STUDIES ON IONOMER-POLYANILINE AND IONOMER-POLYANILINE-MWCNT COMPOSITES FOR ELECTRICAL AND ELECTROMAGNETIC INTERFERENCE SHIELDING APPLICATIONS

Thesis submitted to

Cochin University of Science and Technology

in partial fulfilment of the requirements

for the award of the degree of

Doctor of Philosophy

by

Kingsley Kema Ajekwene

Department of Polymer Science and Rubber Technology
Cochin University of Science and Technology
Cochin- 682 022, Kerala, India

May 2019

Studies on Ionomer-Polyaniline and Ionomer-Polyaniline-MWCNT Composites for Electrical and Electromagnetic Interference Shielding Applications

Ph.D. Thesis

Author

Kingsley Kema Ajekwene
Lecturer I
Department of Polymer and Textile Technology,
Yaba College of Technology,
P.M.B. 2011, Yaba, Lagos, Nigeria.
E-mail: kemaking@gmail.com
kingsley.ajekwene@yabatech.edu.ng

Supervising Teachers

Dr. Thomas Kurian
Professor
Department of Polymer Science and Rubber Technology
Cochin University of Science and Technology
Cochin- 682 022, Kerala, India
E-mail: drtkurian@gmail.com

Dr. Honey John
Professor
Department of Polymer Science and Rubber Technology
Cochin University of Science and Technology
Cochin- 682 022, Kerala, India
E-mail: honey@cusat.ac.in

Department of Polymer Science and Rubber Technology
Cochin University of Science and Technology
Cochin- 682 022, Kerala, India

May 2019

Department of Polymer Science and Rubber Technology
Cochin University of Science and Technology
Cochin- 682 022, Kerala, India

26-04-2019

Certificate

This is to certify that the thesis entitled **“Studies on Ionomer-Polyaniline and Ionomer-Polyaniline-MWCNT Composites for Electrical and Electromagnetic Interference Shielding Applications”** is a report of the original work carried out by **Mr. Kingsley Kema Ajekwene** under our supervision and guidance in the Department of Polymer Science and Rubber Technology, Cochin University of Science and Technology, Cochin-22. No part of the work reported in this thesis has been presented for any other degree from any other institution. All the relevant corrections and modifications suggested by the audience during the pre-synopsis seminar and recommended by the Doctoral committee have been incorporated in the thesis.

Dr. Thomas Kurian
Professor
Department of Polymer Science and
Rubber Technology
Cochin University of Science and
Technology
Cochin- 682 022, Kerala, India

Dr. Honey John
Professor
Department of Polymer Science and
Rubber Technology
Cochin University of Science and
Technology
Cochin- 682 022, Kerala, India

Cochin-22

Declaration

I hereby declare that the thesis entitled “**Studies on Ionomer-Polyaniline and Ionomer-Polyaniline-MWCNT Composites for Electrical and Electromagnetic Interference Shielding Applications**” is the original work carried out by me under the supervision of **Dr. Thomas Kurian** (Professor) and under the co-supervision of **Dr. Honey John** (Professor), Department of Polymer Science and Rubber Technology, Cochin University of Science and Technology, Cochin-22 and has never been included in any other thesis submitted previously for the award of any degree.

Cochin-22
26-04-2019

Kingsley Kema Ajekwene

Dedication

……to the MEMORY of my Late Dad Ajekwene J. C. for the foundation and legacy he bequeathed us.

Above all, the work is dedicated to the GRAND-CREATOR; Almighty God whose invisible qualities are clearly seen from the world's creation.

Acknowledgements

To God alone be all the Glory.

Special thanks and gratitude to my supervisor Prof. Dr. Thomas Kurian and co-supervisor and HOD PSRT Prof. Dr. Honey John who despite their crowded schedules were always open and accessible to me. They gave invaluable assistance, contributive criticism and suggestions, cordial and warm reception and patience at all times of my consultation with them, advice and encouragement during the course of the development of this work until the very end. I have learned so much from your diverse research background and techniques. Without your help, I would not have grown this much as a research scholar and as an individual who has adequately grown over the past three years. Above all, the deep concern for my psychological and spiritual wellbeing is sincerely appreciated here. God bless your you and your household.

My gratitude to Prof. Dr. Sunil K. Narayanankutty (Former Head of the Dept. of Polymer Science and Rubber Technology) for giving me the privilege of admission to the department and his special understanding of tackling issues without creating anxiety.

I am thankful to Emeritus Professors - Dr. C.P. Reghunathan Nair, Dr. Rani Joseph and Dr. K.E. George for their special concerns and well wishes. My acknowledgement and thanks to faculty members of the department; Dr. Sailaja G.S., Dr. Prasanth Raghavan, Dr. Jayalatha Gopalakrishnan, Dr. Jinu Jacob George and Dr. Abitha K. for their encouragement and support. I am also indebted to other teachers; Sona Stanly, Dhanya V for my course works and Emeritus Prof. V.P.N. Nampoori for the unforgettable manner he taught research methodology.

A special thanks to the administrative office staff of PSRT; Anson P. Antony (section officer), Usha Joseph Ma'am (now retired), Manju C., Rajan S., Soumya J. and Raseena A., for their prompt support with the administrative procedures. My warm appreciation also go to Raveendran A. V. (store in-charge) for his kind assistance with every nature of my request at all times, as well as the supporting technical staff; Devi, Biji, Abhil, Sreekanth and Sreenath for all their support and help.

Special thanks to the PDFs; Dr. Bipinbal, Dr. Jelmy and Dr Sreeja S for their support and encouragements.

My sincere thanks go to my PSRT friends and colleagues, Dr. Sobha, Dr. Sunitha, Dr. Sona, Dr. Sreejesh, Dr Teena, Dr. Renju, Dr. Dennymol, Dr. Resmi Dr. Molice Thomas, Dr. Neena Satheesh, Dr. Neena Jibi, Dr. Julie, Dr. Bhavya, Dr. Shadiya, Dr. Muralidharan, Dr. Manoj, Dr. Jolly Anthony, Dr. Anju, Dr. Dhanya Vijanyan, Midhun, Neethu, Jisha J.P., Dr. Remya, Sona Stanly, Dr. Nishad, Sreedevi, Shinu K.P, Asha Paul (my sister), Rahnamol A.M., Divya Jose, Sirajunnisa P., Sumitha N.S., Sneha K.R., Liz Hannah, Ananjana, Aswin A., Praseetha R.N., Meera sathyan, Nisha T.P., Rijoy, Poornima, Jesna Louis, Dhanu, Akhila Das, Neethu T.H., Resmi K.R., Shincy, Athul S. Basil, Irthasa, Liya Rose, Bashida V.B. (Bukola) for their support.

Grateful to my good friends - Venu Gopal, Gean Varghese, Bhaghesh and Dileep for their help, concern, love and companionship.

I wish to express my gratitude to Prof. Dr. C.K. Aanandan, Department of Electronics, CUSAT for permitting me to carry out the EMI shielding measurements and Neeraj for helping to carry out the measurement. I thank Prof. Dr. Junaid Bushiri (HOD) and Prof. Dr. Jayalakshmi S. (now retired) Dept. of Physics, CUSAT for permitting me to carry out the electrical conductivity and ATR spectroscopy and Dr Anil Kumar, Manoj, Ratheesh for helping out with the use of instruments. I also extend my gratitude to the scientists and staff of STIC, Kochi especially Dr. Shibu Eapen and Adarsh for all my analysis.

Deep appreciation and thanks to the Vice Chancellor of CUSAT Prof. Dr. J. Letta for her assistance when I needed help most, the Registrar Prof. Dr. Peters cordial reception and assistance whenever I come for help. The Pro VCs – Prof. Dr. K. Poulose Jacob (immediate past Pro VC) and the present - Prof. Dr. P.G. Sankaran are also warmly appreciated for the willingness and zeal to help at all times. The University Syndicate board and entire administrative of CUSAT are here acknowledged for their role in ensuring that every documentation that relates to me gets due and prompt attention at all times. I am most grateful.

I specially thank the director of International Relations and Academic Admissions (IRAA), Prof. Dr. K.K. Saju who gave so much attention and assistance *in ensuring that my stay at CUSAT is so comfortable as if I am at my home country. The entire staff of IRAA are appreciated for their readiness at all times to help me and other foreign nationals studying at CUSAT.*

Sincere thanks to the, former Rector Dr. Mrs. M.K. Ladipo of Yaba College of Technology, former Deputy Rectors; Sir I.A. Akhuemonkhan (Academics) and Dr. M.A. Adebakin (Admin) and former Registrar B.C. Amakakpabor, Dean of School of Technology Mrs. B. Dada and the former Dean School of Technology Dr. R. Adigun for their support, assistance and constant motivation. My immense gratitude to Dr. C.O. Ogunleye HOD Polymer/Textile Technology for his invaluable support, encouragement and constant motivation.

My profound thanks and appreciation to my mentor Dr. O.A.S. Adeakin who is always there for me at all times; his prayers, encouragement and motivation is immeasurable.

I heartily acknowledge Dr. O.F. Biotidara, Mrs. M.A. Bello (retired), P.B. Kayode (retired), D.N. Ichetaonye, Engr. N.C. Igwe, O.A. Olupinla (Femidodo), Mrs. M.U. Okhuarobo, G.D. Diriyah, O.A. Oderinde, F.O. Oladiran, Dr. S.O. Alebiosu, G.A. Apeh, O.L. Idemudia, M.M. Owen, S.I. Ichetaonye, A. Awosanya, K.U. Ugonna, O.I. Akindiya, J.O. Odubunmi, E.M. Yibowei, J.G. Adekoya, R.A. Muhammed, T.O. Adekeye, for their encouragement and push to carry on. You are all appreciated. I also appreciate R.R. Omolola, Femi Ariyibi, Olusegun (Shegeh), Seun, Nike, Anuoluwapo Janet and Mrs Egunjobi for you warm affection.

Dr P.N. Okolie is specially appreciated for his deep love and concern for my wellbeing. I thank Kennex Paints and Ruth Akinola and family for their support and generosity towards me.

My thanks and gratitude to all my teachers at all the levels of education I have undertaken for all the training and discipline you impacted on me. The LORD will replenish you all. I specially thank Mr. Otoede, Mr. Orukpe, Mr. Ogboi, Mr. Ije, Mr. Obos Peter, Mr. Enihenhena, Mr. Izuaje, Mr. Usifor, Mr. Oyamhendan, Dr. Ihimhinre G., Mr. Ebuade Julus, Mr. Ighalo, Mr. Emafoh, Mr. Elabor, Mr Ogwogho, Mr. Akande, Mr. Ihaza (late), Mr. Okosor (late), Mr.Okongun, Mr. Steve Ugbodaga, Mrs Isibor and Mrs Amiegbebhor. Dr (Mrs) F.A.O. Akpa, Engr. Dr. S.O. Ohikhena, Dr. J.E. Imanah, Prof. J.D. Udonne, Dr. E.J. Asore

(Late) Mr J.A. Idiaghe, Mrs S.O. Ugbesia, Prof. E.O. Osabohien, Mr B.O. Kuale, Prof. N.A. Oladoja are fondly acknowledged. Prof. Popoola A.V., Prof. Oshodi A.A., Prof. Lajide Labunmi, Prof. Ajayi O.O., Prof. Amoo I.A., Prof. Adetuyi A.O., Prof. Aiyesanmi A.F., Prof. Okoronkwo A.E., Prof. Oladimeji (retired), Prof. Ipinmoroti (late), Dr. Owolabi B.J., Dr. Adebayo A.O., Dr. Owokotomo I.A., are all appreciated for their role in my journey so far.

My wonderful family friends are not left out in this acknowledgement-Aigbokhan Edwin and family, Oborkhale Christopher and family, Iriogbe Charles and family, Iluobe Makun and family, Ileogben Alex and family, Momoh Patrick and family, Oboh Johnson and family, Ogunleye Idowu and family and all my good friends not mentioned here due to space constrains. I say thank you for your unending support.

I am also indebted to my entire family members especially my mum Mrs Maureen Ajekwene, Patrick, Barr ThankGod., Stanley, Dr. Agbonmherele, Innocent, Dominic, Uyor, Ibe, Elizabeth, Michael, Chukwudi, Oiko Daniel and many too numerous to mention. I appreciate the support and encouragement of Ajemi Daniel and Aunty Ladi.

I specially thank Jean Gerald Etibou, my friend and brother for being always there for me. Mr. Kioko Nwania and Fadhili Kyao are appreciated. My Liberian friend and brother Mr Sam Browne is warmly appreciated for his encouragement and motivation at moments of anxiety and discouragement. I am indebted to Iscelia Taweh for being a source of encouragement and motivation to me.

I thank Akindele Elijah who has been very humble and loyal to attending to my day to day needs. Simon Baba and my Adhithi Bhavan crew are fondly remembered here; Abdoulie, Mariama, Titos, Fernando, Jyotirmoy, Bimal, Jeza, Daniel Jecca, Philips, Pascal, Hadi, Nosihullah. I appreciate your companionship. I appreciate the entire membership of Kerala International Students Association (KISA) for honour accorded me.

I thank my numerous students; old and new for their constant encouraging and motivational messages. I appreciate you all.

I sincerely and specially acknowledge with thanks and gratitude the financial support from Tertiary Education Trust Fund (TETFUND) of the Federal Republic of Nigeria through Yaba College of Technology.

I have made so many wonderful friends during my life and at the same time have so many more family relations. I wish I could mention everyone, but the list would be too numerous and I would feel bad for leaving anyone out. The path to the time would have been much more difficult without them since their support was a great resource althrough. I say thank you all for being there for me.

Finally I acknowledge the indissoluble connections of my family. I thank my beloved Wife – Angela for her quiet patience and unyielding love and my understanding children – Joseph, Joan and Justus for their unconditional love and patience while the sufferings lasted to stand by me althrough the course of my work.

Above all, my immense gratitude to GOD Almighty for his Abundant Grace, Unfailing Love, Endless Mercy and for the Gift of Life.

Kingsley Kema Ajekwene

Preface

The growth in the application of electrical and electronic devices across a broad spectrum of military, industrial, commercial and consumer sectors such as wireless device systems, navigation, air space technology, military installations, etc. has resulted in the rapid boom of electronic devices ranging from simple to sophisticated. The consequence has created a peculiar form of pollution known as noise or electromagnetic interference (EMI). EMI can cause serious harm to the effective performance of electrical and electronic devices, different life forms as well as human beings. And so, there is a greater need for the effective shielding of electronic devices from the adverse effects of EMI noise with effective shielding materials. Materials for this purpose are prepared by adding ferrites, carbon black or other conducting fillers in a polymeric matrix. Conventionally, EMI shielding techniques focused on metallic materials and their composites, which effectively reflect the electromagnetic waves. Metals have good mechanical strength but have the disadvantages of higher density, easy corrosion and uneconomic processability. Additionally, it is difficult to retain a uniform distribution of the metal filler throughout the matrix in which it is mixed during its composites fabrication. This could result in deficiency of the metallic filler in corners, edges and surfaces which tends to result in gaps in the shield composite materials causing disconnection in the conducting path and leakages of the radiation and thus diminishing the conductivity and effectiveness of the shield. Hence, the need for conducting polymers that displays several characteristics of organic polymers such as lightweight, lower cost, resistance to corrosion and chemical attack, flexibility and greater workability as well.

Conducting polymers in recent years have gained wide usage in electrical/electronic devices, energy storage devices, sensors and EMI shielding materials. Among the conducting polymers, polyaniline (PANI) and PANI based materials have been researched most comprehensively for the reason that they possess easier and inexpensive preparation methods, good environmental stability in both doped and undoped forms, excellent physical and chemical properties and high conductivity. But the main limitations of PANI are that it requires a large amount of protons attached to the polymer to be electrically conducting and it is a very poor conductor when the pH is greater than 5. Therefore PANI tends to experience loss of conductivity in neutral and high pH environments and it is highly unstable even at moderate temperatures (>100 °C). Therefore, there is the need to further expand the application possibilities of conducting PANI in order to meet the requirements of sophisticated technologies. Such a situation needs materials with stable conductivity and opaque to microwaves. Conducting fillers can offer an attractive solution for this. In this regard, CNTs based composites can provide a vital role due to their stable conductivity, non-corrosiveness, nominal processing cost and thermal and environmental stability.

Incorporation of CNTs in PANI and polymer matrices to make composites, have been intensively studied. The unique structure of CNT promotes several outstanding properties including thermal stability and electrical conductivity. The act of incorporating CNTs into PANI to form composites (PANI-CNTs) could extend the properties and applications of PANI and CNTs. Despite this, however, the problem of processability is unabated. This justifies the necessity to fabricate either a binary composites of polymer matrix-PANI, polymer matrix-CNT or hybrid composites of polymer matrix-PANI-CNTs.

Polymer materials (thermoplastics, thermosets, elastomers, etc.) possess good melt strength to bind PANI, CNT or PANI-CNT particles together in order to make it processable without compromising its conductivity and other properties. One of the ways to achieve these benefits lies in the exfoliation of PANI, CNTs or PANI-CNTs into the polymer matrix to generate particles of high aspect ratio. Mechanical and electrical properties of polymers are significantly influenced by the presence of fillers. Mixing polymers with the electroconductive PANI, CNTs or PANI-CNTs besides an increase of electroconductivity, lead to an increase of modulus and tensile strength accompanied by a decrease of deformability resulting in lower elongation at break and diminished toughness of the material. Since the conducting polycomposites are stable and retain the mechanical properties of the host polymer, films can be fabricated by solvent evaporation or by melt-processing for use in anti-static applications, for electromagnetic shielding, microwave absorption devices, etc.

Addition of CNTs into PANI with unstable electrical conductivity and the addition of PANI, CNTs or PANI-CNTs into polymer matrix that is intrinsically highly insulating is of paramount industrial interest for enhancing the processability of PANI, CNTs or PANI-CNTs as well as enhancing the electrical conductivity of the insulating polymer. The present work is an attempt to formulate an effective preparative route by which composite blends with high conductivity and processability could be obtained by chemical oxidative polymerization of aniline, insitu chemical oxidative polymerization of aniline in carbon nanotube and solution mixing PANI or PANI-CNTs with ionomers (sodium salt of poly(ethylene-co-methacrylic acid) (EMAANa) or zinc salt of poly(ethylene-co-methacrylic acid) (EMAAZn) using a blend of polar and non-polar solvents at 65°C to improve the processability of the composites to facilitate their effective utilization as EMI shielding materials. The emphasis is in solution processing as it is a more economical way to achieve good homogeneity and rapid mixing of the component materials with minimum energy consumption.

The thesis consists of seven chapters. The first chapter reviews literatures on ionomers, conducting polyaniline, carbon nanotubes and blending of polymers. Scope and objectives of the present work are also presented in this chapter.

The details of materials used, the experimental methods and characterization techniques applied for the study are outlined in the second chapter.

Chapter three describes the synthesis and characterization of hydrochloric acid (HCl) doped polyaniline (PANI) in bulk and nano dimensions (bulk PANI-HCl and nano PANI-HCl) and toluene sulfonic acid (TSA) doped polyaniline in nano dimensions (nano PANI-TSA). The nanocomposites of polyaniline with MWCNT were prepared by in situ polymerization of aniline in the presence of non-functionalized carbon nanotube and functionalized multi-walled carbon nanotubes (amine and carboxylic acid) using ammonium persulfate as initiator and TSA as dopant tagged PANI-pristine CNT, PANI-ACNT and PANI-CCNT. Scanning electron microscopy (SEM) was used to characterize the morphology of the PANI and PANI-CNT nanocomposites. X-ray diffraction (XRD) spectroscopy, Fourier Transform Infrared (FTIR) spectroscopy and UV-Vis spectroscopy were used to characterize the synthesized PANI and PANI-MWCNT nanocomposites. Thermogravimetric analysis (TGA) was used to study the thermal behaviour of the samples. The electrical conductivity of composites at room temperature was measured and their percolation threshold was determined.

Chapter four is divided into two parts: A and B.

Part A reports the design and development of poly(ethylene-methacrylic acid copolymer) neutralized with zinc salt (EMAAZn) and polyaniline (PANI: bulk PANI-HCl, nano PANI-HCl and nano PANI-TSA) binary composite films, with the aim of modifying EMAAZn in order to achieve improved electrical conductivity and high electromagnetic interference (EMI) shielding effectiveness (SE). EMAAZn-PANI binary composites were prepared in solution by dissolving EMAAZn in solvent using a solvent mixture of toluene/1-butanol (90:10) at 65 °C and mixing PANI in it. These binary composites were characterized and evaluated by FTIR, UV-Vis spectroscopy, XRD spectroscopy and thermogravimetric analysis (TGA). The electrical conductivity of the PANI, EMAAZn-PANI binary composites were measured by conventional four-probe method. The EMI shielding effectiveness was studied using a wave-guide coupled to an Agilent Synthesized Sweeper 8375A and a Hewlett-Packard spectrum analyzer 7000 in the X band frequency range (8-12 GHz).

Part B reports the fabrication of poly(ethylene-methacrylic acid copolymer) neutralized with sodium salt (EMAANa) and polyaniline (PANI: bulk PANI-HCl, nano PANI-HCl and nano PANI-TSA) binary composite films, with the aim of modifying EMAANa in order to achieve improved electrical conductivity and high electromagnetic interference (EMI) shielding effectiveness (SE). The composites are prepared by following the same procedure as described in PART A with sodium salt of poly(ethylene-co-methacrylic acid) (EMAANa)) as ionomer instead of EMAAZn ionomer. The characterization techniques was done using the same methods as detailed in PART A.

Chapter Five is divided into two parts: A and B.

Part A describes the preparation, evaluation and applications of zinc salt of poly(ethylene-co-methacrylic acid) ionomer-polyaniline-multi walled carbon nanotubes tripartite hybrid composites. Zinc ionized ionomer with as prepared PANI-pristine CNT, PANI-ACNT and PANI-CCNT were fabricated into tripartite hybrid composite films of EMAAZn-PANI-MWCNT by solution mixing in blend of solvents (toluene (90%)/ 1-butanol (10%)) at 65°C. The electrical properties and EMI shielding effectiveness characteristics of the conducting hybrid composites were evaluated.

Part B describes the electromagnetic interference shielding effectiveness of polyaniline functionalized carbon nanotubes filled sodium ionomer hybrid composites. Sodium ionized ionomer with as prepared PANI-pristine CNT, PANI-ACNT and PANI-CCNT were fabricated into tripartite hybrid composite films of EMAANa-PANI-MWCNT by solution mixing in blend of solvents (toluene (90%)/ 1-butanol (10%)) at 65°C. The electrical properties and EMI shielding effectiveness characteristics of the conducting hybrid composites were also evaluated.

Chapter six presents the mechanical characteristics of ionomer-PANI binary composites and ionomer PANI-MWCNT tripartite hybrid composites. The mechanical properties of solution processed ionomer-PANI binary composites and ionomer-PANI with different carbon nanotubes at ratio 1:1 were examined.

The conclusions of the investigations are presented in the last chapter of the thesis.

Contents

Chapter 1

Chapter 2

EXPERIMENTAL .... 63 - 85

Chapter 3

STUDIES ON BULK AND NANO POLYANILINE AND NANO POLYANILINE-MULTI WALLED CARBON NANOTUBE (PANI-MWCNT) NANOCOMPOSITES .... 87 - 117

Chapter **4**

Part A

STUDIES ON ZINC IONOMER-POLYANILINE BINARY COMPOSITES

Part B

STUDIES ON SODIUM SALT OF POLYETHYLENE
METHACRYLATE-BASED IONOMER WITH DOPED PANI

Part A

ZINC SALT OF POLY(ETHYLENE-CO-METHACRYLIC ACID) IONOMER-POLYANILINE-MULTI WALLED CARBON NANOTUBES HYBRID COMPOSITES: PREPARATION, EVALUATION AND APPLICATIONS.

Part B

ENHANCED ELECTROMAGNETIC INTERFERENCE SHIELDING EFFECTIVENESS OF POLYANILINE FUNCTIONALIZED CARBON NANOTUBES FILLED SODIUM IONOMER HYBRID COMPOSITES

Chapter 6

Chapter 7

List of Abbreviations and Symbols

$(NH_4)_2S_2O_8$	Ammonium persulfate
[P(E-MAA-Na)]	Sodium salt of poly(ethylene-co-methacrylic) acid
$[P(E\text{-}MAA\text{-}Na^+)]$	Poly(ethylene-co-methacrylic acid) neutralized with sodium salt
[P(E-MAA-Zn)]	Zinc salt of poly(ethylene-co-methacrylic) acid
$[P(E\text{-}MAA\text{-}Zn^{2+})]$	Poly(ethylene-co-methacrylic acid) neutralized with zinc salt
$[P(MMA\text{-}BA\text{-}(AA)_2Zn)]$	Poly(methyl methacrylate-butyl methacrylate-zinc acrylate)
[P(MMA-BA-AANa)]	Poly (methyl methacrylate-butyl methacrylate-sodium acrylate)
AdB	Absorption loss
A	Absorbance
ACNT	Amine functionalized - Carbon nanotubes
Ag_2O	Silver oxide
APS	Ammonium persulfate
ASTM	American Society for Testing and Materials
CB	Carbon black
C-C	Carbon-Carbon
CCNT	Carboxylic acid functionalized - Carbon nanotubes
$Ce(SO_4)_2$	Cerium sulphate
CNTs	Carbon nanotubes
COOH	Carboxyl
CPs	Conducting polymers
CuO	Copper oxide
dB	Decibels
DBSA	Dodecyl benzene sulfonic acid
DBSNa	Sodium dodecylbenzene sulfonate
DC	Direct Current
DMA	Dynamic mechanical analyzer

DMF	Dimethylformamide
DSC	Differential scanning calorimetry
DTA	Differential thermal analysis
EB	Emeraldine base
EM	Electromagnetic
EMI	Electromagnetic interference
EPDM	Ethylene–propylene–diene rubber
ES	Emeraldine salt
ESD	Electrostatic dissipation
FTIR	Fourier transform infrared spectroscopy
H_2O_2	Hydrogen peroxide
H_2SO_4	Sulphuric acid
HCl	Hydrochloric acid
HPC	Hydroxypropylcellulose
ICPs	Intrinsically conducting polymers
IR	Infrared spectroscopy
$K_2Cr_2O_7$	Potassium dichromate
$K_3(Fe(CN)_6$	Potassium ferricyanide
KIO_3	Potassium iodate
LDPE	Low-density polyethylene
LEB	Leucoemeraldine base
$LiNO_3$	Lithium nitrate
MdB	Multiple reflections
MBS	Methyl methacrylate-butadiene-styrene
MMT	Montmorillonite
MUT	Material under test
MWCNTs	Multiwalled carbon nanotubes
$NaVO_3$	Sodium vanadate
NH_2	Amine
NMP	N-methyl-2-pyrrolidinone
P_I (E_I or H_I)	Power of incident EM waves

P_T (E_T or H_T)	Power of transmitted EM waves
PA	Polyacetylene
PANDB	Polyaniline doped by dodecyl benzene sulfonic acid
PANI	Polyaniline
PEDOT	Poly(3,4-ethylene dioxythiophene)
PF	Polyfuran
PMMA	Poly(methyl methacrylate)
PNB	Pernigraniline base
PPV	Poly(p-phenylene-vinylene)
PPy	Polypyrrole
PS	Polystyrene
PSS	Poly(styrenesulfonate)
PSSA	Polystyrene sulfonic acid
PTh	Polythiophene
PVA	Poly(vinyl alcohol)
PVP	Poly (vinyl pyrrolidone)
RdB	Reflection loss
R&D	Research and Development
RF	Radio frequency
S/cm	Siemens per centimetre
SE_R	Reflection
SE_A	Absorption
SEdB	Shielding effectiveness
SE	Shielding effectiveness
SEM	Scanning electron microscopy
SPEEKK	Sulfonated poly(ether ether ketone ketone)s
SWCNTs	Single-walled carbon nanotubes
S_{11} (S_{22})	R- Reflectance
S_{12} (S_{21})	T- Transmittance
TC	Thermoplastic constituent
Tc	Cooling temperature

TEM	Transmission electron microscopy
Tg	Glass transition temperature
TGA	Thermogravimetric analysis
THF	Tetrahydrofuran
Ti	Increased temperature
Tm	Melting temperature
TPU	Polyurethane thermoplastic
TSA	Toluene Sulphonic acid
UV – vis	Ultraviolet – visible spectroscopy
VOCs	Volatile organic compounds
XRD	X – ray diffraction
n	Integer
d	Distance between atomic layers in the crystal
λ	Wavelength
θ	Angle of incidence
α	Absorption coefficient
σ	Electrical conductivity (S/m)
I	Current (amperes)
V	Voltage (volts)
l	Thickness of the sample (m)
A	Area of contact of electrodes with sample (m^2)

* * *

Chapter 1

LITERATURE REVIEW

Contents

1.1 Introduction

Polymers were regarded as electrically non-conducting materials until the oxidation of polyacetylene in the presence of iodine vapour which resulted in a significant increase in electrical conductivity of polyacetylene (PA) in 1977 [1,2]. Conducting polymers possess electrical properties like that of metals and the characteristics of organic polymers such as lightweight, lower cost, resistance to corrosion and chemical attack, flexibility and greater workability [3, 4, 5]. They are widely used in electrical/electronic devices and a myriad of applications. However, they have limitations despite their unique characteristic properties and ever growing areas of applications. The limitations are due to high manufacturing costs, material inconsistencies, toxicity, insolubility in many organic solvents, inherent brittleness, poor mechanical properties and poor processability [6]

Carbon nanotubes (CNTs) have become one of the most interesting nanomaterials in the past three decades and have received significant attention in terms of fundamental properties and potential applications. It was first discovered and reported in 1991 by Iijima when he discovered multiwalled carbon nanotubes (MWCNTs) [7]. They possess some impressive and interesting structural, mechanical, electrical, optical, thermal and chemical characteristics which are attributed to their small size and mass, strong mechanical potency and high electrical and thermal conductivity. Carbon nanotubes are allotropes of carbon, made of graphite and constructed in cylindrical and tubular shapes with diameters in nanometer and length in millimeters [8-11]. Composite materials reinforced by either carbon nanotubes or conducting polymers have been prepared and significant enhancement in mechanical and electrical properties have been reported by many researchers.

Ionomers are classes of polymeric materials that comprise repeat units of both electrically neutral units and a fraction of ionized units usually not more than 15 mole % [12]. Ionomers have unique physical properties including electrical conductivity and high melt viscosity. The ionic interactions in ionomers allow for the control of physical and mechanical properties of the polymers such as elastic modulus, glass transition temperature, viscosity, melt strength, fatigue resistance and transport properties [13-17]. However, it has a low and poor conductivity which is dependent on water absorption. The resulting deficiencies in electrical applications include operating temperatures restricted to below 100°C, poor durability of wet membranes and poor mechanical and chemical stability at elevated temperatures.

Based on the features of ionomers, conducting polymers and carbon nanotubes highlighted above, proper enhancement of properties will be possible if these uniquely special materials are blended together. Numerous attempts have been made by researchers by the use of long chain organic dopants, functionalization of monomer rings and preparation of conducting polymer-thermoplastic composites by either chemical blending (insitu polymerization or copolymerization) or mechanical blending (melt or solution mixing) thereby allowing the fabrication of composite films which exhibit a good balance of electrical conductivity, mechanical properties and processing characteristics [18].

1.2 Ionomers

As the name sounds, they are ion containing copolymeric materials with either positive [+] or negative [-] electric charge [12, 19] in which up to 15 mol % of the repeat units contain ionic groups. They comprise of both electrically neutral repeating units (nonionic) and a fraction of ionized units covalently bonded to the polymer backbone as pendant group moieties. The level of substitution of ionic groups as well as how the ionic groups are incorporated into the polymer structure determines the classification of polymers as ionomers. The non-polar polymer backbone present in ionomers is incompatible with the polar ionic groups thereby resulting in the microphase separation of the ionic groups into ion-rich domains [12, 13, 14, 20, 21].

1.2.1 Classes of Ionomers

Ionomers can be classified by the type of the ion chemically attached to the backbone chains, the position of the ionic groups, and the distribution of the ionic groups on the polymer backbone, the counterion used, the chemistry of reaction and the geometry of the polymer backbone. The polymer architectures could be a linear macromolecule, macrocyclic, branched, grafted (comb-like) chains, stars, dendrimers and tridimensional networks [15, 22]. The chemical nature of the components in the backbone can be organometallic, organic or inorganic [14]. Different types of ionic groups such as sulfonic, ammonium, carboxylic, phosphonic and phosphonium and imidazole can be introduced into the polymer backbone [14, 15]. Ionomers can also be classified as cationomers (quaternary ammonium polymers, polyurethane, etc.), anionomers (sulfonated polystyrene, poly(ethylene-co-meth-acrylic acid) and polyampholytes or zwitter ionomers (poly aminocarboxylic acids, proteins, etc.) depending on the type of ionic group chemically attached to the polymer backbone [14].

1.2.2 Production of Ionomers

There are two techniques for the preparation of ionomers of practical interest:

a) Copolymerization of a low level functionalized monomer with an olefinic unsaturated monomer.

b) Direct functionalization of a preformed polymer.

The synthesis of ionomers involves a polymerization process referred to as copolymer neutralization. The process involves ionomers being derived from precursor copolymers containing both ionic and non-ionic repeat groups. The ionic component is then neutralized to form an ionic pair with the attachment of metallic cation. Ionic groups are usually formed as part of the polymer structure. The amount of acid groups neutralized during the neutralization process influences the amount of ionic content that will be present in the ionomer [23]. Typically, ionomers are obtained by copolymerization of acrylic acid or methacrylic acid with ethylene, styrene, or similar co-monomers by free-radical copolymerization. The resulting copolymer is available as a free acid, which could be neutralized to the desired degree with metal acetates, hydroxides and similar salts [22, 24].

The direct functionalization of a preformed polymer is utilized when only a low degree of functionalization is desired as in the case of sulfonated ionomers. This reaction is done typically in a homogeneous solution, using the sulfonating agent - acetyl sulphate, generated in situ from acetic anhydride and concentrated sulphuric acid. After neutralization to the desired degree by a suitable agent, the ionomer is isolated by coagulation in a non-solvent or by solvent flashing [22]. One of the examples of a popular ionomer is poly(ethylene-co-methacrylic acid). This polymer is a sodium or zinc salt (which provides the ions) of copolymers derived from ethylene and methacrylic acid [12].

1.2.3 Poly(ethylene-co-methacrylic acid)

It is a commercial thermoplastic ionomer produced by DuPont in the early 1960's and was trademarked "Surlyn" It is a random copolymer consisting of poly(ethylene-co-methacrylic acid). It contains 5.4 mol % methacrylic acid and neutralized with alkali metals or zinc hydroxide [23].

The production of Surlyn involves the copolymerization of ethylene and methacrylic acid via a high-pressure free radical reaction. After synthesis, the copolymer is then dissolved using tetrahydrofuran and the solvent is thereafter removed leaving the neutralized copolymer (ionomer) as the final product [13, 23].This is illustrated in Figure 1.1 below.

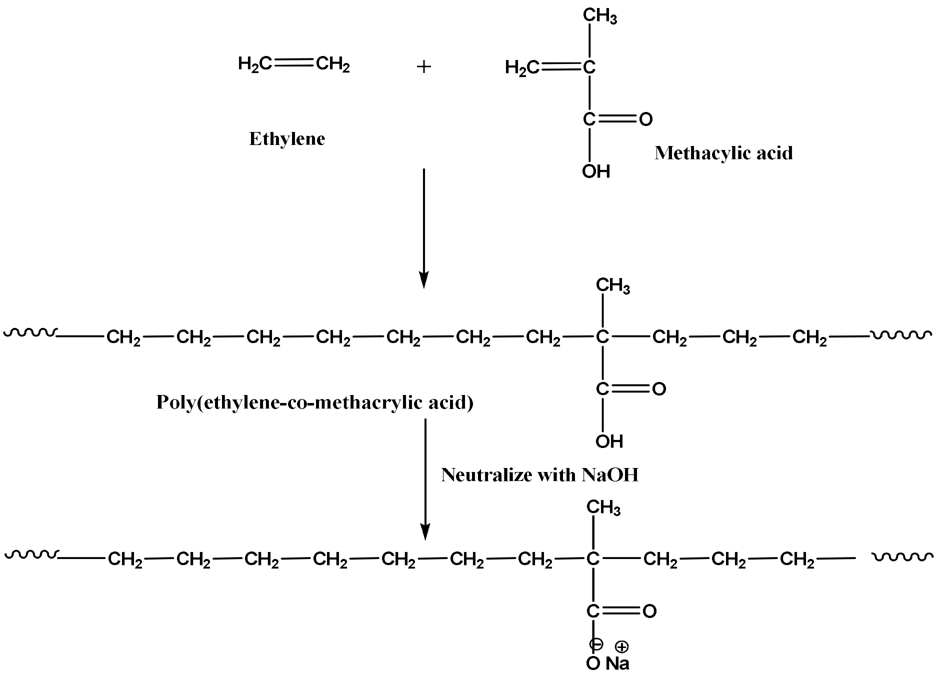

Figure 1.1. Diagram of EMAA neutralized with sodium [12, 23].

1.2.4 Structure-Properties Relationship and Applications of Ionomers

In a typical ionomer, the nonpolar chains are grouped together and the polar ionic groups are attracted to each other. As a result, the ionic groups would prefer to go off into a little corner by themselves which is not usually possible due to the restriction imposed by their attachment to the polymer chain. This allows thermoplastic ionomers to act in ways similar to that of crosslinked polymers or block copolymers [12, 19, 24]. The ionic attractions that results strongly affect the polymer properties. The phenomenon is illustrated in figure 1.2.

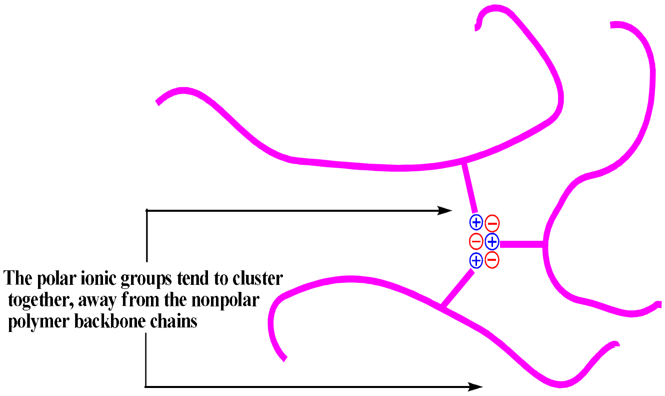

Figure 1.2. Polar ionic group clustering [12 – with permission]

When these clustered ionic groups are heated, they tend to lose their attractions for each other and the chains will move around freely. This is because ionomers are not crosslinked polymers; in fact, they are a type of thermoplastics known as reversible crosslinkers. As the temperature increases, the mobility of the chains increases and the groups can no longer stay in their clusters (Figure 1.3). This allows for a polymer with the properties of an elastomer and the processability of a thermoplastic and is in most instances known as thermoplastic elastomers [12, 19, 24].

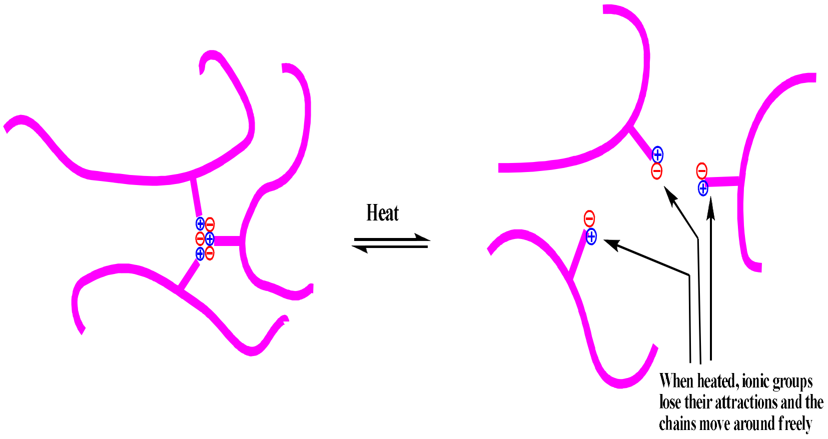

Figure 1.3. Thermoplasticity of ionomers [12 – with permission]

The combination of a stable backbone with an acidic sulfonic acid groups in the case of sulfonated ionomers gives characteristic properties such as high conductivity to cations (making it suitable for many membrane applications), ability to resist chemical attack, high operating temperature (up to 190 °C as a result of its backbone interlaced with the ionic sulfonate groups), superacid catalyst and proton conductivity up to 0.2 S/cm depending on temperature and hydration state. However, it is selectively and highly permeable to water and gases which is a drawback for energy conversion devices such as artificial leafs, fuel cells, alkali cells, sensors and water electrolyzers [25]. Other properties such as water management, hydration stability at high temperatures, electro-osmotic drag, as well as the mechanical, thermal and oxidative stability are also affected especially at higher temperatures [26, 27].

Properties such as sealing performance, clarity and oil/grease resistance are desirable features needed for packaging products such as food; hence, making ionomers highly suitable for food packaging. Its high strength and toughness properties makes it useful in sporting applications (such as golf ball covers and ski boots), semipermeable membranes, sealing tapes and thermoplastic elastomers. They have been utilized successfully in various industrial fields including diffusion and electrodialysis, electrolysis, solid polymer electrolyte for batteries, potentiometric sensors, membranes for water treatment, solution recycling and filtering, proton exchange membranes for fuel cells, packaging, coatings, optics, medical and biological fields (as sensors, membranes and dental restorative materials, etc.) [21, 28, 29, 30].The exceptional chemical inertness and thermal stability coupled with favourable electrical conductivity are of particular advantage in this application. The three main characteristics of ionomer membranes that determine their applications are ion conductivity, hydrophilicity and fixed carriers. Ion conductivity plays an important role in electro-dialysis, concentration and desalination of electrolytes, separation between electrolyte and non-electrolyte, bipolar ion exchange membrane process to produce acid and alkali, ion-exchange reaction across the membrane, electro-deionization, electrolysis (chlor-alkali production, organic synthesis), diffusion dialysis (acid or alkali recovery from waste), neutralization dialysis (desalination of water), Donnan dialysis (recovery of precious metals, softening of hard water, pre-concentration of a trace amount of metal ions for analysis), up-hill transport (separation and recovery of ions), piezodialysis and thermo-dialysis (desalination or concentration), battery (alkali battery, redox-flow battery, concentration cell), fuel cell (hydrogen-oxygen, methanol-oxygen) and an actuator (catheter for medical use). Hydrophilicity is applied in the field of pervaporation (dehydration of water-miscible organic solvent), dehumidification (dehumidification of air and gases) and sensors (gas, chemical and biosensors). While fixed carriers (ions incorporated into ionomer membrane) facilitates the selective transport of certain gases through the membranes due to the formation of polymer coordinate complexes in the ionomer (removal of acidic gas, separation of olefins from alkanes, separations of sugars) and modified electrodes [20, 31, 32, 33].

They have unique structures that consist of hydrophobic main backbones and pendant side chains with hydrophilic terminated sulfonic groups. The hydrophobic main backbones endow them with superior properties of structural integrity while the pendant hydrophilic side chains give them desirable proton conductivity when fully hydrated. [34, 35].

In the case of sulfonated ionomers higher degree of sulfonic acid substitution to achieve higher proton conductivity results in the loss of mechanical strength as the ionomer becomes soluble in water. This could result in the microphase separation of ionomers into hydrophilic and hydrophobic domains [31, 36]. The hydrophobic domains consist of the main chain backbone while the hydrophilic domains bear the sulfonic acid groups. Water absorbs into the polymers associating with the sulfonic acid groups and swelling the hydrophilic domains. Proton conduction occurs through the hydrophilic domains. Ionomers have hydrophilic domains dispersed in a continuous hydrophobic matrix. At high water content, ionomers show good proton conductivity. At low water content, the hydrophilic domains may not be sufficiently connected to carry a proton current. As water is absorbed into the material, the hydrophilic domains swell and creates percolation path for proton conduction to take place [31, 36, 37, 38, 39]. This drawback can be effectively managed by optimizing the concentration of sulfonic acid groups which balance the increased conductivity and decreased mechanical strength with increased acid concentration; as well as several different approaches for the modification of ionomers, including physical and or chemical treatment, reinforcement by porous support materials and fillers (conducting polymers, CNTs) and the addition of organic or inorganic compounds.

1.3 Conducting Polymers

Traditionally, polymers are considered as insulators. However, in 1977, a discovery by Alan G. MacDiarmid, Hideki Shirakawa, and Alan J. Heeger changed this age long traditional concept and belief about polymers. They found that conductivity of polyacetylene after doping with electron-withdrawing AsF_5 increased ninefold, reaching the order of 10^3 S/cm but was very unstable [1]. After this discovery, a series of more stable conducting polymers, including polypyrrole (PPy), polyaniline (PANI), and polythiophene (PTh), were reported from the end of the 1970s to the beginning of the 1980s, which opened up the unprecedented research on conducting polymers. Conducting polymers include electronically and ionically conducting polymers. Ionically conducting polymers are usually called polymer electrolytes while electronically conducting polymers are referred to as conjugated conducting polymers. The conductivity of almost all conjugated polymers can reach the order of 10^{-3}–10^3 S/cm after doping [3, 40].

Because of some of their special and unique properties such as being a conducting mechanism, electrical properties, reversible doping-dedoping process, controllable chemical and electrochemical properties and easy processability, a variety of conducting polymers e.g., polyacetylene (PA), polyaniline (PANI), polypyrrole (PPY), poly(p-phenylene-vinylene) (PPV), poly(3,4-ethylene dioxythiophene) (PEDOT), polyfuran (PF) and other polythiophene (PTh) derivatives, etc., have drawn special attention in the field of nanoscience and nanotechnology [41]. For the purpose of this work, polyaniline is the conducting polymer of choice.

1.3.1 Polyaniline (PANI)

Polyaniline (PANI) is a semi-flexible semiconducting rod-like organic polymer. Because of its many attractive processing properties and rich chemistry, polyaniline is one of the most studied conducting polymers.

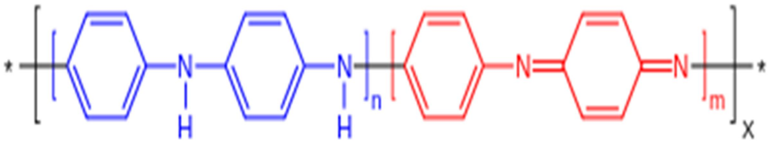

Figure 1.4. Main polyaniline structures

Depending on the acidity conditions, PANI possess a globular, nano-fibrillar or nano-tubular morphology. The salt of polymer can convert to non-conducting PANI base under alkaline conditions. Polyaniline displays both the electronic and ionic conductivity. Its electrical and thermal stability at high temperature and in unfavorable media is quite good.

Polyaniline is polymerized from aniline monomer in the presence of an acid as a dopant and oxidizing agent. PANI could be found in one of three different idealized oxidation states. The synthetic methods to produce PANI are quite simple. On the contrary, the mechanism of the reactions are quite complex.

The formation of Leucoemeraldine can be described as follows, where [O] is a generic oxidant.

$$nC_6H_5NH_2 + [O] \rightarrow [C_6H_4NH]_n + H_2O$$

The most common oxidant is ammonium persulfate. The components are each dissolved in 1 M hydrochloric acid (other acids can be used), and the two solutions slowly combined. The reaction is very exothermic. The polymer precipitates is an unstable dispersion with micrometer-scale particulates.

Pernigraniline is prepared by oxidation of the emeraldine base, one typical oxidant being Meta-chloroperoxybenzoic acid.

$$\{[C_6H_4NH]_2[C_6H_4N]_2\}_n + RCO_3H \rightarrow [C_6H_4N]_n + H_2O + RCO_2H$$

Leucoemeraldine with n = 1, m = 0 is the fully reduced state. Pernigraniline is the fully oxidized state (n = 0, m = 1) with imine links instead of amine links. It is white/clear & colorless $(C_6H_4NH)_n$

The emeraldine (n = m = 0.5) form of polyaniline, often referred to as emeraldine base (EB) is neutral, when it is doped (protonated) it is called emeraldine salt (ES) in which the imine nitrogens are protonated by an acid to give a green coloured material [2, 42].

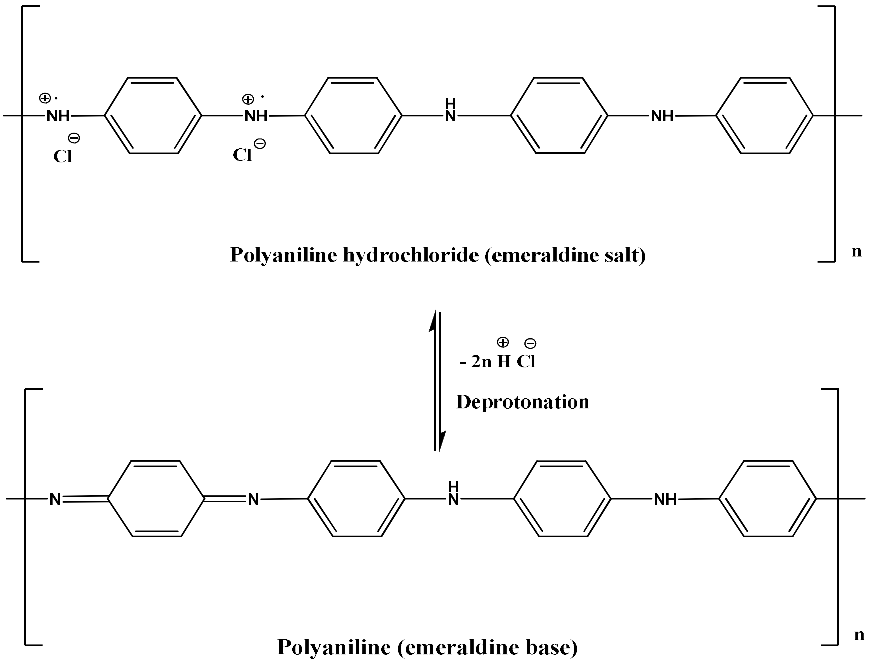

Figure 1.5. Protonation and deprotonation of emeraldine base [2]

Emeraldine base is regarded as the most useful form of polyaniline due to its high stability at room temperature and the fact that, upon doping with acid, the resulting emeraldine salt form of polyaniline is highly electrically conducting. It is blue colour for the emeraldine base $([C_6H_4NH]_2[C_6H_4N]_2)_n$

Leucoemeraldine and Pernigraniline are poor conductors, even when doped with an acid. This is blue/violet coloured $(C_6H_4N)_n$.

1.3.2 Synthesis of Conducting Polymers

Many synthetic strategies (both physical and chemical) have been adopted for the preparation of conducting polymers (CPs). Conducting polymers can be synthesized by reacting aniline in acidic aqueous media through techniques such as interfacial polymerization, reverse emulsion polymerization, chemical, electrochemical, photochemical, metathesis, concentrated emulsion, inclusion, solid-state, plasma polymerization. It could also be obtained as thin films, coatings or as a colloidal dispersion. and a variety of techniques. Pyrolysis and soluble precursor polymer preparation could as well be used in the synthesis of conducting polymers. Among the synthesis methods highlighted above, chemical and electrochemical polymerization processes are reportedly the most prominent and commonly used [2]. The mechanism (scheme) of chemical polymerization is illustrated in figures 1.6 below.

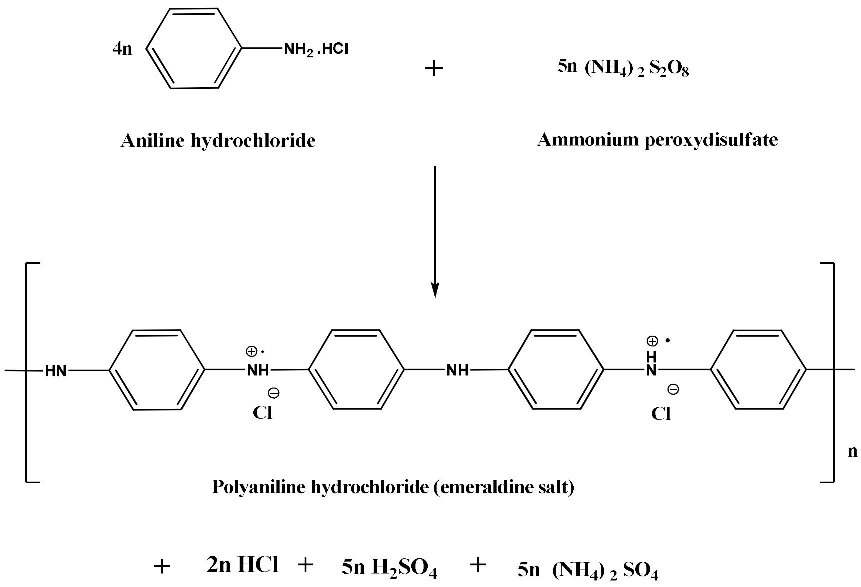

Figure 1.6. Chemical polymerization of aniline [2].

In chemical polymerization (oxidative coupling), the monomers are oxidized to a cation radical and coupled to form di cations to generate the polymer with repetition of the reaction e.g., the oxidation of aniline by peroxydisulfate in acid media leading to the conducting polymer (Polyaniline) [2, 43, 44]. All the classes of conjugated polymers could be synthesized by this technique. Chemical polymerization route is reportedly the most useful method for preparing large amounts of conducting polymers since it is performed without electrodes. A variety of conducting polymers like polypyrrole, polythiophene, polyaniline, polyphenylene oxide, polyazulene, polycarbazole, polyaniline/polymeric acid composite and several other polymers have been synthesized using this approach. Some of these conducting polymers are highlighted in table 1.1.

Table 1.1: Structures, Synthesis, Doping Agents, Solubilities, Applications and Conductivities of some representative Conjugated Polymers [Adapted from 40]

Conjugated polymers	Structures	Stable structure	Preparation method	Doping Agents	Solubility	Application fields	Conductivity (S cm−1)
Polyacetylene (PA)	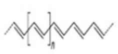	p-type, inorganic, redox	chemical oxidation polymerization	I_2, AsF_3, $AlCl_3$, Li $FeCl_3$, K,	Soluble in some solvents	Polyacetylene has no commercial applications due to its poor stability and processability	10^3–1.7×10^5
Polypyrrole (PPy)	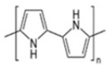	p-Doped conducting state	PPy films can be obtained by electrochemical oxidation polymerization from aqueous or organic solution. PPy powder can be prepared by chemical oxidation polymerization	$FeCl_3$, $Cu(ClO_4)_2$, AsF_5	Insoluble	Modified electrode, enzyme electrodes (biosensors), electrochromics, conducting polymer films	10^2–7.5×10^3
Polyaniline (PAn)		p-Doped conducting state (proton-acid doping)	Electrochemical or chemical oxidation polymerization from strong acidic aqueous solution	HCl, $HClO_4$, Camphor, Sulphonic acid	Insoluble for the PAn doped with common anions, but it can become soluble bycounteranion doping induced solubility	Modified electrodes, enzyme electrodes (biosensors), electrochromics, electrode materials for batteries and solid capacitors, anti-corrosion, microwave absorption, electrode buffer layer for optoelectronic devices	30–200
Polythiophene (PTh)	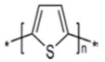	Intrinsic semiconducting state	Electrochemical oxidation polymerization from organic solution, or chemical oxidation polymerization in organic solvent	SO_3, CF_3-, ClO_4-, BF_3	Insoluble	Electrochromics, conducting polymer Films	10–10^3
Poly(3,4-ethylenedioxythiophene) (PEDOT)	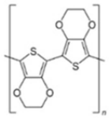	p-Type doped conducting state	Electrochemical oxidation polymerization from organic solution, chemical oxidation or chemical synthesis in organic solvent	Camphorsulfonic acid (CSA), Aniline-2-sulfonic acid	Aqueous solution	Transparent conducting polymer films, anode buffer layer materials in organic/polymer light emitting diodes and organic/polymer solar cells, anti-static-electricity coating layer materials, electrode materials in solid state capacitors, etc.	10^2–10^3
Poly(3-hexyl thiophene) (P3HT)	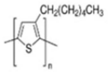	Intrinsic semiconducting state	Chemical synthesis in organic solvents	BF_4-, ClO_4-, $FeCl_4$-	Soluble in THF, chlorobenzene,	Donor material in polymer solar cells, semiconductors in field effect transistors	10^3-10^4
Poly(p-phenylene vinylene) (PPV)	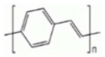	Intrinsic semiconducting state	Chemical synthesis in organic solvents	AsF_5, $AlCl_3$, $FeCl_3$, K, Li	dichlorobenzene, etc. Soluble in organic solvents	Orange electroluminescent material for polymer light-emitting diodes	3–5×10^3
Poly (p-phenylene sulphide) (PPS	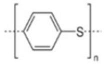	Intrinsic semiconducting state	Chemical synthesis in organic solvents	AsF_5, FSO_3, H, SbF_5	Soluble in organic solvents	Photovoltaic cells, gas sensors, and supercapacitors	10^{-9}-10^1

To understand the specific behavior and working of conducting polymers and their wide range of applications such as in chemical and bio-sensors, field-effect transistors, field emission and electrochromic display devices, supercapacitors, actuators and separation membranes, etc., the properties has to be understood [41].

1.3.3 Properties of Conducting Polymers

Conducting polymers do not only exhibit electrical conduction properties, but also exhibit some extraordinary properties such as electronic, magnetic, wetting, optical, mechanical, and microwave-absorbing properties (Figure 1.7).

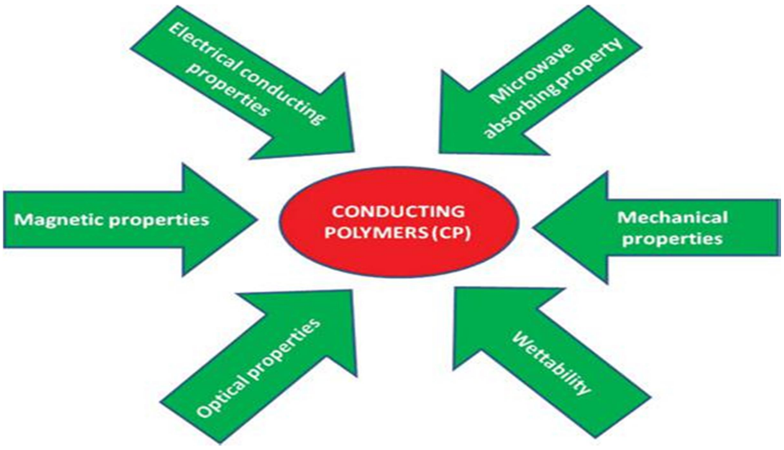

Figure 1.7. Properties of conducting polymers [41].

1.3.3.1 Electrical/Electronic Properties

After doping, the electrical conductivity of conducting polymers can reach the metallic conducting regime up to the order of 10^{-3}-10^{3} S/cm [25, 41, 45, 46].

1.3.3.2 Magnetic Properties

The magnetic properties of conducting polymers have been extensively studied because they provide important information on charge-carrying species and unpaired spins which is controlled by the level of doping and doping type [25, 41, 45, 46, 47].

1.3.3.3 Optical Properties

The unique optical properties of conducting polymers have been extensively explored because of their applicability in nanophotonic devices. The materials are suitable for the fabrication of photodetectors, photochemical sensors, and photonic wire lasers [25, 41].

1.3.3.4 Microwave Absorbing Properties

Conducting polymers as microwave absorbing materials have been explored due to their lower density and excellent electromagnetic loss. This indicates that conducting polymers can be used as high absorption, wide frequency and lightweight microwave absorbents. Doped polyaniline with fiber-like morphology has a better electromagnetic wave-absorbing property than that of polyaniline with particle-like morphology [25, 41, 45-49]. The conductivity of the polymers can be tailored for a given application. High conductivity and dielectric constant of the materials contribute to high EMI shielding efficiency (SE). Therefore, conducting polymers find their application in EMI shielding technology.

1.3.4 Applications of Conducting Polymers

Conducting polymers exhibit unique properties which are multifunctional. Therefore, they are expected to find applications in many fields. The most documented are: as corrosion inhibitors, compact capacitors, anti-static coating, smart windows, transistors, light emitting diodes, lasers used in flat screen televisions, nanoelectronic devices, chemical or biological sensors, catalysis or electrocatalysis, energy, electro rheological fluids and biomedicine, drug delivery and protein purification, tissue engineering, neural interfaces, actuators, microwave absorption and electromagnetic shielding[25, 40-54]. This is represented in Figure 1.8.

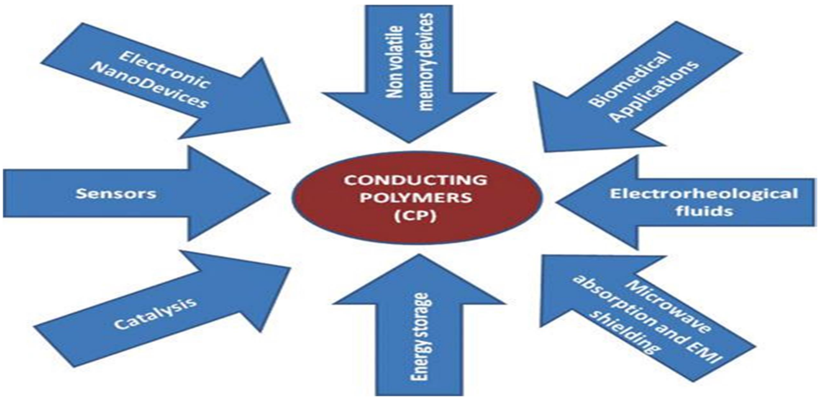

Figure 1.8. Applications of conducting polymers [41].

1.4 Carbon Nanotubes

Carbon nanotubes (CNTs) have become one of the most interesting nanomaterials in the past three decades and have received significant attention in terms of fundamental properties, measurements and potential applications. It was first discovered and reported in 1991 by Iijima when he discovered multiwalled carbon nanotubes (MWCNTs) [7]. Since then, there has been a drastic revolution in the field of nano materials science and technology culminating in great interest in application from both immediate (fundamental and technical) to futuristic applications [55, 56]. They possess some impressive and interesting structural, mechanical, electrical and electronic, optical, thermal and chemical characteristics, which is attributed to their small size and mass, their strong mechanical potency, their high electrical and thermal conductivity etc. These unique characteristic features have opened an array of limitless channels for present day and future applications. Their length to width ratio (greater than 1,000,000) makes them exhibit unique mechanical properties such as stiffness, strength and high elastic moduli. Their electrical properties make them show semiconducting as well as metallic behaviour which makes them useful in thermoelectricity, superconductivity, electroluminescence and photoconductivity [56, 57].

Carbon nanotubes are allotropes of carbon, made of graphite and constructed in cylindrical and tubular shapes with nanometer in width and several millimetres in length [9, 58]. They contain at least two layers or more ranging from about 3 nm to 30 nm in the outer diameter. Other allotropes of carbon are diamond and graphite which are considered as the two natural crystalline forms of pure carbon. Another allotrope form of carbon known as Buckminster Fullerene (C60) molecule was first discovered in 1985 by a research team led by Korto et al [57, 58].

1.4.1 Structure and Morphology

Carbon atoms exhibit sp^3 hybridization in the diamond form in which four bonds are directed towards the corners of a regular tetrahedron resulting in an extremely rigid three-dimensional network, resulting in its hardness while in the graphite form, the carbon exhibits sp^2 hybridization in which each atom is evenly connected to the three carbons at 120° in the xy

plane and a weak $\pi\pi$ bond in the zz axis to form the hexagonal (honeycomb) lattice typical of a sheet of graphite [7]. The bonding in carbon nanotubes is sp^2 with each atom joined to three neighbours, as in graphite. The tubes can, therefore, be considered as rolled-up graphene sheets (graphene is an individual graphite layer). This bonding structure, which is stronger than the sp^3 bonds found in diamond, provides the molecules with their unique strength [59]. Structure of nanotubes is as shown in Figure 1.9.

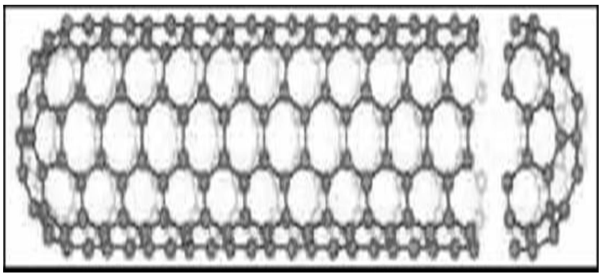

Figure 1.9. Structure of carbon nanotube [60]

1.4.2 Classification of Carbon Nanotubes

Carbon nanotubes are classified into two types. Single-walled carbon nanotubes-SWCNTs and Multiple-walled carbon nanotubes-MWCNTs

1.4.2.1 Single-Wall Carbon Nanotubes (SWCNT)

Single-walled carbon nanotubes (SWCNTs) synthesized about two years later in 1993 by Dresselhaus and co-workers [11] though Iijima had made the observation of single-walled carbon nanotubes (SWCNTs) earlier in that same year. Single-wall carbon nanotubes exhibit novel properties as a result of their unusual structure. They comprise of a hollow cylinder of carbon ~ 1nm in diameter and a tubular length of up to

1,000,000 times as long as its width [59, 60]. The structure has an extremely unique optical and electronic properties, high strength and flexibility with high thermal and chemical stability. Therefore, it is expected to have a sensational effect on a number of industries; including electronics, displays, health and composites. The structure of a SWCNT can be conceptualized by wrapping a one-atom-thick layer of graphite of graphene into a consistent cylinder. The way the graphene sheet is wrapped is represented by a pair of indices (n, m) called the chiral vector. If m = 0, the nanotubes are called "zigzag, which is named for the outlook of hexagons. On the other hand, if n = m, the nanotubes are called "armchair", which depicts one of the two conformers of cyclohexene; a hexagon of carbon particles. Else, they are called "chiral", in which the m values lies between zigzag and armchair structures [56, 57, 61-67].

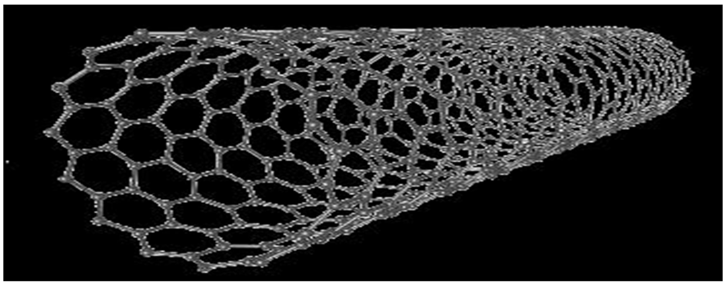

Figure 1.10. Single-wall carbon nanotubes [61]

1.4.2.2 Multi-Walled Carbon Nanotubes (MWCNTs)

Multiwalled carbon nanotubes (MWCNTs) was discovered in carbon soot by Iijima in 1991 [10]. The structures of multi-walled carbon nanotubes (MWCNT) can be described by two models; the Russian Doll and Parchment models. In the Russian Doll model, sheets of graphite are arranged in concentric cylinders i.e. a single-walled carbon nanotube (SWCNT) inside a bigger single-walled nanotube while in the Parchment model, a single sheet of graphite is rolled in around itself, looking like a scroll or rolled up paper. The interlayer distance in multi-walled nanotubes is close to the clearance distance, approximately 3.3 Å (330 pm) separating graphene layers in graphite [57, 60, 61, 62, 63]. The layers, constituting the individual cylinders, are found close in pairs at the very tip of MWCNT and its detailed structure plays a very important role in electronic and field emission properties of nanotubes. The structure is a barrel-shaped tube including six-membered carbon rings like graphite [60, 61]. Comparably MWCNTs consists of several tubes in concentric cylinders. The quantity of these concentric walls may shift from 6 to at least 25. The width of MWCNTs might be 30 nm when contrasted with 0.7– 2.0 nm for average SWCNTs. Comparisons between SWCNT and MWCNT is as presented in Table 1.2.

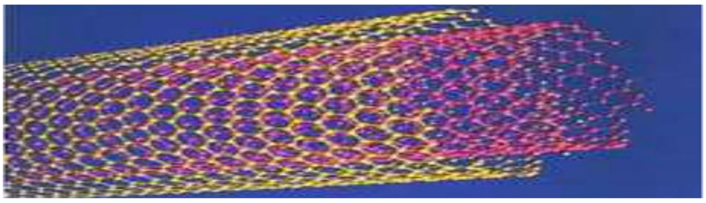

Parchment models

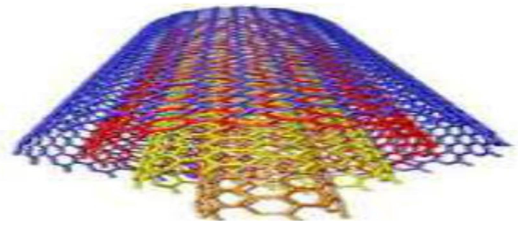

Russian Doll models

Figure 1.11. Multi-Walled Nanotubes [61]

Table 1.2. Comparison between SWCNT and MWCNT [57, 59]

Sr. No	SWNT	MWNT
1	A single layer of graphene which is beneficial in establishing a conducting network.	Multiple layers of graphene.
2	Catalyst is required for the synthesis.	Can be produced without catalyst.
3	Bulk synthesis is difficult as it requires proper control over growth and atmospheric condition.	Bulk synthesis is easy.
4	Purity is poor.	Purity is high.
5	Chance of defect is more during functionalization. Tubes may fracture during dispersion at defect sites, bringing down the number of electrical pathways and the resulting conductivity.	Chance of defect is rare but once occurred it is difficult to improve.
6	Less accumulation in the body.	More accumulation in body.
7	Characterization and evaluation are easy.	It has very complex structure hence characterization and evaluation is fairly difficult.
8	They are more pliable and easily twisted. An increased aspect ratio is needed in order to develop a conductive network in the polymer matrix at a low loading of additives.	It cannot be easily twisted and plied.

1.4.3 Functionalization of CNTs

The lack of solubility of carbon nanotubes in a wide range of media has been a major technical limitations to its applications. To overcome this problem, the modification of the surface of CNTs is done. This modification is known as functionalization. This could be achieved by adsorption, electrostatic interaction or covalent bonding of different molecules and chemistries that render them more hydrophilic. Chemical modification through Amine (NH_2) and Carboxyl (COOH) have made it possible to solubilize and disperse carbon nanotubes in water, thus opening the path for their facile manipulation and processing. Through such modifications, the water solubility of CNT is improved and their compatibility profile is completely transformed. Moreover, the bundling/aggregation of individual tubes through van der Waals forces are also reduced by the functionalization of their surfaces [55, 56, 57, 59].

1.4.4 Properties of CNTs

Morphologically, CNTs have a high aspect ratio with lengths typically more than 100 times the diameter, and in certain cases much higher. Their performance and application are based not just on aspect ratio, but also on the degree of entanglement and the straightness of the tubes, which in turn is a function of both the degree and dimension of defects in the tubes [60]. Carbon nanotubes are endowed with exceptionally high material properties, such as electrical and thermal conductivity, strength, stiffness and toughness. Three major properties of CNTs are specifically interesting for the industry; the electrical conductivity (as conductive as copper), mechanical strength (Up to 15 to 20 times stronger compared to steel and at the same time 5 times lighter) and thermal conductivity (same as that of diamond but five times more than that of copper) [68]. Other impressive properties that endeared CNTs are chemical, optical and field emission properties. A combination of these impressive properties enables a whole new variety of useful and beneficial applications.

1.4.4.1 Mechanical Properties

The tensile strength and elastic modulus of carbon nanotubes have been reported to be the strongest and stiffest materials discovered thus far. CNTs have an excellent tensile strength and when integrated into a composite, such as a thermoplastic or thermoset compounds, can significantly increase its strength [60]. This strength is attributed to the covalent sp^2 bonds formed between the individual carbon atoms. A nanotube’s strength can be weakened by defects in the structure of the tube. Defects occur from atomic vacancies or a rearrangement of the carbon bonds. Defects in the structure can cause a small segment of the nanotube to become weaker, which in turn causes the tensile strength of the entire nanotube to weaken. The tensile strength of a nanotube is dependent on the strength of the weakest segment in the tube similar to the way the strength of a chain depends on the weakest link in the chain.

CNTs are extremely strong along their axes and exhibit a very large Young‘s modulus in their axial direction because of the presence of carbon-carbon (C-C) bonds making it suitable for the application as probe tips for scanning microscopy.

A single perfect nanotube is about 10 to 100 times stronger than steel per unit weight. The Young's modulus of the best nanotubes can be as high as 1000 GPa which is approximately 5 times higher than steel. The tensile strength or breaking strain of nanotubes can be up to 63 GPa, around 50 times higher than steel. These properties, coupled with the lightness of carbon nanotubes, gives it great potential in applications such as aerospace. It has also been suggested that nanotubes could be used in the space elevator, an Earth-to-space cable first proposed by Arthur C. Clarke.

1.4.4.2 Electrical/Electronic Properties

Not only are carbon nanotubes extremely strong, they have very interesting electrical properties. They can be highly conducting, hence, can be said to be metallic. Their conductivity has been shown to be a function of their chirality, the degree of twist, their diameter as well as its high aspect ratio. The needed conductivity level can be achieved with much lesser loadings than for conventional solutions such as metal particulates or carbon black. CNTs can be either metallic or semi-conducting in their electrical behaviour [60]. The structure of a carbon nanotube determines the conductivity of the nanotube. The structure of atoms in a carbon nanotube minimizes the collisions between conduction electrons and atoms, making carbon nanotube highly conductive. The strong bonds between carbon atoms also allow carbon nanotubes to withstand higher electric currents than copper. Electron transport occurs only along the axis of the tube. Carbon nanotubes can transmit electrical signals at speeds up to 10 GHz when used as interconnects on semi-conducting devices. Nanotubes also possess a constant resistivity.

A single graphite sheet is a semimetal, which means that it has properties intermediate between semiconductors (like the silicon in computer chips, where electrons have restricted motion) and metals (like the copper used in wires, where electrons can move freely). When a graphite sheet is rolled into a nanotube, not only do the carbon atoms have to line up around the circumference of the tube, but the quantum mechanical wave functions of the electrons must also match up. In theory, metallic nanotubes can carry an electrical current density of 4 × 109 A/cm^2 which is more than 1,000 times greater than metals such as copper [55, 57].

The electronic properties of carbon nanotubes are also extraordinary. There are several areas of technology where carbon nanotubes are already being used in electronics. These include flat-panel displays scanning probe microscopes and sensing devices. A nanotube with a natural junction (where a straight metallic section is joined to a chiral semiconducting section) behaves as a rectifying diode (a half-transistor in a single molecule) [55, 57, 60].

1.4.4.3 Thermal and Expansion Properties

There is a common claim that all nanotubes are expected to be very good thermal conductors along the tube, exhibiting a property known as ballistic conduction, but good insulators laterally to the tube axis. CNTs have been revealed to display superconductivity below 20°K (approx. -253°C). The thermal stability of carbon nanotubes is estimated to be up to 2800 °C in a vacuum and about 750 °C in the air based on the level of defects and to a certain extent on the purity as a residual catalyst in the product can also catalyze decomposition. It is also assumed that carbon nanotubes can transmit up to 6000 $W{\cdot}m^{-1}{\cdot}K^{-1}$ at room temperature compared to a metallic copper well-known for its good thermal conductivity, but transmits 385 $W{\cdot}m^{-1}{\cdot}K^{-1}$ [60]. Many applications properties such as in nanoscale molecular electronics, sensing and actuating devices, or as reinforcing additive fibres in functional carbon-carbon composite materials, have been utilized [55, 57, 60].

1.4.4.4 Chemical Properties

CNTs are an allotrope of sp^2 hybridized carbon similar to graphite and fullerenes and as such have high chemical stability. The chemical reactivity of a CNT as compared with a graphene sheet is enhanced as a result of the curvature of the CNT surface. This curvature causes the mixing of the π and σ orbital which leads to hybridization between the orbitals. The degree of hybridization becomes larger as the diameter of the CNTs gets smaller. Hence, carbon nanotube reactivity is directly related to the π-orbital mismatch caused by an increased curvature. For the same reason, a smaller nanotube diameter results in increased reactivity. Covalent chemical modification of either sidewalls or end caps has shown to be possible. For example, the solubility of CNTs in different solvents can be controlled this way. Covalent attachment of molecular species to fully sp^2-bonded carbon atoms on the nanotube sidewalls proves to be difficult. From the foregoing, nanotubes can be considered as chemically inert. However, one can functionalize the nanotubes to enhance both the strength and dispersibility of composites. [55, 57, 60].

1.4.4.5 Optical Properties

Optical properties of CNTs are related to their one-dimensional nature especially. Studies have revealed that the optical activity of chiral nanotubes disappears if the nanotubes become larger. Therefore, it is expected that other physical properties are influenced by these parameters too. Use of the optical activity might result in optical devices in which CNTs play an important role [55, 57].

1.4.4.6 Field Emission

Field emission results from the tunneling of electrons from a metal tip into vacuum, under application of a strong electric field. Field emitters are superior to conventional electron sources, hence finding their way into all kind of applications, most importantly flat-panel displays. The small diameter and high aspect ratio of CNTs is very favorable for field emission. They are probably the best electron field-emitter known, largely due to their high length-to-diameter ratios. Even for moderate voltages, a strong electric field develops at the free end of the supported properties of CNTs because of their sharpness [60].

1.4.5 Applications of Carbon Nanotubes

Because of their special physicochemical properties, CNTs are expected to play a major role in numerous applications. There are a large number of present and evolving applications as illustrated below in Figure 1.12).

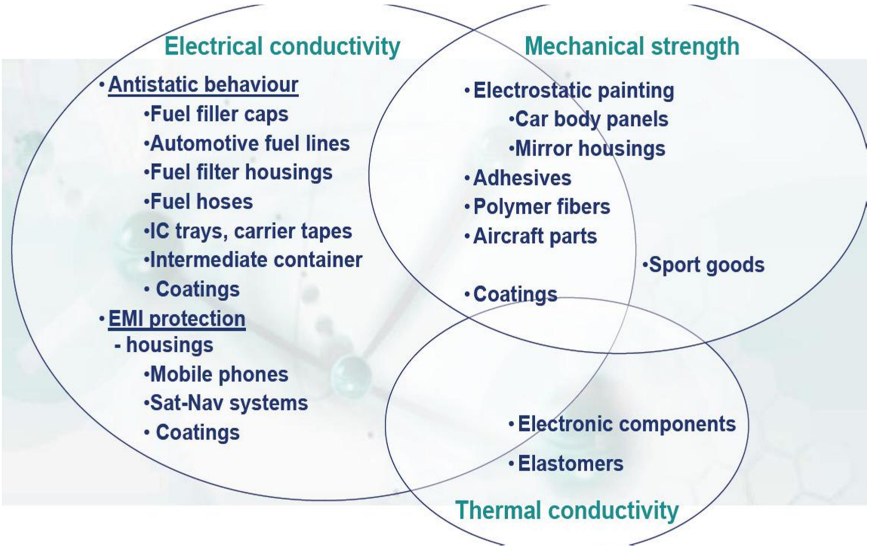

Figure 1.12. Properties of CNTs and potential application fields [68].

Development time is an essential criterion that determines when an application will reach the market. When plotted against time, several broad categories of applications can be recognized: those in place currently or available in the short term, those to be expected mid-term, and those still in the realm of early R&D, classified as long-term (see Table 1.3).

Table 1.3. Applications classification of CNTs in the short, mid and long-term [68].

Current / Short-term	Mid-term	Long-term
Conductive polymers & composites (automobiles and electronics)	Coatings (conductive thin films)	Microwaves antennas
Sensors and Instruments (microscope probe tips, gas leak detectors)	Catalysts (petrochemical)	Self-assembling yarns
	Textiles &fibres	
	Lithium-ion batteries	
	Membrane and filters	
Electromagnetic Shielding	Lamps	Aerospace
Sporting goods (tennis rackets)	Semiconducting materials	Medical implants
	Advanced Ceramics	Drug delivery
	Fuel Cells	
	Caulks and sealants	

Carbon Nanotubes are an example of true nanotechnology. They have opened an incredible range of applications in materials science, electrical, electronics, chemical processing, energy management, electrostatic discharge protection in wafer processing fabrication, antistatic elastomeric and plastic components for automobile fuel line components, plastics rendered conductive to enable electrostatic spray painting of automobile body parts, RFI shielding materials, spray-coatable heater elements; thermal interface and other heat conduction materials; enhanced carbon fiber waterproof and tear resistant cloth fabrics, concrete and steel like applications (a space elevator has even been proposed) based on the property of strength, electrical circuits based on the property of electrical conductivity, sensors based on the property of thermal conductivity, vacuum proof food packaging, batteries and capacitors, solar cells, transistors, nano-electronics, flat panel display, fuel cells, water filtration membranes, composites and even as a vessel for delivering drugs and many other present and evolving applications.

1.5 Conducting Composite Blends

A polymer blend is a mixture of two or more polymers blended together to form a new material with different physical properties encompassing the component polymers. The properties of the blends can be manipulated depending on their intended end use by correct selection of the component polymers [69, 70, 71]. Generally, there are five main types of polymer blends: thermoplastic-thermoplastic blends, thermoplastic-rubber blends, thermoplastic–thermosetting blends, rubber-thermosetting blends and polymer-filler blends (ionomer/ conducting polymer binary blends, conducting polymer/CNTs composites and ionomer/conducting polymer/CNTs ternary blends). All these types of blends have been extensively studied by other researchers previously. While modern blending technology can greatly extend the performance capabilities of polymer blends for specific applications, they must perform under specific conditions too (e.g., mechanical, chemical, thermal or electrical) [72].

Polymer blends are classified as either homogeneous (miscible) or heterogeneous (immiscible). Miscible blends are usually optically transparent and are homogeneous to the polymer segmental level. Compatibility between the polymer phases decides the properties of a heterogeneous polymer blend. Various processing techniques such as solution, melt (hot compression and extrusion) and in-situ polymerization are being used to prepare conducting polymer blends [71, 73].

Different methods have been described to prepare conducting polymer-ionomer blends, such as mechanical mixing, casting of a solution containing the components of the blend or polymerization of one polymer into the other (either chemically or electrochemically). If the synthesis of conducting polymer is performed in the presence of ionomers and CNTs with the appropriate groups that are able to interact with the conducting polymer, then the enhancement of the thermal stability, electrical conductivity and its processability via methods briefly described below may be possible.

1.5.1 Solution mixing

In solution mixing, a solution of the ionomer is prepared, the conducting polymer is separately dispersed in a suitable solvent by sonication, both are blended and the solvent is removed by evaporation [74]. Rajik and Pillai [75] performed solution blending on conducting polyaniline with elastomeric EVA and evaluated the properties. Castillo-Ortega et al. [16] studied and reported the preparation and characterization of electroconductive polypyrrole-thermoplastic composites. They prepared homogenous films of polypyrrole-poly(vinyl chloride) blends by casting in the presence of poly(vinyl methyl ether) or poly(vinyl ethyl ether) dispersants. Cheng-Ho Chen et al. [26] reported preparation and characterization of conductive poly(vinyl alcohol)/polyaniline doped by dodecyl benzene sulfonic acid (PVA/PANDB) blend films by solution-blend method to prepare conductive poly(vinyl alcohol)/polyaniline doped by dodecyl benzene sulfonic acid (PVA/PANDB) blend films. Emeraldine base (EB)-type polyaniline (PANI) was dissolved in N-methyl-2-pyrrolidinone (NMP) and then blended with PVA/dodecyl benzene sulfonic acid (DBSA) solution at varying proportions. They found that the electrical conductivity and the thermal degradation onset temperature of the PVA/PANDB blend film was increased as the amount of EB-type PANI solution is increased. Kingslin et al [27] worked on lithium ion-conducting polymer electrolyte based on PVA–PANI doped with lithium nitrate prepared by solution casting technique using DMF as solvent. Blend polymer (92.5 PVA: PANI 7.5) electrolytes with different wt. % of lithium nitrate ($LiNO_3$) was prepared by solution casting technique using DMF as solvent. Denice et al [76] prepared and evaluated electrical conductivity of polyaniline/thermoplastic polyurethane blends. The aim was to obtain and evaluate the electrical conductivity of polyaniline doped with dodecylbenzenesulfonic acid (PANI.DBSA)/polyurethane thermoplastic (TPU) blends. The PANI.DBSA was synthesized from DBSA-aniline (DBSAn) salt through an emulsion polymerization in tetrahydrofuran (THF) or in the presence of polyurethane thermoplastic solution, resulting in pure PANI.DBSA or PANI.DBSA/TPU blends. Blends of PANI.DBSA/TPU were also prepared through casting, at room temperature, after dissolving both components in THF as a common solvent**.**

1.5.2 Melt Blending

In melt blending process, the conducting polymer is mixed with the ionomer in molten state at elevated temperatures using conventional methods such as extrusion. It has the advantage of being free of solvents. It is the most widely used and convenient method to prepare thermoplastic nanocomposites compared to other methods because it is simple, industrially favorable, low cost, and environmentally friendly. It is also known that the processing method strongly affects the distribution and dispersion of filler or conducting polymer layers, interfacial interactions, and resulting structural and physical properties of the blends [77].Castillo-Castro and co-workers [78] reported the synthesis and characterization of composites of DBSA-doped polyaniline and polystyrene-based ionomers in which DBSA-doped polyaniline blends were synthesized in the presence of poly(styrene-metallic acrylate) ionomers. In a similar way, composites of polystyrene sulfonic acid (PSSA)-polyaniline and montmorillonite clay was synthesized and characterized by Yu-Feng Li and co-workers [79]. They reported an exfoliated layered structure in the XRD patterns indicating the presence of MMT clay in the composites while the TEM photograph shows that the composites have a mixed nanomorphology, indicating that some silicate layers were exfoliated in the polyaniline matrix. The FTIR spectroscopy was reported to have demonstrated the interaction between the PSSA-PANI chain and the surface of the MMT clay layer in the composite. Kunteppa et al [80] reported the AC conductivity and battery application of polyethylene oxide/PANI/sodium chlorate composites. The blends showed good conductivity which is attributed to ionic polarization and electrode polarization. They reported that as the PANI content increases in PEO there is an increase in the polarization current and in the voltage stability. Chang-hsiu Chen and co-workers [81] reported the electrical conductivity of polymer blends of poly(3,4-ethylenedioxythiophene),: poly(styrenesulfonate): N-methyl-2-pyrrolidinone and polyvinyl alcohol. They reported that the use of NMP in the blend increased the electrical conductivity by two to three orders of magnitude and films of the blended polymers with a PEDOT: PSS: NMP concentration equal to or greater than 50 wt. % have a conductivity greater than 1 S/cm. Dhawal and Sadhan [82] produced of electrically conducting networks in immiscible polymer blends by chaotic mixing by using formic acid to dissolve polyamide 6 (PA6) and polypropylene PP-phase at different stages of mixing. The conductive compound of PP was prepared by mixing 10% by volume of carbon black (CB) in twin screw extruder.

1.5.3 Latex processing

Latex processing technique for preparing ionomer/conducting polymer blend involves the preparation of an aqueous colloidal dispersion of the conducting polymer, mixing with a polymer latex to form a two-component colloidal mixture and drying (lyophilization) of the colloidal mixture in order to yield a composite [25]. This method facilitates direct incorporation of conducting polymer into a highly viscous ionomer matrix as well as the formation of three dimensional framework of conducting polymer in the ionomer matrix. But due to the hydrophobicity of conducting polymers, generating a homogenous dispersion in aqueous latex is highly challenging, even after ultrasonication or intense mechanical mixing. Taghipour and co-workers [83] modified polyaniline/polystyrene and polyaniline/metal oxide structure using surfactants by polymerizing aniline and styrene in aqueous solution by polymerization of styrene and aniline in two-stages. Styrene has been polymerized using ammonium persulfate (APS) as an oxidant in the presence of various surfactants such as poly (vinyl pyrrolidone) (PVP), hydroxypropylcellulose (HPC), poly(vinyl alcohol) (PVA) and surfactive dopant sodium dodecylbenzene sulfonate (DBSNa) in the first stage. In the next stage, aniline has been polymerized using potassium iodate (KIO_3) as an oxidant in the presence of PS latex. In addition, nanocomposites of polyaniline containing nanometer-size CuO (Copper oxide) and Ag_2O (Silver oxide) were synthesized by a chemical method using DBSNa as a surfactant. Hong-Quan et al [84] prepared conducting polyaniline-sulfonated EPDM ionomer composites from in-situ emulsion polymerization and studied their properties. They prepared composites of polyaniline (PANI) and zinc sulfonated ethylene–propylene–diene rubber (EPDM) ionomer by polymerization of aniline in the presence of the ionomer by using a direct, one-step in situ emulsion polymerization technique. The ionomers were prepared by sulfonation of EPDM rubber with acetyl sulfate in petroleum ether, followed by neutralization with zinc acetate solution. The in situ polymerization of aniline was carried out in an emulsion comprising water and xylene containing the ionomer in the presence of dodecyl benzene sulfonic acid, acting as both a surfactant and a dopant for the PANI. The composite obtained can further be processed by melt method. Yuming et al [85] polymerized aniline with stable poly(methyl methacrylate-butyl methacrylate-sodium acrylate) [P(MMA-BA-AANa)] and poly(methyl methacrylate-butyl methacrylate-zinc acrylate) [P(MMA-BA-$(AA)_2Zn$)]

ionomer emulsions to improve the processability of polyaniline (PANI). The results indicated that the two ionomer emulsions not only improved the tensile strength of PANI but also maintained the conductivity of PANI at room temperature. Hossein Eisazadeh and Amin Kavian [86] carried out copolymerization of aniline and styrene using various surfactants in aqueous media to obtain polyaniline/polystyrene (PANI/PS) copolymer. The reaction was carried out by using potassium iodate (KIO_3) and ammonium persulfate ($(NH_4)_2S_2O_8$) as an oxidant in the presence of various surfactants such as poly(ethylene glycol), hydroxypropyl cellulose, and surfactive dopant sodium dodecylbenzene sulfonate.

1.5.4 In-situ Polymerization

While in the in situ polymerization method, the conducting polymer is mixed with the liquid ionomer monomer in the presence of a suitable initiator and polymerization is initiated either by heat or radiation. This method is extensively used for the preparation of ionomer/ conducting polymer binary blends, conducting polymer/CNTs composites and ionomer/conducting polymer/CNTs ternary blends due to an advantage of formation of a covalent bond between the conducting polymer and the ionomer matrix [25, 74]. This technique allows the preparation of blends with high conducting polymer loading for enhanced conductivity. Terlemezyan et al [87] reported a research work on electrically conducting polymer blends comprising polyaniline (PANI) as conducting constituent and poly(methyl methacrylate) (PMMA), polystyrene (PS) and methyl methacrylate-butadiene-styrene (MBS) copolymer as a thermoplastic constituent (TC). It was shown that the highest conductivity values were obtained by the in situ prepared PANI/PMMA blends than the other systems studied. Anupam Singh and co-workers [88] researched on in situ blending and characterizations of aniline blended with polymethylmethaacrylate metal containing polymer (Ba acrylate). They examined the physical properties of the prepared polymer films such as appearance, polymerization yield and absorption quality. Xian Feng Li and co-workers [89] synthesized sulfonated poly(ether ether ketone ketone)s (SPEEKK)/Polyaniline (PANI) composite membranes for direct methanol fuel cell usages by studying the membrane morphology. Fernando and Bluma [90] devised a methodology for determination of polyaniline doped with dodecylbenzene sulfonic acid (Pani.DBSA) content in SBS/Pani. DBSA blends prepared by in-situ polymerization based on UV-Vis spectrometry.

The list of works carried out by researchers (individual or groups) on blending and composites of ionomers, conducting polymers and CNTs in the bid to bridging their draw backs has been enormous in the last two decades. New and emerging horizons are opening up regularly due to technological advancement. In this regard, therefore, scientists and researchers are challenged to meet up with the dynamics of these unique materials and their applicability.

For the purpose of this work, we have synthesized polyaniline by chemical oxidative polymerization, insitu polymerization of polyaniline-CNT composite and solution blended ionomer/polyaniline binary composites and ionomer/polyaniline/MWCNT hybrid composites.

1.6 Microwave Absorption and Electromagnetic Interference (EMI) Shielding

Electromagnetic radiation (EMI) in term of conventional theory, is the flow of energy at the universal speed of light through free space or through material medium in the form of electric and magnetic fields [91]. It may possibly come in the form of lightning strikes, interference from radio emitters, nuclear electromagnetic pulses or even high power microwave threats. For these reasons, there is a pressing need for the effective shielding of electronic devices from the adverse effects of EMI noise and protection of human being from radiations with shielding materials such as conducting polymers and composites [92, 93]. Materials for this purpose are usually prepared by adding ferrites, boron, tungsten, titanium, tantalum, silver, gold, carbon black or other conducting fillers or some form of combination of these materials etc., in a polymeric matrix. But then, these fillers possess the disadvantage of higher density values, prone to corrosion and difficulty in processing.

EMI shielding refers to the reflection and absorption of electromagnetic radiation by material. In case of reflection of the radiation by the shielding material, the shield material must possess electron or holes (mobile charge carriers) which interact with the electromagnetic field in the radiation. As a result, the shield material tends to be electrically conducting. Electromagnetic interference (EMI) shielding effectiveness (SE) is defined as the attenuation of the propagating electromagnetic (EM) waves produced by the shielding material [94-108]. In general, SE is expressed in decibels (dB). This is schematically illustrated in the diagram (Figure 1.13) below.

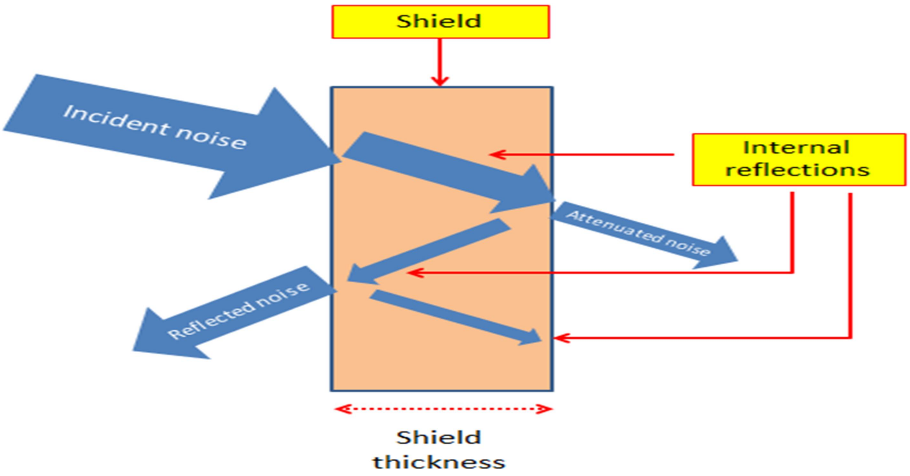

Figure 1.13. Scheme of shielding principles [105]

When electric fields are applied to the surface of an ideal conductor or simply hit to a shield material, it induces a current that causes displacement of charge inside the conductor that cancels the applied field, at which point the current stops. Electric fields will produce forces on the charge carriers within the conductor [105, 106].

EMI Shielding puts impedance discontinuity to the path of a propagating radiated EM wave, either reflecting it or absorbing it. When an incident noise hit a shield, some portion of it will be reflected, absorbed and pass through with an attenuated magnitude. In a good shield, a weak noise wave can pass through. Below illustrates the scenario. The effectiveness of a shield depends on the three factors; reflections, absorption and multiple reflections. Reflection means an instant reflection of incident wave when hit a shield surface. Multiple reflections include internal reflections and re-reflections of waves or noise [105-108] and can be expressed as:

$$\mathrm{SE}_{\mathrm{T}}\,(\mathrm{dB}) = 10\log_{10}(P_{\mathrm{T}}/P_{\mathrm{I}}) \quad (1)$$

$$= 20\log_{10}(\mathrm{ET}/E_{\mathrm{I}}) \quad (2)$$

$$= \log_{10}(H_{\mathrm{T}}/20H_{\mathrm{I}}) \quad (3)$$

Where; P_I (E_I or H_I) and P_T (E_T or H_T) are the power (electric or magnetic field intensity) of incident and transmitted EM waves, respectively. The scattering parameters S_{11} (S_{22}) and S_{12} (S_{21}) of VNA are related to reflectance (R) and transmittance (T) respectively, i.e., $T = |E_T/E_I|^2 = |S_{12}|^2$ $(=|S_{12}|^2)$, $R = |E_R/E_I|^2 = |S_{11}|^2$ $(=|S_{22}|^2)$. Once, the values of R and T are known, absorbance (A) can be calculated as $A = (1 - R - T)$. Further, the relative intensity of the EM wave inside the shield (after primary reflection from the face of incidence) is based on the quantity $(1 - R)$, and effective absorbance (A_{eff}) can be described as $A_{eff} = (1 - R - T)/(1 - R)$. From the foregoing, attenuations owing to reflection (SE_R) and absorption (SE_A) can appropriately be stated as:

$$\mathrm{SE}_{\mathrm{R}} = 10\log_{10}(1 - \mathrm{R}) \quad (4)$$

$$\mathrm{SE}_{\mathrm{A}} = 10\log(1 - \mathrm{Aeff}) = 10\log_{10}[T/(1- R)] \quad (5)$$ [105-108]

The below equation can be used to mathematically define shielding effectiveness.

$$\mathrm{SE}_{\mathrm{dB}} = \mathrm{R}_{\mathrm{dB}} + \mathrm{A}_{\mathrm{dB}} + \mathrm{M}_{\mathrm{dB}}$$

Where;

SEdB – Shielding effectiveness

RdB – Reflection loss

AdB – Absorption loss

MdB – Multiple reflections

In far field, reflection loss is the predominant shielding mechanism at the lower frequencies while at higher frequencies absorption loss is dominant. For near field electrical sources, reflection loss is the predominant at the lower frequencies while absorption loss is predominant at higher frequencies. For near field magnetic sources, absorption loss is the predominant mechanism at all frequencies [105].

The electrical conductivity of a shielding material is not a specific scientific criteria for shielding since conduction only requires connectivity in its path [89]. Metals are therefore the most common materials for EMI shielding and they function mainly by reflection due to the free electrons in them. The metal sheets are bulky, so metal coating made by electroplating, electroless plating and vacuum deposition are commonly used for shielding [88, 108]. But it suffers from poor wear or scratch resistance. However, absorption of shield material depends on the electric or magnetic dipoles, which interact with electromagnetic field of the radiation. Carbon-based polymer composites are attractive compared to conventional metal and polymer based EMI shielding materials due to their light weight, corrosion resistance, flexibility, and processing advantages. Therefore, research efforts in the past two decades have been on exploring conducting polymer materials as alternative shielding materials [90-111].

The uses of conducting polymers as microwave absorbers and electromagnetic interference shielding materials have attracted increased attention due to their good electrical conductivity and processability especially when combined with nanocomponents like CNT to enhance the shielding performance [25, 41, 49]. Among the conducting polymers, polyaniline (PANI) and polyaniline based materials have been studied most extensively because of their easier and inexpensive preparation methods, good environmental stability in both doped and undoped forms, excellent physical and chemical properties and high conductivity at microwave frequencies [3-5, 112]. The disadvantage of using conducting polymers such as PANI or PANI-CNTs composites alone is its processability, which can be overcome by preparing blends with polymers [25, 41]. Ionomers are polymers which possess unique properties including electrical conductivity and high melt viscosity [6, 12]. The ionic interactions in ionomers controls the properties of the polymers such as elastic modulus, glass transition temperature, viscosity, melt strength, fatigue resistance, processability and transport properties [13-17, 113]. These characteristics makes the ionomer based on poly(ethylene-co-methacrylic acid) a potential host matrix for the development of conducting polymer systems. There are several studies in literature concerning blends of polymers with conducting polymers such as polyaniline and MWCNTs [16, 17, 82, 114-130].

In this study, we have prepared blends of zinc or sodium salt of poly(ethylene-co-methacrylic acid ionomer (EMAAZn or EMAANa) with polyaniline (PANI) and polyaniline-MWCNT for EMI shielding applications. PANI doped with HCl and TSA under different synthesis conditions to tailor the particle size in both bulk and nano dimensions and were synthesized and characterised. PANI-MWCNT composites were prepared by insitu polymerization of aniline monomer in the presence of multi-walled carbon nanotubes (MWCNT). Composites of EMAA-PANI and EMAA-PANI-MWCNT were prepared by solution mixing in solvent blends (toluene-1 butanol) at 65°C. The electrical properties and EMI shielding effectiveness characteristics of the conducting blends were evaluated.

1.7 Scope and Objectives of the Work

Conducting polyaniline (PANI) possess electrical properties like that of metals and the characteristics of organic polymers such as lightweight, lower cost, resistance to corrosion and chemical attack, flexibility and greater workability. These unique characteristics have led to its wide usage in electrical/electronic devices and a myriad of applications. However, unsolved issues, still remain concerning good conductivity with good mechanical and thermal properties which have limited the full utilizations of these unique characteristic properties it possess in the ever growing areas of applications due to material inconsistencies, insolubility in many organic solvents, inherent brittleness, poor mechanical and thermal properties, poor processability and low conductivity. If combined with CNTs to form composites, these limitations could be overcomed since CNTs possess some impressive and interesting structural, mechanical, electrical and electronic, optical, thermal and chemical characteristics, which is attributed to their small size and mass, their strong mechanical potency, their high electrical and thermal conductivity/stability. Carbon nanotubes is utilized to form electronically conductive nanocomposites. The aim with carbon nanotube composites is to form a stable dispersion of individual carbon nanotubes in the PANI matrices with improved electrical and mechanical properties by using in-situ polymerization techniques. Still, these composites are limited using them alone in terms of processability, which can be overcome by preparing blends with polymers such as thermoplastics, thermosets, elastomers, etc. to significantly balance electrical properties, mechanical properties, thermal characteristics, processability, etc. Ionomers are polymers which possess unique properties including electrical conductivity and high melt viscosity, elastic modulus, glass transition temperature, fatigue resistance, processability and transport properties. These characteristics makes the ionomer based on poly(ethylene-co-methacrylic acid) a potential host matrix for the development of conducting polymer systems. However, despite its uniqueness as a class of polymeric materials that comprise repeat units of both electrically neutral units and a fraction of ionized units; yet, it has a low and poor conductivity which is dependent on water absorption resulting in electrical applications restricted to below 100°C operating temperatures, poor durability of wet films and poor mechanical and chemical stability at elevated temperatures. Based on the drawbacks of both ionomers, conducting PANI and CNTs highlighted above, proper enhancement of properties will be possible if the synthesis of conducting PANI is performed in the presence of ionomers and CNTs with the appropriate groups that are able to interact with the conducting polymer, hence the enhancement of the thermal stability, electrical conductivity and its processability.

The aim of the thesis is to formulate a effective preparative route by which composite blends with high conductivity and processability could be obtained via chemical oxidative polymerization of aniline, insitu chemical oxidative polymerization of aniline in carbon nanotube and solution mixing PANI or PANI-CNTs with ionomers of poly(ethylene-co-methacrylic acid) neutralized with sodium salt [P(E-MAA-Na)] or poly(ethylene-co-methacrylic acid) neutralized with zinc salt [P(E-MAA-Zn)] using a blend of polar and non-polar solvents at 65°C to improve the processability of electrically conducting PANI and PANI-CNTs composites to facilitate their effective utilization as EMI shielding materials. The emphasis is in solution processing as it is a more economical way to achieve good homogeneity and rapid mixing of the component materials without large energy consumption of blends.

The objectives of this work are-

- To synthesize and characterize bulk and nano PANI with different acid dopants by adopting a novel technique.
- To prepare and characterize PANI-MWCNTs hybrid core-shell nanocomposites through insitu chemical oxidative polymerization process to achieve high and stable electrical conductivity.
- To develop, prepare and characterize binary blends of PANI-ionomer blends of poly(ethylene-co-methacrylic acid) neutralized with sodium salt [P(E-MAA-Na)] or poly(ethylene-co-methacrylic acid) neutralized with zinc salt [P(E-MAA-Zn)].
- To develop, prepare and characterize ternary blends of PANI-MWCNTs-ionomer blends of poly(ethylene-co-methacrylic acid) neutralized with sodium salt [P(E-MAA-Na)] or poly(ethylene-co-methacrylic acid) neutralized with zinc salt [P(E-MAA-Zn)].
- To evaluate the binary and ternary blends for utility and EMI shielding applications.

Reference

[1] Shirakawa H, Lewis EJ, MacDiarmid AG, Chiang CK and Heeger AJ, 1977. Synthesis of electrically conducting organic polymers: halogen derivatives of polyacetylene, (CH)x. J Chem Society, Chem Communications, 16 578-580.

[2] Inzelt G, 2002. Conducting Polymers: A New Era in Electrochemistry, Springer-Verlag Berlin Heidelberg, Monographs in Electrochemistry book series, p123-148.

[3] Ameen S, Akhtar SM, Song M and Shin HS, 2013. Solar cells - research and application perspectives. In Arturo Morales-Acevedo (Eds) Metal oxide nanomaterials, conducting polymers and their nanocomposites for solar energy. InTech, p203-259.

[4] Palaniappan S and John A, 2008. Polyaniline materials by emulsion polymerization pathway. Prog Polym Sci, 33 732-758.

[5] Bakhishi AK and Bhalla G, 2004. Electrically conducting polymers: Materials of the twenty-first century. J Sci and Ind Res, 63 715-728.

[6] Subrahmanyam AR, Geetha V, Kumar A, Alakanandana A and Siva KJ, 2012. Mechanical and electrical conductivity studies of PANI-PVA and PANI-PEO blends. Int J Mater Sci, 2 (1) 27-30.

[7] Saifuddin N, Raziah AZ and Junizah AR, 2013. Carbon nanotubes: A review on structure and their interaction with proteins. J Chem, 2013 1-18, doi.org/10.1155/2013/676815.

[8] Varshney K, 2014. Carbon nanotubes: A review on synthesis, properties and applications. Int J Eng Res General Sci, 2 (4) 660-677.

[9] He H, Pham-Huy LA, Dramou P, Xiao D, Zuo P and Pham-Huy C, 2013. Carbon nanotubes: applications in pharmacy and medicine. Biomed Res Int, 2013, 1-12, doi.org/10.1155/2013/578290.

[10] Iijima S, 1991. Helical microtubules of graphitic carbon. Nature, 354 (6348) 56-58.

[11] Dresselhaus MS, Dresselhaus G and Avouris PH, 2001. Carbon nanotubes: Synthesis, structure, properties and applications. Springer-Verlag, Berlin Heidelberg, Germany, Topics Appl Phys Book Series, 80 p1-9.

[12] Mathias LJ, 2018. Available: www.pslc.ws/macrog/Polymer Science Learning Center/ionomer. Accessed 2 June 2018.

[13] Tant M and Wilkes GL, 1987. Viscoelastic behaviour of ionomers in bulk and solution, in structure and properties of ionomers, Pineri M and Eisenberg A(Eds), Reidel, Dordrecht, NATO ASI Series, p191-226.

[14] Schlick S, 1996. Ionomers: characterization, theory and applications. Boca Raton, Florida: CRC Press LLC.

[15] Eisenberg A and Joon-Kim J-S, 1998. Introduction to ionomers. Wiley Interscience, New York, p327.

[16] Castillo-Ortega MM, Encinas JC, Rodriguez DE, Olayo R, 2001. Preparation and characterization of electroconductive polypyrrole–thermoplastic composites. J Appl Polym Sci, 81 1498-1506.

[17] Castillo-Ortega MM, Rodriguez DE, Encinas JC, Plascencia M, Mendez-Velarde FA, Olayo R, 2002. Conductometric uric acid and urea biosensor prepared from electroconductive polyaniline-poly (n-butylmethacrylate) composites. Sens Actuat B 85 19-25.

[18] Castillo-Ortega MM, Del Castillo-Castro T, Encinas JC, Perez-Tello M, De Paoli M-A and Olayo R, 2003. Electrically conducting polyaniline-PBMA composite films obtained by extrusion. Appl Polym Sci, 89 179-183.

[19] Nandi A, Gupta DG and Banthia AK, 2002. Sulfonated polybutadiene random ionomer as a stabilizer for colloidal copper nanoparticles. Colloids and Surfaces A: Physicochemical and Eng Aspects, 197 119-124.

[20] Sata T, 2004. Ion exchange membrane, preparation, characterization, modification and application. SC, 1-307, doi: 10.1039/9781847551177-FX001.

[21] Capek I, 2005. Nature and properties of ionomer assemblies II. Adv Colloid Interface Sci, 118 73-112.

[22] Samuel J, Xavier T and Kurian T, 2000. Ionomers. Prog Rubber Plast Technol, 16 (1) 1-15.

[23] Reynolds PJ, 2012. A Surlyn® Ionomer as a self-healing and self-sensing composite. MRes Thesis, Department of Metallurgy and Materials, University of Birmingham, UK.

[24] Eisenberg A, Hird B and More RB, 1989. A new multiplet-cluster model for the morphology of random ionomers. Macromol, 23 (18) 4098-4107.

[25] Bhadra S, Khastgir D, Singha NK and Lee JH, 2009. Progress in preparation, processing and applications of polyaniline. Prog Polym Sci, 34 (8) 783-810.

[26] Chen C-H, Mao C-F, Su S-F and Fahn Y-Y, 2007. Preparation and characterization of conductive poly (vinyl alcohol)/polyaniline doped by dodecyl benzene sulfonic acid (PVA/PANDB) blend films. J Appl Polym Sci, 103 3415-3422.

[27] Francis KMG, Subramanian S, Shunmugavel K, Naranappa V, Pandian SSM and Nadar SC, 2016. Lithium Ion-conducting blend polymer electrolyte based on PVA–PAN doped with lithium nitrate. Polym-Plast Technol Eng, 55 (1) 25-35.

[28] Pinnau I and Freeman BD, 2000. Membrane formation and modification. ACS Symposium Series, Oxford University Press, p376.

[29] Green DW and Perry RH, 2007. Perry's Chemical Engineers' Handbook. 8th edition, McGraw-Hill Education, New York, United States, p2400.

[30] ZemanLJ and Zydney AL, 1996. Microfiltration and ultrafiltration, principles and applications. Marcel Dekker, Inc., New York, United States, p618.

[31] Plazaneta M, Sacchetti F, Petrillo C, Deme B, BartoliniP and Torred R, 2014. Water in a polymeric electrolyte membrane: sorption/ desorption and freezing phenomena. J Membrane Sci, 453 419-424.

[32] Wang D, 2014. Ionomer morphology, solution to film thermodynamics, molecule transport, physical properties, and water desalination via electrodialysis. Doctorial Theses and Dissertation, University of Connecticut Graduate School.

[33] Hensley JE and Way JD, 2007. Synthesis and characterization of perfluorinated carboxylate/ sulfonate ionomer membranes for separation and solid electrolyte applications. Amer Chem Society, Chem Mater, 19 4576-4584.

[34] Eikerling M, Kornyshev AA and Stimming UJ, 1997. Electrophysical properties of polymer electrolyte membranes: a random network model. Phys Chem B, 101 (50) 10807-10820.

[35] Yang Y, Siu A, Peckham TJ and Holdcroft S, 2008. In Fuel Cells I, Structural and morphological features of acid-bearing polymers for PEM fuel cells. Adv Polym Sci, 215 (1) 55-126.

[36] Wu X, Wang X, He G and Benziger J, 2011. Differences in water sorption and proton conductivity between Nafion and SPEEK. J Polym Sci Part B: Polym Phys, 49 1437-1445.

[37] Teocoli F, Paolone A, Palumbo O, Navarra MA, Casciola M and Donnadio A, 2012. Effects of water freezing on the mechanical properties of Nafion membranes. J Polym Sci Part B: Polym Phys, 50 1421-1425.

[38] Swier S, Shaw MT and Weiss RA, 2004. Design of polymer blend for proton exchange membranes in fuel cells. Amer Chem Soc, Fuel Chem, 49 (2) 532-533.

[39] Zhang H and Shen PK, 2012. Recent development of polymer electrolyte membranes for fuel cells. Amer Chem Soc, Chem Rev, 112 2780-2832.

[40] Yongfang Li, 2015. Organic optoelectronic materials, Yongfang Li (ed.), Springer International Publishing Switzerland, Lecture Notes in Chemistry 91 p23-50.

[41] Das TK and Prusty S, 2012. Review on conducting polymers and their applications. Polym-Plast Technol Eng, 51 (14) 1487-1500.

[42] https://en.wikipedia.org/wiki/File:Polyaniline_structure.svg. Accessed 7th November 2017.

[43] Gerard M, Chaubey A and Malhotra BD, 2002. Review application of conducting polymers to biosensors. Biosensors Bioelectronics, 17 345-359.

[44] Kumar D and Sharma RC, Advances in Conductive Polymers. Eur Polym J, 34 (8) 1053-1060.

[45] Ciric-Marjanovic G, 2013. Recent advances in polyaniline research: Polymerization mechanisms, structural aspects, properties and applications. Synth Metals 177 1– 4.

[46] Jangid NK, Chauhan NPS, Meghwal K, Ameta R and Punjabi PB, 2014. A review: conducting polymers and their applications. Res J Pharm, Bio Chem Sci, 5 (3) 383-412.

[47] Bai H and Shi G, 2007. Gas sensors based on conducting polymers. Sensors, 7 267-307.

[48] Fogel R and Limson J, 2016. Developing biosensors in developing countries: South Africa as a case study. Biosensors, 6 (5) 1-17.

[49] Thomassin J-M, Jerome C, Pardoen T, Bailly C, Huynen I and Detrembleur C, 2013. Polymer/carbon based composites as electromagnetic interference (EMI) shielding materials. Mater Sci and Eng R: Reports, 74 (7) 211-232.

[50] Gupta N, Sharma S, Mir IA and Kumar D, 2006. Advances in sensors based on conducting polymers. J Sci Ind Res, 65 549-557.

[51] https://en.wikipedia.org/wiki/Brain–computer_interface. Accessed 7th November 2017.

[52] https://www.kaspersky.com/blog/direct-neural-interfaces/8560. Accessed 7thNovember 2017.

[53] https://en.wikipedia.org/wiki/Actuator. Accessed 7thNovember 2017.

[54] https://www.thomasnet.com/articles/pumps-valves-accessories/types-of - actuators. Accessed 7thNovember 2017.

[55] Chavan R, Desai U, Mhatre P and Chinchole R, 2012. A review: Carbon nanotubes. Int J Pharm Sci Review Res, 13 (1) 125-134.

[56] Mahajan D, 2017. Carbon nanotubes: A review on synthesis, electrical and mechanical properties and applications. Asian J Appl Sci Technol, 1 (7) 15-20.

[57] Kuzmany H, Kukovecz A, Simona F, Holzweber M, Kramberger C and Pichler T, 2004. Functionalization of carbon nanotubes. Synth Metals, 141 113-122.

[58] Kroto HW, Heath JR, O'Brien SC, Curl RF, and Smalley RE, 1985. C60: Buckminsterfullerene. Nature, 318 (6042) 162–163.

[59] Hirlekar R, Yamagar M, Garse H, Vij M and Kadam V, 2009. Carbon nanotubes and its applications: A review. Asian J Pharm Clinical Res, 2 (4) 17-27.

[60] https://www.nanoshel.com/applications-and-benefits-of-multi-walledcarbon/Nanoshel LLC News on April 9, 2016, by Abhishek. Accessed 7thNovember 2017.

[61] http://en.wikipedia.org/www/Carbon%nanotube. Accessed 7th November 2017

[62] Odom TW, Huang J-L, Kim P and Lieber CM, 2000. Structure and electronic properties of carbon nanotubes. J Phys Chem B, 104 2794-2809.

[63] Ganesh EN, 2013. Single-walled and multi-walled carbon nanotube structure, synthesis and applications. Int J Innov Technol Exploring Eng, 2 (4) 311-320.

[64] Odom TW, Huang J-L, Kim P and Lieber CM, 1998. Atomic structure and electronic properties of single-walled carbon nanotubes. Nature, 391 62-64.

[65] Mamedov AA, Kotov NA, Prato M, Guldi DM, Wicksted JP and Hirsch A, 2002. Molecular design of strong single-wall carbon nanotube/ polyelectrolyte multilayer composites. Nature Mater, 1 190-194.

[66] Rafique MMA and Iqbal J, 2011. Production of carbon nanotubes by different routes-A review. J EncapsAdsorp Sci, 1 29-34.

[67] Che G, Lakshmi BB, C. R. Martin CR and Fisher ER, 1998. Chemical vapour deposition based on synthesis of carbon nanotubes and nanofibers using a template method. Chem Mater, 10 260-267.

[68] Applications and Benefits of Multi-Walled Carbon Nanotubes (MWCNTs). http://www.cefic.org/Documents/Other/Benefits%20of%20Carbon%20Nanotubes.pdf. Accessed 7thNovember 2017, 1-6.

[69] Gogotsi Y, Naguib N and Libera JA, 2002. In situ chemical experiments in carbon nanotubes. Chem Phys Letters, 365 354–360.

[70] Gazotti Jr WA, Casalbore-Miceli G, Mitzakoff S, Geri A, Gallazzi MC and De Paoli MA, 1999. Conductive polymer blends as electrochromic materials. Electrochimica Acta 44 1965-1971.

[71] Olabisi O and Adewale K, 2015. Handbook of thermoplastics. 2nd Edition, CRC Press,doi: 10.1201/b19190-1.

[72] Parameswaranpillai J, Thomas S and Grohens Y, 2015. Polymer Blends: State of the art, new challenges and opportunities. Wiley-VCH Verlag GmbH & Co. KGaA, 1-5, doi.org/10.1002/9783527645602.ch01

[73] Rahate AS, Nemade KR and Waghuley SA, 2012. Polyphenylene sulfide (PPS): state of the art and applications. Reviews Chem Eng, 29 (6) 471-489.

[74] Kaur G, Adhikari R, Cass P, Bown M and Gunatillake P, 2015. Electrically conductive polymers and composites for biomedical applications. RSC Adv, 5 37553-37567.

[75] Paul R and Pillai CKS, 2002. Melt/solution processable conducting polyaniline: Elastomeric blends with EVA. J Appl Polym Sci, 84 1438-1447.

[76] Vicentini DS, Barra GMO, Bertolino JR and Pires ATN, 2007. Polyaniline/thermoplastic polyurethane blends: Preparation and evaluation of electrical conductivity. Euro Polym J, 43 4565-4572.

[77] Ercan N, DurmusA and Kasgoz A, 2015. Comparing of melt blending and solution mixing methods on the physical properties of thermoplastic polyurethane/organoclay nanocomposite. J Thermoplast Comp Mater 30 (7) 950-970.

[78] Del Castillo-Castro T, Castillo-Ortega MM, Villarreal I, Brown F, Grijalva H, Perez-Tello M, Nun˜o-Donlucas SM and Puig JE, 2007. Synthesis and characterization of composites of DBSA-doped polyaniline and polystyrene-based ionomers. Composites: Part A, Appl Sci Manufacturing, 38 639-645.

[79] Li Y-F, Wang Y-P, Gao X-H and Gao J-M, 2006. Composites of polystyrene sulfonic acid (PSSA)-polyaniline and montmorillonite clay: Synthesis and characterization. J Macromol Sci, Part A, 43 (2) 405-415.

[80] Kunteppa H, Parveen A, Kumar HGH and Roy AS, 2013. AC conductivity and battery application of polyethylene oxide/PANI/sodium chlorate composites. Adv Mater Letters, 4 (11) 856-861.

[81] Chen C-H, LaRue JC, Nelson RD, Kulinsky L and Madou MJ, 2012. Electrical Conductivity of polymer blends of poly (3, 4-ethylenedioxythiophene): Poly (styrenesulfonate): N-Methyl-2-pyrrolidinone and polyvinyl alcohol. J Appl Polym Sci, 125 (4) 3143–3141.

[82] Dharaiya DP and Jana SC, 2006. Production of electrically conductive networks in immiscible polymer blends by chaotic mixing. Polym Eng Sci, 46 (1) 19-28.

[83] Taghipour Z, Eisazadeh H and Tanzifi M, 2014. Modification of polyaniline/polystyrene and polyaniline/metal oxide structure by surfactant. Int J Eng Transactions B: Applications, 27 (2) 227-238.

[84] Xie H-Q, Pu Q-L and Xie D, 2004. Preparation of conductive polyaniline-sulfonated epdm ionomer composites from in situ emulsion polymerization and study of their properties. J Appl Polym Sci, 93 2211-2217.

[85] Wang Y, Xie H, Cai Y and Guo J, 1997. Synthesis and properties of polyaniline/sodium and zinc ionomer composites. Polym J, 29 875-880.

[86] Eisazadeh H and Kavian A, 2009. Copolymerization of aniline and styrene using various surfactants in aqueous media. Polym Comp, 30 (1) 43-48.

[87] Terlemezyan L, Mihailov M, and Ivanova B, 1992. Electrically conductive polymer blends comprising polyaniline. Polym Bull, 29 283-287.

[88] Singh A, Jaiswar GL and Dhakarey R, 2010. Conducting polymer of aniline blended by polymethylmethaacrylate metal containing polymer: Insitu blending and characterizations. J Chem Pharm Res, 2 (3) 647-655.

[89] Li X, Chen D, Xu D, Zhao C, Wang Z, Lu H and Na H, 2006. SPEEKK/polyaniline (PANI) composite membranes for direct methanol fuel cell usages. J Membrane Sci 275 134-140.

[90] De Souza Jr FG and Soares BG, 2006. Methodology for determination of Pani.DBSA content in conductive blends by using UV-Vis spectrometry. Polym Testing 25 512–517.

[91] Nandanwar DV, Modak P, Kondawar SB, Dhakate SR and Dudhe CM, 2014. Electromagnetic interference shielding of multi-walled carbon nanotubes/polyaniline nanocomposites. Int J Res Biosci Agric Technol, 2 (1) 918-926.

[92] John H, Thomas RM, Jacob J, Mathew KT and Joseph R, 2007. Conducting polyaniline composites as microwave absorbers. Polym Comp, 28 (5) 588-592.

[93] Geetha S, Kumar SKK, Rao CRK, Vijayan M and Trivedi DC, 2009. EMI shielding: Methods and materials-A review.J Appl Polym Sci, 112 (4) 2073-2086.

[94] Faez R, Martin IM, De Paoli M-A, Rezende MC, 2001. Microwave properties of EPDM/PANI-DBSA blends.Synth Metals, 119 (1) 435-436.

[95] Saini P and Arora M, 2012. Microwave absorption and EMI shielding behavior of nanocomposites based on intrinsically conducting polymers, graphene and carbon nanotubes, in Newpolymers for special applications, De Souza Gomes A, (Ed.), InTech p73-112.

[96] Ott HW, 2009. Electromagnetic Compatibility Engineering, John Wiley &Sons, Hoboken, NJ, USA, p3-4.

[97] Saini P, Choudhary V, Singh BP, Mathur RB and Dhawan SK, 2011. Enhanced microwave absorption behavior of polyaniline-CNT/ polystyrene blend in 12.4-18.0 GHz range. Synth Metals, 161(15-16) 1522-1526.

[98] ColaneriNF and Shacklette LW, 1992. EMI shielding measurements of conductive polymer blends. IEEE Transactions Instrum Measur, 41 (2) 291-297.

[99] Chung DDL, 2000. Materials for electromagnetic interference shielding. J Mater Eng Performance, 9 (3) 350-354.

[100] Saini P and Choudhary V, 2013. Enhanced electromagnetic interference shielding effectiveness of polyaniline functionalized carbon nanotubes filled polystyrene. J Nanopart Res, 15 1-7.

[101] Wu J and Chung DDL, 2002. Increasing the electromagnetic interference shielding effectiveness of carbon fiber polymer-matrix composite by using activated carbon fibers. Carbon, 40 (3) 445-447.

[102] Yang Y, Gupta MC, Dudley KL, and Lawrence RW, 2005. Novel carbon nanotube-polystyrene foam composites for electromagnetic interference shielding. Nano Letters, 5 (11) 2131-2134.

[103] Shacklette LW, Colaneri NF, Kulkarni VG and Wessling B, 1992. EMI Shielding of intrinsically conductive polymers. J Vinyl Additive Technol, 14 (2) 118-122.

[104] Yang Y, Gupta MC, Dudley KL and Lawrence RW, 2005. A comparative study of EMI shielding properties of carbon nanofiber and multi-walled carbon nanotube filled polymer composites. J Nanosci Nanotechnol, 5 (6) 927-931.

[105] Electronicsbelieverhttp://electronicsbeliever.com/emi-shielding-techniques/March 21, 2017. Accessed on 23rd of August, 2018.

[106] https://en.wikipedia.org/wiki/Electromagnetic_interference. Accessed on 23rd of August, 2018.

[107] Saini P, Choudhary V and Dhawan SK, 2012. Improved microwave absorption and electrostatic charge dissipation efficiencies of conducting polymer grafted fabrics prepared via in situ polymerization. Polym Adv Technol, 23 343-349.

[108] Saini P, Choudhary V, Vijayan N and Kotnala RK, 2012. Improved electromagnetic interference shielding response of poly (aniline)-coated fabrics containing dielectric and magnetic nanoparticles. J Phys Chem C, 116 13403-13412.

[109] Khan S, Arora M, Wahab MA and Saini P, 2014. Permittivity and electromagnetic interference shielding investigations of activated charcoal loaded acrylic coating compositions. J Polym, 2014 1-7.

[110] Gupta TK, Singh BP, Mathura RB and Dhakate SR, 2014. Multi-walled carbon nanotube-graphene-polyaniline multiphase nanocomposite with superior electromagnetic shielding effectiveness. Nanoscale, 6 842-851.

[111] Basuli U, Chattopadhyay S, Nah C and Chaki TK, 2012. Electrical properties and electromagnetic interference shielding effectiveness of multiwalled carbon nanotubes-reinforced EMA nanocomposites. Polym Comp, 33 (6) 897-903.

[112] Yanmin Wang, (2014). Microwave absorbing materials based on polyaniline composites: A review. Int J Mater Res, 105 (1) 3-12.

[113] Yong Li, Changxin Chen, Song Zhang, Yuwei Ni and Jie Huang, 2008. Electrical conductivity and electromagnetic interference shielding characteristics of multiwalled carbon nanotube filled polyacrylate composite films. Applied Surface Science, 254 (18) 5766-5771. DOI: 10.1016/j.apsusc.2008.03.077.

[114] Li YL, Li MJ, Pang ML, Feng SY, Zhang J and Zhang CQ, (2015). Effects of multi-walled carbon nanotube structures on the electrical and mechanical properties of silicone rubber filled with multi-walled carbon nanotubes. J Mater Chem C, 3 5573-5579.

[115] Wang HB, Teng KY, Chen C, Li XJ, Xu ZW, Chen L, F HJ, Kuang LY, Ma MJ and Zhao LH, 2017. Conductivity and electromagnetic interference shielding of graphene-based architectures using MWCNTs as free radical scavenger in gamma-irradiation. Mater Lett, 186 78-81.

[116] Wang R, Yang H, Wang JL and Li FX, 2014. The electromagnetic interference shielding of silicone rubber filled with nickel coated carbon fiber. Polym Test, 38 53-56.

[117] Zeng ZH, Jin H, Chen MJ, Li WW, Zhou LC and Zhang Z, 2016. Lightweight and anisotropic porous MWCNT/WPU composites for ultrahigh performance electromagnetic interference shielding. Adv Funct Mater, 26 303-310.

[118] Wang GL, Zhao GQ, Wang S, Zhang L and Park CB, 2018. Injection-molded microcellular PLA/graphite nanocomposites with dramatically enhanced mechanical and electrical properties for ultra-efficient EMI shielding applications. J Mater Chem C, 6 6847-6859.

[119] Jin L, Zhao XM, Xu JF, Luo YY, Chen DQ and Chen GH, 2018. The synergistic effect of a graphene nanoplate/Fe_3O_4@$BaTiO_3$ hybrid and MWCNTs on enhancing broadband electromagnetic interference shielding performance. RSC Adv, 8 2065.

[120] Poothanari, M.A.; Abraham, J.; Kalarikkal, N.; Thomas, S. Excellent electromagnetic interference shielding and high electrical conductivity of compatibilized polycarbonate/polypropylene carbon nanotube blend nanocomposites. Ind Eng Chem Res, 57 4287-4297.

[121] Abraham J, Arif MP, Kailas L, Kalarikkal N, George SC and Thomas S, 2016. Developing highly conducting and mechanically durable styrene butadiene rubber composites with tailored microstructural properties by a green approach using ionic liquid modified MWCNTs. RSC Adv, 6 32493.

[122] Wang P, Xu P, Zhou YY, Yang YW and Ding YS, 2018. Effect of MWCNTs and P[MMA-IL] on the crystallization and dielectric behavior of PVDF composites. Eur Polym J, 99 58-64.

[123] Al-Saleh MH, 2015. Influence of conductive network structure on the EMI shielding and electrical percolation of carbon nanotube/polymer nanocomposites. Synth Met, 205 78-84.

[124] Ajitha AR, Mohammed AP, Aswathi MK, Lovely PM, Geethamma VG, Nandakumar Kalarikkal, Sabu Thomas and Tatiana Volova, (2018). An effective EMI shielding material based on poly(trimethylene terephthalate) blend nanocomposites with multiwalled carbon nanotubes. New J Chem, 42 13915-13926. DOI: 10.1039/C8NJ02410C.

[125] Yang H, Yu Z, Wu P, Zou H and Liu P, 2018. Electromagnetic interference shielding effectiveness of microcellular polyimide/insitu thermally reduced graphene oxide/carbon nanotubes nanocomposites. Appl Surf Sci, 434 318-325.

[126] Duan H, Zhao M, Yang Y, Zhao G and Liu Y, 2018. Flexible and conductive PP/EPDM/Ni coated glass fiber composite for efficient electromagnetic interference shielding. J Mater Sci: Mater Electron, 29 10329-10336. Doi:10.1007/s10854-018-9089-x.

[127] Na R, Liu J, Wang G and Zhang S, 2018. Light weight and flexible poly(ether ether ketone) based composite film with excellent thermal stability and mechanical properties for wideband electromagnetic interference shielding. RSC Adv, 8 3296-3303. Doi:10.1039/C7RA11675F.

[128] Zhang K, Li GH, Feng LM, Wang N, Guo J, Sun K, Yu KX, Zeng JB, Li T, Guo Z and Wang M, 2017. Ultralow percolation threshold and enhanced electromagnetic interference shielding in poly(l-lactide)/multi-walled carbon nanotube nanocomposites with electrically conductive segregated networks. J Mater Chem C, 5 9359-9369. Doi:10.1039/C7TC02948A.

[129] Bhawal P, Ganguly S, Das Tushar K, Mondal S and Das NC, 2018. Mechanically robust conductive carbon clusters confined ethylene methyl acrylate-based flexible composites for superior shielding effectiveness. Polym Adv Technol, 29 95-110. Doi:10.1002/pat.4092.

[130] Ajekwene KK, Johny JE and Kurian T, 2018. Sodium salt of polyethylene-co-methacrylic acid ionomer/polyaniline binary blends for EMI shielding applications. PIER C, 88 207-218. doi:10.2528/PIERC18093003.

…..ഌ൯…..

Chapter 2

EXPERIMENTAL

Contents

In this chapter, the materials used and the experimental techniques adopted are outlined and described. The various characterizations and tests performed to investigate the prepared samples (PANI, PANI-MWCNTs and the composites (PANI/ionomer and PANI/MWCNT/ionomer)) are also described.

2.1 Materials

Chemicals and solvents: Ammonium persulphate (APS), p-toluene sulfonic acid monohydrate (TSA) and aniline obtained from Sigma Aldrich Chemical Company were of very high purity (99.9%). Hydrochloric acid (HCl) 98%, and acetone were obtained from Spectrochem Pvt. Ltd., Mumbai, India. The aniline was distilled before use. All other materials were used without any pre-processing.

Carbon nanotubes (CNT): Ordinary non-functionalized multi-walled carbon nanotubes (pristine CNT), carboxylic acid functionalized MWCNT (CCNT) and amine functionalized MWCNT (ACNT)) were obtained from AdNano Technologies Pvt. Ltd., Bangalore, Karnataka, India.

Ionomers: The ionomers used in this study were:

a) Zinc salt of poly(ethylene-co-methacrylic acid) (HIMILAN 1702 EMAAZn) with melt flow index (190 °C/2.16 kg) of 16 g/10 min, and

b) Sodium salt of poly(ethylene-co-methacrylic acid) (HIMILAN 1555 EMAANa) with melt flow index (190°C/2.16 kg) of 10 g/10 min.

These ionomers were supplied by Mitsubishi Plastics, Inc., Japan.

2.2 Synthesis and Preparation Methods

2.2.1 Chemical oxidative polymerization

The synthesis of polyaniline (PANI) by chemical oxidation polymerization involves the use of either sulphuric or hydrochloric acid in the presence of ammonium persulphate as the oxidizing agent in the aqueous medium. The main function of the oxidant is to withdraw a proton from the aniline moleculе, without forming a strong co-ordination bond either with the intermediate /substrate or with the final product. Polymer chains proceeds by a redox process between the growing chain and aniline with addition of monomer to the chain end [1]. The high concentration of a strong oxidant, $(NH_4)_2S_2O_8$, at the initial stage of the polymerization enables the fast oxidation of oligomers and polyaniline, as well as their existence in the oxidized form. However, to avoid oxidative degradation of the polymer formed only a small quantity of oxidant is used.

PANI is usually synthesized by aniline oxidation either with a chemical oxidant (chemical route) or through electrochemistry. Chemical synthesis requires three reactants: aniline, an oxidant and an acidic medium (aqueous or organic). The most common acids used as acidic medium are fundamentally sulphuric acid (H_2SO_4) and hydrochloric acid (HCl). The recommended oxidants are mostly ammonium persulphate ($(NH_4)_2S_2O_8$), cerium sulphate ($Ce(SO_4)_2$), potassium dichromate ($K_2Cr_2O_7$), hydrogen peroxide (H_2O_2), sodium vanadate ($NaVO_3$), potassium iodate (KIO_3) and potassium ferricyanide ($K_3(Fe(CN)_6)$). Usually, the most popular synthesis is run with a 1 mol aqueous hydrochloric acid solution (pH between 0 and 2), ammonium persulfate as oxidant with an oxidant/aniline molar ratio ≤ 1.15 in order to obtain high conductivity and yield [1]. The solution temperature is within the range of 20 and 25°C (room temperature). The reaction time is usually between 9 and 48 hrs.

For the purpose of this study, ammonium persulphate (APS) as oxidant and toluene sulfonic acid monohydrate (TSA) and hydrochloric acid (HCl) were the acid dopants respectively. The experimental procedure consists of adding slowly (drop by drop) the aqueous ammonium persulfate solution to the aniline/HCl or TSA solution. The material obtained is polyemeraldine salt: polyemeraldine hydrochloride (PANI-HCl) or polyemeraldine toluene sulfonic acid (PANI-TSA), which is green in colour [1]. The process is illustrated in the figure 2.1:

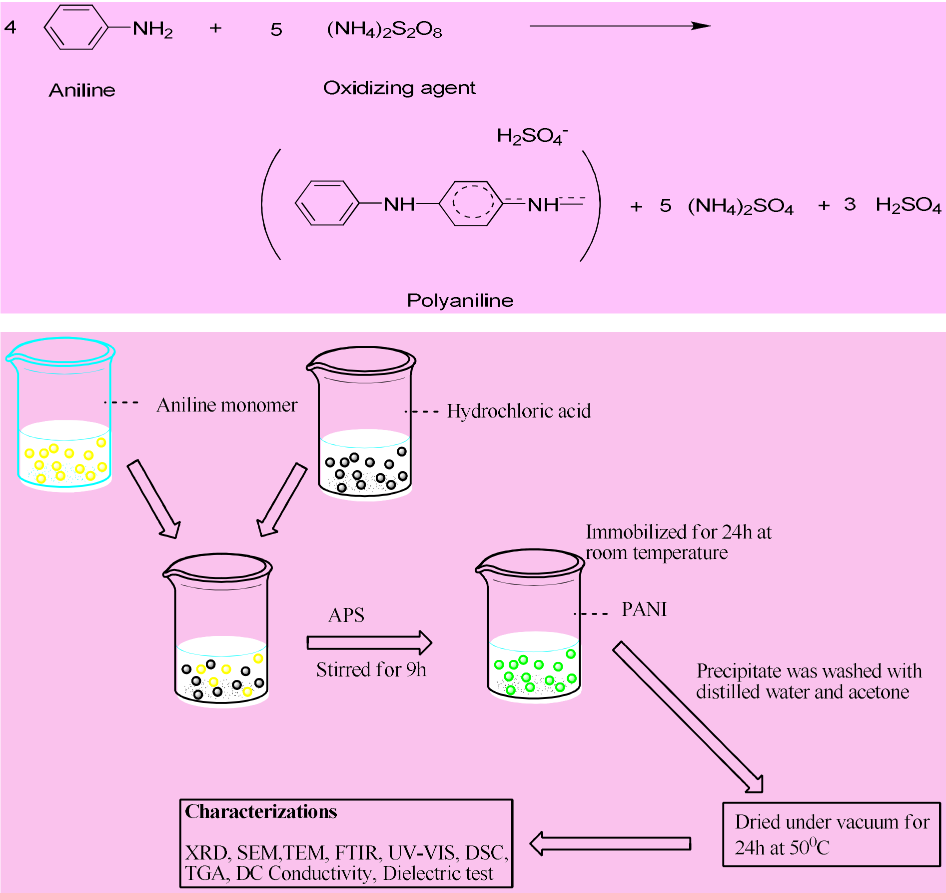

Figure 2.1. Chemical oxidative polymerization of aniline monomer

2.2.2 In-situ chemical oxidative polymerization

Several synthesis methods of polyaniline and multi walled carbon nanotube (PANI-MWCNT) nanocomposites have been reported in literature. Among these various methods, insitu polymerization is mostly used. Insitu polymerization is a chemical reaction that results in the formation of a very fine and thermodynamically stable reinforcing phase within a matrix, in which nanoparticles are dispersed in liquid monomer or precursor with relatively low-molecular weight and also in their solution, thereby allowing the formation of a homogeneous mixture. This enables grafting of polymer molecules on CNT, resulting to a better interaction and better dispersion coefficient between CNT and polymer matrix.

For this research work, the basic starting materials used are the different functionalized MWCNTs (amine and carboxylic acid functionalized), non functionalized MWCNT (Pristine MWCNT) and aniline, using ammonium persulphate (APS) as a radical initiator with TSA as the acid dopant. MWCNTs are dispersed by ultrasonication in the prepolymer, introducing MWCNT at prepolymer gives a good dispersion in the low viscosity of the prepolymer. As the polymerization progresses, there is an increase in the viscosity of the solution while the polymer grows and is wrapped around the dispersed MWCNTs. This results in a composite with enhanced electrical, mechanical and tribological properties with higher interfacial strengths, because of the interaction between the MWCNTs and growing polymer, this forms stronger MWCNTs-polymer bonds via covalent or non-covalent interactions. The temperature of the reaction is within 25°C (room temperature). The reaction time is between 9 and 24 hrs. The experimental procedure consists of aniline monomer and MWCNT in aqueous solution of the acid dopants homogenization by sonication, then adding slowly (drop by drop) the aqueous ammonium persulfate solution to the aniline/MWCNT dispersion. The material obtained is polyemeraldine-toluene sulfonic acid (PANI-TSA)-MWCNT, which is greenish-black in colour. Incorporating MWCNTs as fillers into PANI enhances the conductivity of PANI nanocomposites as the MWCNTs can have much higher electrical conductivity than PANI. The MWCNT can behave as conducting bridge between the conducting domains of PANI which results in an enhancement of the electrical conductivity of PANI. The reaction process is illustrated in Figure 2.2 bellow.

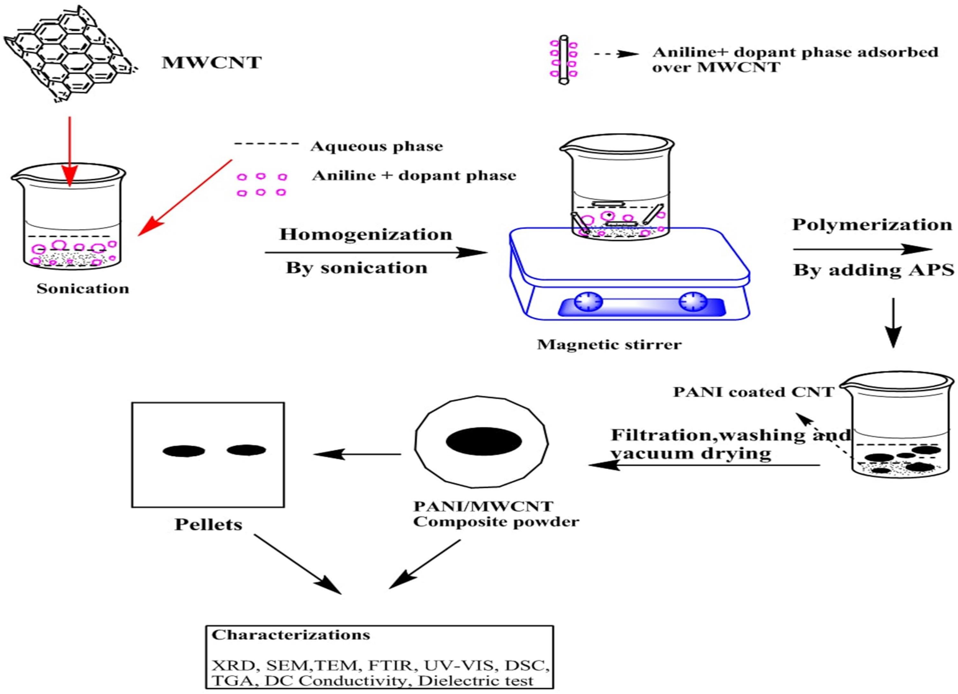

Figure 2.2. Insitu chemical oxidative polymerization of aniline monomer in MWCNTs

2.2.3 Blending

Polymer blends or mixtures represent an important class of materials, in which at least two polymers are mixed together to generate a new material with different properties. Blending may be the simplest and cheapest way to obtain polymeric materials with tailored properties because of the combination of advantageous properties of each component [2, 3].

In this study, we have used the solution blending method.

2.2.3.1 Solution blending

Solution blending is usually used for preparation of polymer blends on a laboratory scale. The components of the blend are dissolved in a common solvent and stirred intensively. The blend is separated by evaporation or precipitation of the solvent. Advantages of the process are rapid mixing of the system without large energy consumption and the potential to avoid unfavourable chemical reactions [4].

In this research work, two different solution blending were carried out, the binary solution blend and ternary solution blend. The binary solution blend was done with ionomers Poly(ethylene-co-methacrylic acid) partially ionized with zinc or sodium salts and PANI, while the ternary blend was done with PANI, MWCNT and ionomers or mixing of composite of PANI-MWCNTs obtained by in situ chemical oxidative polymerization with ionomers.

2.2.4 Solvent blend optimization for ionomer dissolution

Ionomer is an ion containing copolymeric material with either positive [+] or negative [-] electric charge in which up to 15 mol % of the repeat units contain ionic groups. They comprise of both electrically neutral repeating units (non-ionic) and a fraction of ionized units covalently bonded to the polymer backbone as pendant group moieties. This makes the dissolution of ionomer with a single polar or non-polar solvents practically impossible. Hence, the need for solvent blending (polar and non-polar solvents). Toluene and 1-Butanol were selected for this purpose. The following table shows the optimization of the solvent blend ratios for the dissolution of the ionomer.

Table 2.1. Solvent blend ratio optimization for ionomer dissolution

Ionomer (g)	Solvents Toluene/1-Butanol	% of the ionomer dissolved
1.0	10/90	100
1.0	20/80	100
1.0	30/70	100
1.0	40/60	100
1.0	50/50	100
1.0	60/40	100
1.0	70/30	100
1.0	80/20	100
1.0	90/10	100

A constant weight of ionomer (1 g) was introduced into the solvent blends at varying ratios at a temperature of 65°C for 15 minutes with stirring. All the ionomers were completely dissolved each case. The dissolved solutions were allowed to evaporate to a solid film in a petri dish and then dried in vacuum oven at 50°C for 24 hours.

The films formed on the petri dishes were physically observed for smoothness and consistency of film. It was observed that the solvent combination of ratio 90/10 (Toluene/1-Butanol) gave the best film with good spread, smoothness of film and better consistency. The smoothness, consistency and good spread decreased with increase in the 1-Butanol content of the solvent blend. There was also a severe loss of strength and film becomes flaky and powdery as the volume of 1-Butanol content of the solvent blend increased (60-90). Based on these observations, 90/10 solvent blend was chosen for further work. However, the film of the chosen solvent blend was not smooth and uniform enough for testing and analysis. Hence, the dried films were compression moulded using a flat mould at 70°C and test pieces cut out for testing and characterization.

2.3 Characterization Techniques

A detailed description of the characterization techniques employed in interpreting the various sample properties are highlighted here.

2.3.1 Morphological Characterization

The morphology and microstructure of the samples were investigated through the sscanning electron microscopy (SEM) and transmission electron microscopy (TEM). It involves scanning by an electron beam across a sample surface and secondary electrons are ejected from the surface.

2.3.1.1 Scanning Electron Microscopy (SEM)

Scanning electron microscopy (SEM) is a method for high resolution surface imaging. The SEM uses an electron beam for surface imaging. The samples are mounted on SEM stubs using carbon tape and then sputter coated with a thin layer of gold to avoid charging during analysis. For a typical SEM, a beam in a cathode ray tube and an electron beam are simultaneously scanned across the surface of the sample. A signal is then produced by scattered electrons resulting in an image that gives a three dimensional appearance.

The advantages of SEM over light microscopy are greater magnification and much larger depth of field. Different elements and surface topographies emit different quantity of electrons, due to which the contrast in a SEM micrograph (picture) is representative of the surface topography and distribution of elemental composition on the surface. Qualitative elemental analysis, standard less quantitative analysis, X-ray line scans and mapping can be performed with SEM-EDS combination [5]. In this work, we have employed JEOL Model JSM - 6390LV with magnification range of 5X - 300000X.

2.3.1.2 Transmission Electron Microscopy (TEM)

Transmission electron microscopy (TEM) is a microscopy technique in which electrons are transmitted through an ultra-thin specimen, interacting with the specimen as it passes through. An image is formed from the interaction of the electrons transmitted through the specimen [5]. Using TEM, the principle involves an electron beam, which is transmitted through a specimen that must be less than 200 nm thick, in a stable high vacuum system. The samples can be magnified between 100-100,000 times [6]. TEM provides very useful information for crystalline materials while amorphous materials are more difficult to analyze using TEM [7]. In this work JEOL/JEM 2100 with magnification of 2000X – 1500000 X was employed for this characterization.

2.3.2 X-Ray Powder Diffraction Analysis (XRD)

Wide Angle X-Ray powder diffraction is used to obtain information about the structure, composition and state of a material. Some typical applications are identification of an unknown sample based on the crystalline peaks, variable temperature studies, precise measurements of lattice constant and residual strains, and refinement of atomic coordinates.

The structure determination is based on the interference of monochromatic X-rays and the crystalline sample [8]. In XRD, X-Rays are impinged and reflected X-Rays are collected at a known angle relative to the sample [9]. The scattered beam is used to determine the atomic structure of the lattice. For an incident ray, at an angle θ, according to Bragg's equation, path difference is given by:

$$n\lambda = 2d \sin \theta$$

Where; n is an integer, d is the distance between atomic layers in the crystal, λ is the wavelength, and θ is the angle of incidence.

If Bragg's equation is satisfied, a peak will be observed. By comparing the obtained peaks in the XRD pattern to database information about crystalline structures, the material could be identified. For polymers, as they contain both crystalline and amorphous regions, the X-ray diffraction patterns may contain a mixture of sharp and diffused patterns. Hence the diffractograms contains sharp peaks, corresponding to the ordered regions and the diffused and broader portions corresponding to the irregular ones. It is well-established that for intrinsically conducting polymers, crystallinity has a significant influence on the conductivity retention. At elevated temperature, conductivity ageing happens to amorphous regions easily when compared to the crystalline regions.

X-Ray Powder Diffractometry is one of the most powerful and established technique for material structural analysis, capable of providing information about the structure of a material at the atomic level [5]. Bruker AXS D8 Advance with a configuration of Vertical Theta/2 Theta geometry was used for this work.

2.3.3 Fourier Transform Infrared (FTIR) Spectroscopy

Atoms or atomic groups in molecules are in continuous motion with respect to one another. They vibrate about some mean position. Fourier transform infrared (FTIR) spectroscopic method allows one to characterize vibrations in molecules by measuring the absorption of light of certain energies that correspond to the vibrational excitation of the molecules from lower to higher states. All molecules have specific frequencies at which they rotate or vibrate corresponding to discrete energy levels. As the different functional groups absorb at their unique characteristic frequencies, the resulting spectrum representing the molecular absorption and transmission, is a molecular fingerprint of the sample [10].

IR spectrum of a compound is the superposition of absorption bands of specific functional groups. The subtle interactions with the surrounding atoms or molecules impose the stamp of individuality of the spectrum of each compound. IR absorption has numerous applications in qualitative and quantitative analysis [5]. Thermo Nicolet, Avatar 370 with spectra range of 4000-400 cm^{-1} was employed for this work.

2.3.4 Ultra Violet-Visible (UV-VIS) Spectroscopy

There is a difference in energy between molecular bonding, non-bonding and anti-bonding orbitals ranges from 125 to 650 kJ per mole.

This energy corresponds to the electromagnetic radiation in the ultraviolet region and the visible region of the spectrum. Thus, UV-Visible spectroscopy deals with the measurement of energy absorbed when electrons are promoted to a higher energy levels. The UV-Visible spectrum can be divided into three regions:

- Far or vacuum ultraviolet region (10-200nm)
- Near or quartz ultraviolet region (200-380nm)
- Visible region (380-780nm)

The absorption of light in the ultraviolet (l0 - 420 nm) and visible (420-700 nm) regions by a sample is measured in Ultraviolet–visible spectroscopy. The absorption of light in this region depends on the nature of chemical groups present in the structure. When a radiation of energy in the UV-Vis region falls on the sample, there can be various possible transitions which are σ-σ*, n-σ*, π-π* and n-π* depending on the sample under analysis. Among these transitions, n-π* transition requires the least amount of energy and gives rise to an absorption band at longer wavelengths [11]. By analysing the UV-Vis absorption spectra of materials, it is possible to estimate the absorption coefficient α, direct and indirect band-gap energies and the density of states. Near IR spectroscopy is a valuable tool for analyzing aromatic mixtures. Absorption measurements in the UV and visible regions provide information about electronic transitions in a sample. The applications of the instrument include overtone analysis of X-H containing molecules (X=C, O, N, Si), determination of hydrogen bonds, energy gap measurements in solids, study of molecular structure, concentration measurements etc. In this procedure we have used Varian Cary 5000 with spectra range of 175 – 3300 nm for this purpose.

2.3.5 Thermal Analysis

Thermal analysis can be used to detect the physical or chemical changes in a material related to thermal properties. The glass transition temperatures (Tg) of the polymers can be studied through these methods. This technique includes thermogravimetric analysis (TGA)/differential thermal analysis (DTA) and differential scanning calorimetry (DSC). Thermogravimetric analysis (TGA) determines the weight changes of a sample, whereas differential thermal analysis (DTA) measures changes in temperature between a sample and a reference as a function of temperature or time. We have used only TGA in this study. Applications of the TGA instrument are for compositional analysis, decomposition temperature, oil volatility measurements, flammability studies, heat of transition, thermal stability analysis, oxidative stability analysis, transition temperature detection etc. In this analysis, we have used Perkin Elmer STA 6000 [5].

2.3.6 Conductivity Measurements

DC conductivity

The powdered samples of PANI and PANI-MWCNT were pressed into pellets of 13mm disc diameter with the help of hydraulic press by applying a pressure of 1000 kg/cm^2. The PANI-Ionomer binary blend and PANI-MWCNT-Ionomer ternary blend samples were cut to a disc shape of 13mm diameter to fit closely into the coaxial measurement cell of the instruments. Samples were coated with a silver conducting paste to reduce the sample-electrode contact resistance.

D.C measurements were done using sensitive digital electrometer type Keithley 616 four probe technique (ASTM D 991-89) [12]. Using a Keithley 616 source-measure unit in dry air at room temperature. Disc shaped rubber samples having diameter 13 mm and thickness of about 1 mm were used for the measurements. The sample was mounted between two parallel copper electrodes and conductivity was calculated using the formula [13]

$$\sigma = \left(\frac{I}{V}\right) \times \frac{l}{A}$$

Where σ is the electrical conductivity (S/m), I is the current (amperes), V is the voltage (volts), *l* is the thickness of the sample (m) and A is the area of contact of electrodes with sample (m^2) which is given by [13].

$$A = \pi \text{ x } (5 \text{ x } 10^{-3})^2$$

2.3.7 Electromagnetic Interference (EMI) Shielding

Electromagnetic interference (EMI) is the disruption of operation of an electronic device when it is in the vicinity of an electromagnetic (EM) field in the radio frequency (RF) spectrum that is caused by another electronic device. Blend reflectivity measurements over a frequency range of 8 to 12 GHz were done at room temperature using a wave-guide coupled to an Agilent Synthesized Sweeper 8375A and a Hewlett-Packard spectrum analyzer 7000 [14]. A network analyzer consists of a signal source, a receiver and a display. The source dispatches a signal at a single frequency to the material under test (MUT). The receiver is adjusted to that frequency to detect the reflected and transmitted waves from the material. Scatter parameters, also called S-parameters, were used to calculate shielding parameters in a two-port EMI shielding setup. [15, 16].

2.3.8 Stress-Strain Properties

Mechanical properties of TPU nanocomposites were studied using a Shimadzu Universal Testing Machine (model AG-I) with a load cell of 10 kN capacity. The specimens used were dump bell shaped. The gauge length between the jaws at the start of each test was adjusted to 14 mm and the measurements were carried out at a crosshead speed of 50 mm/min at room temperature. Tensile strength, elongation at break and elastic modulus were measured according to ASTM D-882.

2.4 Sonication Technique

A sonicator is a powerful piece of lab equipment with an ultrasonic electric generator that creates a signal to power a transducer. The transducer converts the electric signal using piezoelectric crystals (crystals that respond directly to electricity) by creating a mechanical vibration. The sonicator preserves and amplifies the vibration until it passes to the probe. The probe moves in time with the vibration to transmit it to agitate the solution [17].

Sonication is the act of applying ultrasonic energy to agitate particles in a sample. It refers to the process of applying sound energy to agitate particles or discontinuous fibers in a liquid. In a laboratory, this is usually accomplished by use of an ultrasonic bath or ultrasonic probe known colloquially as sonicator. Sonication uses an ultrasonic bath or probe to apply sound energy to agitate liquid-containing particles. It converts an electrical signal into a physical vibration to break substances apart. These vibrations or disruptions can mix solutions and accelerate the dissolution of solids such as PANI or CNT into liquids such as water as well as remove dissolved gas from liquids. Sonication typically uses ultrasound waves with ultrasonic frequencies of 20 kHz (20,000 cycles per second) or higher to create a loud shrieking noise. The greater the frequency, the more intense the noise and the stronger the agitation of particles [17-19].

During the sonication of liquids, the sound waves that propagate into the liquid medium result in alternate cycles of low and high pressure (rarefaction and compression respectively) which depends on frequency. During the cycles of low pressure, ultrasonic waves of high intensity creates some empty small bubbles in the liquid. When the bubbles attain a volume at which they can no longer absorb energy, they tend to violently implode during a high-pressure cycle. This occurrence is termed cavitation. The implosion of cavitation bubbles results in micro jets and turbulences of up to 1000 km/h. This results in the mechanical stress on the van der Waals forces between particles. Large particles are subject to wearing away of surface due to cavitation implosion in the surrounding liquid or at least a reduction in size resulting from breaking up through particle-particle collision as well as the collapse of cavitation bubbles formed on the surface to achieve homogenization, dispersing, deagglomeration, milling, emulsification, extraction, lysis, disintegration and sono-chemical effects. During the implosion, temperatures of 5000 K and pressures of up to ~2000 atm can be attained locally [19-21].

However, this localization of energy especially from probe sonication leads to a considerable amount of damage, including buckling, bending, dislocations and rupture in the case of CNTs thereby drastically reducing their aspect ratio or even destroying it partially. It could also cause heating of the sample, hence, the necessity to cool the sample during sonication to prevent degradation (deteriorate the electrical, thermal and mechanical properties of the nanocomposite). For the purpose of this work, ultrasonic probe was used as shown in Figure Figure 2.3.

Figure 2.3 Ultrasonic Probe [20].

Sonication is widely used in the laboratory to disperse nanotubes into the polymer matrix. This process utilizes ultrasound energy to agitate nanoparticles in the polymer matrix. When it passes through the polymer medium, attenuated waves are induced, promoting the ‘peeling off’ of the CNTs located at the outer parts of the nanoparticle bundles/agglomerates. As a result, individual nanoparticles are separated and high quality dispersion can be achieved. When the duration of the process is longer and the intensity of the input energy is higher, better dispersion quality can be obtained.

When dispersing nanoparticles in a low viscosity medium, diffusion process and particle-particle and particle-matrix interactions (distance) play an important role. This distance is comparable to the radius of gyration of a typical polymer molecule. It shows basically that, in a nanocomposite, the entire polymer matrix can behave as if it were part of an interphase. Such effect may influence both processing and final properties of the polymeric phase. The common methods of preparing CNTs/polymer composites are solution processing, melt processing and reaction processing or in situ polymerization [20]. In this work, we have adopted in-situ polymerization and solution processing.

In in-situ polymerization is considered an efficient method to significantly improve the dispersion of CNTs and the interaction between CNTs and the polymer matrix. The CNTs are first mixed with monomers and then CNTs/Polymer composites can be obtained by polymerizing the monomers under specified conditions [20]. Figure 2.4 shows the flowchart for the process.

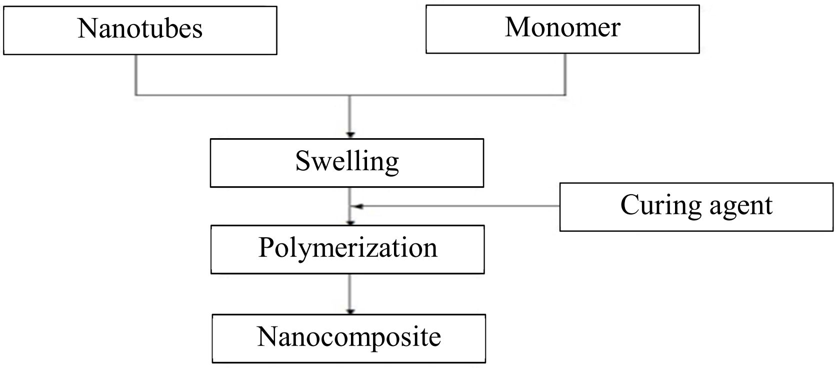

Figure 2.4. Flowchart representing the process stages [20].

In solution processing, CNTs are generally dispersed in a solvent and then mixed with polymer solution by sonication and magnetic stirring. After the dispersion of the CNTs, the composite can be obtained by vaporizing the solvent. This method is considered as a very effective way to prepare composites with CNTs homogeneously distributed and often used to prepare films [20]. Figure 2.5 shows the flowchart for sonication through solution processing.

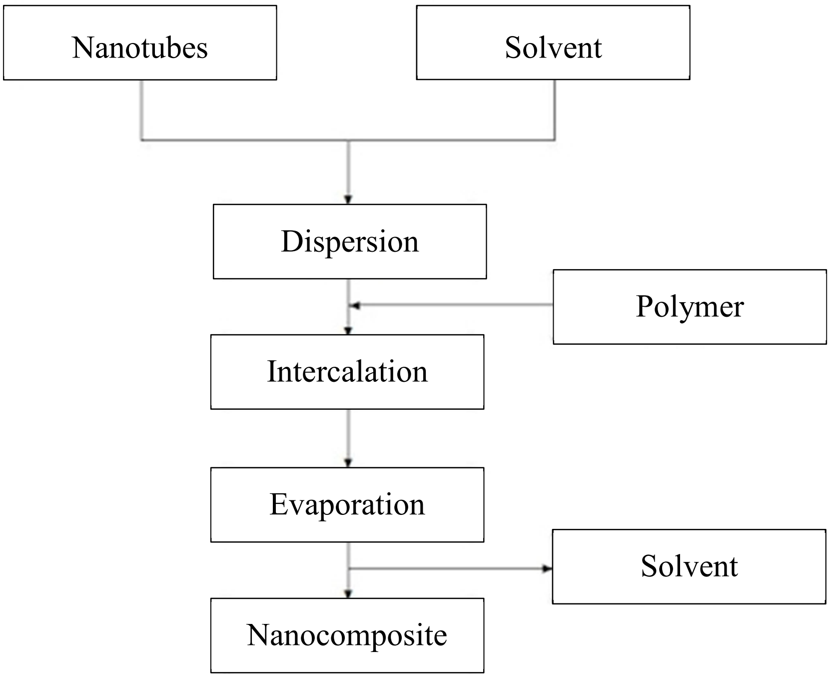

Figure 2.5. Flowchart presenting the different steps of the solution processing of a polymer composite [20].

Reference

[1] Bavane RG, 2014. Synthesis and Characterization of Thin Films of Conducting Polymers for Gas Sensing Applications. PhD Thesis, North Maharashtra University, Jalgaon, Maharashtra, India.

[2] http://ediss.sub.uni-hamburg.de/volltexte/2013/6505/pdf/ Dissertation.pdf. Accessed on 20th March, 2018.

[3] Shodhganga.inflibnet.ac.in/bitstream/10603/229/9/09_chapter1.pdf. Accessed on 20th March, 2018.

[4] Introduction to Polymer Blend, www.uobabylon.edu.iq/eprints/ publication 10_10932_ 1261.pdf. Accessed on 20th March, 2018.

[5] Truong VT, Codd AR and Forsyth M, 1994. Dielectric properties of conducting polymer composites at microwave frequencies. J Mater Sci 29 4331-4338.

[6] Neena G, 2017. Segregated and Random Network formation of MWCNT and Nanosilica in NR and XNBR, PhD Thesis, Cochin University of Science and Technology, Kochi, Kerala, India.

[7] http://www.sticindia.com/saif_instruments. Accessedon 20th March, 2018.

[8] Williams DB, and Carter CB, 1996. Transmission Electron Microscopy: A Text book for Materials Science. Plenum Press, New York, USA.

[9] Shahinpoor M and Kim KJ, 2005. Ionic polymer–metal composites: IV. Industrial and medical applications. Smart Mater Struct, 14 197-214.

[10] Als-Nielsen J and McMorrow D, 2001. Elements of Modern X-Ray Physics, 2nd Edition. Wiley, New York, USA, p 1-159.

[11] Cullity BD and Stock SR, 2001. Elements of X-ray Diffraction. Prentice Hall, New Jersey, USA.

[12] Banwell CN, 1995. Fundamentals of Molecular Spectroscopy, 4th Edition. Tata McGraw Hill Publishing Company Ltd, New Delhi, India.

[13] Heinz-Helmut P, 1992. UV-VIS Spectroscopy and its applications, in Springer laboratory manual. Springer-Verlag Berlin Heidelberg, Germany, p244.

[14] Martins CR, Faez R, Rezende MC and De Paoli M-A, 2004. Microwave absorption properties of a conductive thermoplastic blend based on polyaniline. Polym Bull 51, 321-326.

[15] Joseph N and Sebastian MT, 2013. Electromagnetic interference shielding nature of PVDF-carbonyl iron composites. Materials Letters, 90 64-67.

[16] Arjmand M, 2014. Electrical conductivity, electromagnetic interference shielding and dielectric properties of multi-walled carbon nanotube/ polymer composites. PhD Thesis University of Calgary, Canada.

[17] Deborah D.L.Chung, 2017. Carbon Composites (Second Edition). In Composites with Carbon Fibers, Nanofibers and Nanotubes. Cement-Matrix Composites, Butterworth Heinemann, Published by Elsevier Inc. Pages 333-386. https://doi.org/10.1016/B978-0-12-804459-9.00006-3

[18] Gedanken A, 2001. Encyclopedia of Materials: Science and Technology (Second Edition). In Reference Module in Materials Science and Materials Engineering, Ultrasonic Processing to Produce Nanoparticles, Elsevier Ltd., Pages 9450-9456. https://doi.org/10.1016/B0-08-043152-6/01708-3.

[19] Gou J, Zhuge J and Liang F, 2012. Manufacturing Techniques for Polymer Matrix Composites (PMCs). In Processing of polymer nanocomposites, Woodhead Publishing Series in Composites Science and Engineering, Published by Elsevier Inc., Pages 95-119, https://doi.org/10.1533/9780857096258.1.95

[20] Marcio Loos, 2015. Carbon Nanotube Reinforced Composites, CNR Polymer Science and Technology. In Processing of Polymer Matrix Composites Containing CNTs. William Andrew Applied Science Publishers, Published by Elsevier Inc. Pages 171-188. https://doi.org/ 10.1016/ B978-1-4557-3195-4.00006-0

[21] Sabet SM, Mahfuz H, Hashemi J, Nezakat M and JA and Szpunar JA, 2015. Effects of sonication energy on the dispersion of carbon nanotubes in a vinyl ester matrix and associated thermo-mechanical properties. J Mater Sci, 50 4729. https://doi.org/10.1007/s10853-015-9024-y

……

Chapter 3

STUDIES ON BULK AND NANO POLYANILINE AND NANO POLYANILINE-MULTI WALLED CARBON NANOTUBE NANOCOMPOSITES

Contents

This study reports the synthesis and characterization of hydrochloric acid (HCl) and toluene sulfonic acid (TSA) doped polyaniline (PANI) in bulk and nano dimensions. The composites of polyaniline with MWCNT were prepared by in situ polymerization of aniline in the presence of non-functionalized and functionalized multi-walled carbon nanotubes (using ammonium persulfate as initiator. Scanning electron microscopy (SEM) was used to characterize the morphology of the PANI and PANI-CNT nanocomposites. X-ray diffraction (XRD) spectroscopy, Fourier Transform Infrared (FTIR) spectroscopy and UV-Vis spectroscopy were used to characterize the synthesized PANI and PANI-MWCNT nanocomposites. Thermogravimetric analysis (TGA) was used to measure the thermal behaviour of the samples. Under in situ polymerization, PANI layer was found to wrap over the functionalized MWCNTs especially the carboxylated MWCNT. There was uniform dispersion of functionalized MWCNTs within the PANI matrix with significant interaction between the two compared to the non-functionalized MWCNT. The electrical conductivity of composites at room temperature was measured and their percolation threshold was determined. PANI-MWCNT composites displayed much higher conductivity than PANI composites.

3.1 Introduction

Polymers were regarded as electrically non-conducting materials until Shirakawa et al. in 1977 [1] discovered a significant electrical conductivity in polyacetylene (PA) after its oxidation in the presence of iodine vapour. Conducting polymers or intrinsically conducting polymers (ICPs) are organic polymers that conduct electricity. They possess electrical properties like that of metals (metallic conductivity) and semiconductors. They display several other characteristics of organic polymers such as lightweight, lower cost, resistance to corrosion and chemical attack, flexibility and greater workability also [2-6]. Electrical conductivity of conducting polymers can be tuned from insulating to metallic through adequate doping process. They have a conjugated structure with alternate σ and π bonds, which is delocalized throughout the entire polymer network, resulting in an enhanced electrical conductivity [5, 6]. Conducting polymers include electronically and ionically conducting polymers. Ionically conducting polymers are usually called polymer electrolytes while electronically conducting polymers are referred to as conjugated conducting polymers. The conductivity of almost all conjugated polymers can reach up to the order of 10^{-3}–10^{3} S/cm after doping [2, 7]. They are widely used in many electrical/electronic devices and for a myriad of applications. Among different conducting polymers, polyaniline (PANI) is the most versatile owing to its low cost and desirable properties such as low specific mass, thermal/chemical stability and high conductivity [8]. Polyaniline occurs in 3 different states namely leucoemeraldine base (LEB) - which is the fully reduced state, pernigraniline base (PNB) -which is the fully oxidized form and emeraldine base (EB) - which is the partially oxidized form. Emeraldine salt (ES) occurs as a doped (protonated) form of emeraldine base (EB) and it is the only one that is electrically conducting [6].

The application possibilities of a conducting polymer can be further expanded to meet the requirements of present day sophisticated technologies if their conductivity can be enhanced to a certain extent. Composite preparation is one of the ways to improve the conductivity of conducting polymers. Polyaniline/carbon nanotubes (PANI/CNTs) based composites have been widely explored in which the charge-transfer activities between the two components leads to considerable improvement in conductivity [9]. PANI/CNTs nanocomposites were prepared either through grafting PANI macromolecules on the CNTs or through in situ polymerization of aniline monomer in CNT dispersion. Carbon nanotube was first discovered and reported in 1991 by Iijima et al. with their discovery of multiwalled carbon nanotubes (MWCNTs) [10]. Since then, carbon nanotubes (CNTs) has become one of the most interesting nanomaterials receiving significant attention in many growing micro and nano engineering industries and potential applications with great promise [11]. They possess impressive and interesting structural, mechanical, electrical and electronic, optical, thermal and chemical characteristics due to their small size and mass. There are two types of CNTs – single walled carbon nanotubes (SWCNTs) and multi walled carbon nanotubes (MWCNTs). SWCNTs is comprised of hollow single cylinders of graphene sheets while MWCNTs is comprised of a group of concentric SWCNTs capped at both ends, with diameters reaching tens of nanometers depending on the number of concentric walls [9].

This chapter describes the preparation of PANI in bulk and in nano dimensions through chemical oxidative polymerization of aniline using HCl and TSA as dopants respectively and APS as oxidant. The prepared bulk and nano sized PANI was characterized and its electrical properties were studied. PANI-MWCNTs nanocomposites were prepared by in situ chemical oxidative polymerization of aniline monomer in MWCNTs (non-functionalized (pristine MWCNT), carboxylic acid functionalized (CCNT) and amine functionalized (ACNT)) in the presence of TSA as dopants and APS as oxidant.

3.2 Experimental Methods

3.2.1 Synthesis of polyaniline (PANI)

Polyaniline was prepared by chemical oxidative polymerization of aniline monomer in the presence of 1 M HCl as dopant using ammonium persulfate as redox initiator at room temperature for 12 hrs. The polymer formed was washed with distilled water, dilute HCl solution and finally with acetone until the filtrate became colourless to remove excess HCl, oxidant, aniline and oligomers. The green coloured precipitate was then dried in vacuum oven at 50°C for 24 hours. The dried mass was ground to fine powder using mortar and pestle. The prepared polyaniline is designated as bulk PANI-HCl.

Polyaniline was also prepared in nano dimension by polymerizing 0.2g aniline using 0.66g of ammonium per sulfate dissolved in 1.8 ml water as initiator in the presence of 40 mL aqueous solution of 1M HCl at room temperature for 12 hrs. The same reaction was repeated with 1 M TSA as dopant keeping all other reactants the same as former.

3.2.2 Preparation of PANI-MWCNT composites

Binary composites of PANI-MWCNTs was prepared by in-situ chemical oxidative polymerization of 0.2g aniline using 0.66g of ammonium per sulfate dissolved in 1.8 ml water as initiator in the presence of 40 mL aqueous solution of 1M TSA as dopant in the presence of MWCNT in three forms viz non-functionalized (pristine CNT), carboxylic acid functionalized (CCNT) and amine functionalized (ACNT). The concentration of MWCNTs was varied as 0.05g (25%), 0.1g (50%), 0.15g (75%), 0.2g (100%), 0.25g (125%), and 150% in the reaction mixture of aniline-TSA so as to get the aniline-MWCNTs ratio 1:0.25, 1:0.5, 1:0.75, 1:1, 1:1.25, and 1:1.5.

3.2.3 Characterization

The morphology and microstructure of the samples were examined by using JEOL Model JSM - 6390LV SEM and JEOL/JEM 2100 TEM. The Fourier transform infrared (FTIR) spectra of samples were recorded from KBr sample pellets using a Thermo Nicolet Avatar 370 FTIR spectrometer. The compositional state of the samples were determined using X-Ray Powder Diffractometry (XRD) Bruker AXS D8. The optical absorption by the sample in the UV and visible region was measured with Varian Cary 5000 UV-Visible spectrophotometer in the spectral range 225-1000 nm. Thermo gravimetric analysis (TGA) was performed on a Perkin Elmer STA 6000 thermogravimetric analyzer to determine the decomposition and transition temperatures, and thermal stabilities of the samples. The electrical properties of the PANI samples were measured by four probe technique (D.C conductivity) using sensitive digital electrometer type Keithley Agilent 616.

3.3 Results and Discussions

3.3.1 Characterization of Polyaniline

3.3.1.1 Scanning Electron Microscopy (SEM)

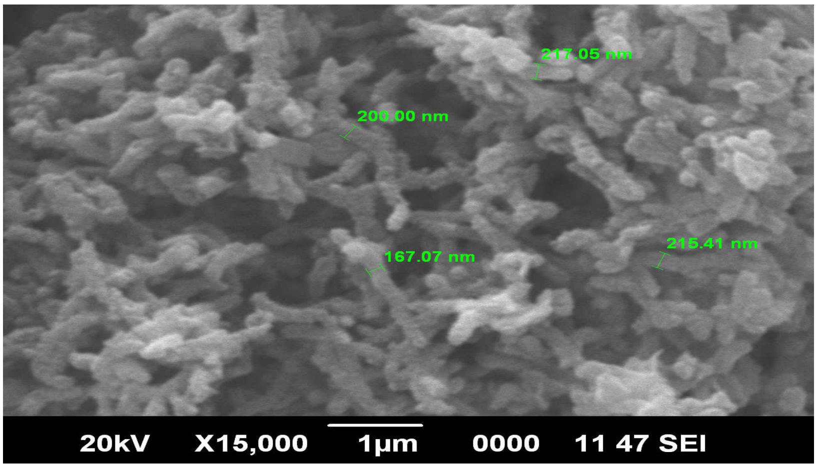

Figure 3.1a. SEM micrograph of bulk PANI-HCl.

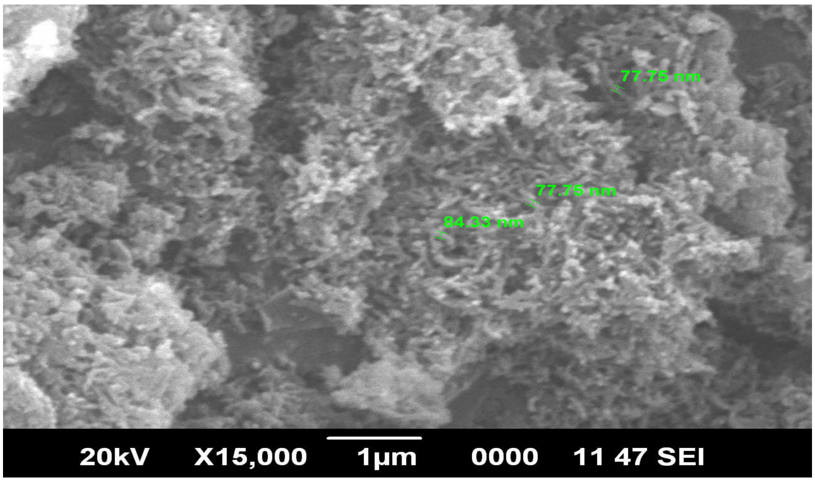

Figure 3.1b. SEM micrograph of nano PANI-HCl.

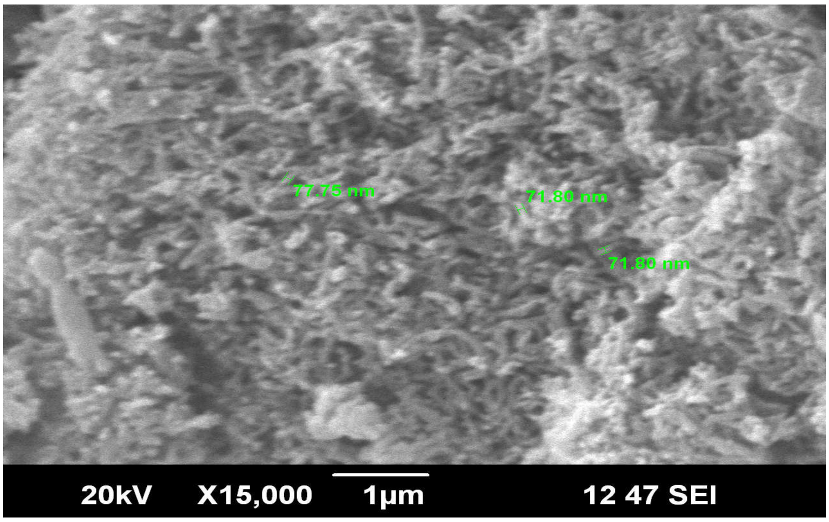

Figure 3.1c. SEM micrograph of nano PANI-TSA.

Figures 3.1a, 3.1b and 3.1c show the SEM micrographs of bulk PANI-HCl, nano PANI-HCl and nano PANI-TSA respectively. All the micrographs reveal the irregular granular morphology of the synthesized polyaniline. Bulk PANI-HCl has a porous structure with particle size of 217 nm. The micrographs of nano PANI-HCl and nano PANI-TSA reveal that the synthesized polyaniline comes under nanodimension with an average particle size of 77 nm and 71 nm respectively and possess a fibrous morphology.

3.3.1.2 Transmission Electron Microscopy (TEM)

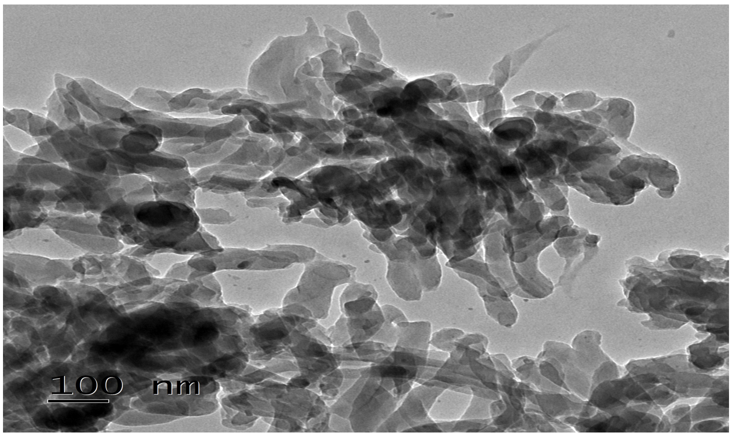

Figure 3.2a. TEM micrograph of nano PANI-HCl.

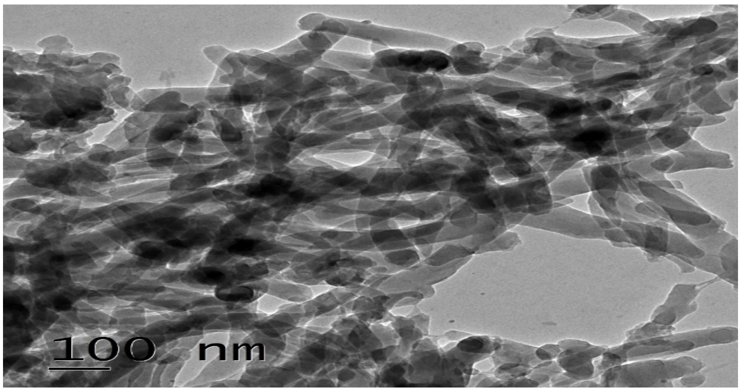

Figure 3.2b. TEM micrograph of nano PANI-TSA.

The transmission electron micrograph (TEM) images of nano PANI-HCl and nano PANI-TSA are shown in Figures 3.2a and 3.2b respectively. The TEM images clearly show a fibrous like morphology in the form of hollow nanorods. The formation of these polyaniline nanorods/nano fibers occurs interfacially at the junction of the organic and aqueous phase during the polymerization process may be due to the controlled and limited availability of the aniline monomer. The limited amount of aniline monomer molecules in the organic phase interacts with the oxidizing agent that is present in the aqueous phase [6, 9].

3.3.1.3 Fourier Transform Infrared (FTIR) Spectroscopy

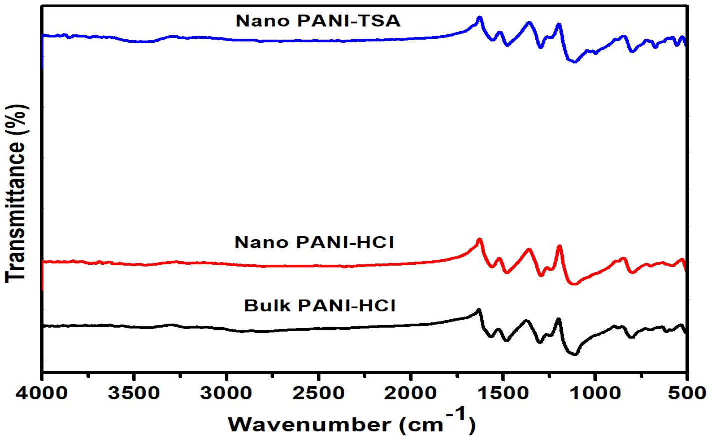

Figure 3.3. FTIR spectra of the Bulk PANI-HCl, Nano PANI-HCl and Nano PANI-TSA.

The FTIR spectra of PANI (bulk PANI-HCl, nano PANI-HCl and nano PANI-TSA) are presented in Figure 3.3. The bands at 1566cm^{-1}, 1560cm^{-1} and 1557cm^{-1} observed in bulk PANI-HCl, nano PANI-HCl and nano PANI-TSA respectively are attributed to the C=C stretching of quinoid and 1482cm^{-1}, 1480cm^{-1} and 1477cm^{-1} attributed to benzenoid rings indicating the oxidation state of emeraldine salt PANI [12-15]. The typical peaks at 1301 cm^{-1}, 1293 cm^{-1}, 1296 cm^{-1} and 1245 cm^{-1}, 1240 cm^{-1}and 1233 cm^{-1} are attributed to the bending vibration of C-N for aromatic amines/imines and C-N^{+} stretching vibrations in the polaronic structures (displacement of π electrons) owing to differing conformation or charge configuration suggesting the presence of protonated conducting PANI induced by acid doping of the polymer [6, 16]. The strong bands at around 1111 cm^{-1} are assigned to C-H in-plane bending vibration considered to be the extent of the degree of delocalization of electrons and thus it is the characteristic peak of PANI [15]. The observed band at 878 cm^{-1}, 769 cm^{-1}, 878 cm^{-1} and 801 cm^{-1}, 697 cm^{-1}, 800 cm^{-1} can be assigned to the aromatic ring out-of-plane deformation vibration bending of C-H bond in the benzene ring and para-distributed aromatic rings indicating polymer formation [16]. Out of plane bending deformation of C–H is observed at 506 cm^{-1} and 500 cm^{-1} [14, 15]. The peak at 997 cm^{-1} in (nano PANI-TSA) can be assigned to SO3^{-} group of the dopant TSA bound to the aromatic rings [15]. The weak and broad signal observed at 3448 cm^{-1} in nano PANI-TSA is assigned to N-H bond stretching indicating the presence of a secondary amine. This peak is broad and weak such that it is not visible in the bulk PANI-HCl and nano PANI-HCl spectrum.

3.3.1.4 X-Ray Diffractometry (XRD)

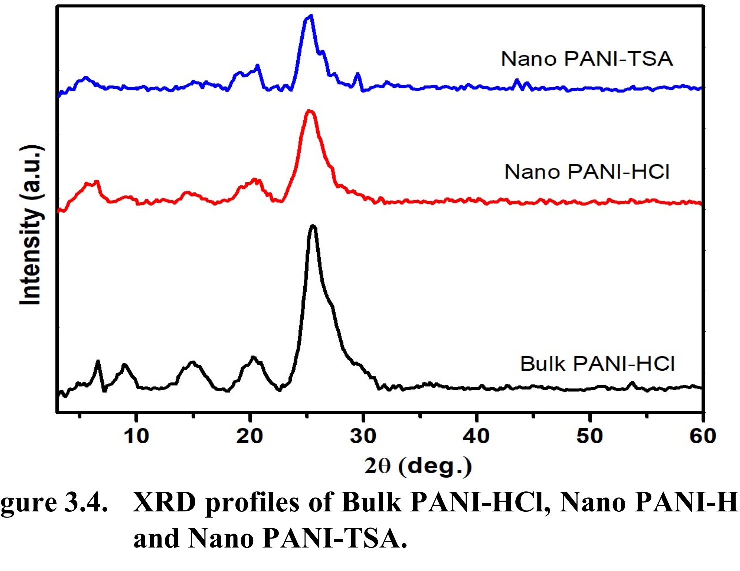

Figure 3.4. XRD profiles of Bulk PANI-HCl, Nano PANI-HCl and Nano PANI-TSA.

Figure 3.4 shows the XRD pattern of bulk PANI-HCl, nano PANI-HCl and nano PANI-TSA. The diffraction pattern of bulk PANI-HCl and nano PANI-HCl showed medium sharp peaks at 2θ = 25° indicates the partially crystalline nature of HCl doped PANI with conducting metallic islands separated by large amorphous regions. The diffraction pattern of the para-toluene sulphonic acid (TSA) doped PANI (nano PANI-TSA) shows peaks at 2θ =20°, 25°, 28°, 43° and 44° indicate the partial crystallinity of the sample. The sharp peak at 2 θ = 29° is a characteristic peak indicating the rigidity and well-ordered nature of some portion of PANI sub chains due to interchain packing between poly-cation and TSA anion [6, 9, 12, 17, 18]. The sharp peak at 2θ = 25° obtained for all the three PANI samples is the characteristic peak of PANI indicating the extent of π conjugation in the polyaniline and sharpness of the peak reveals the degree of order of π conjugation.

3.3.1.5 UV-Visible spectroscopy (UV-Vis)

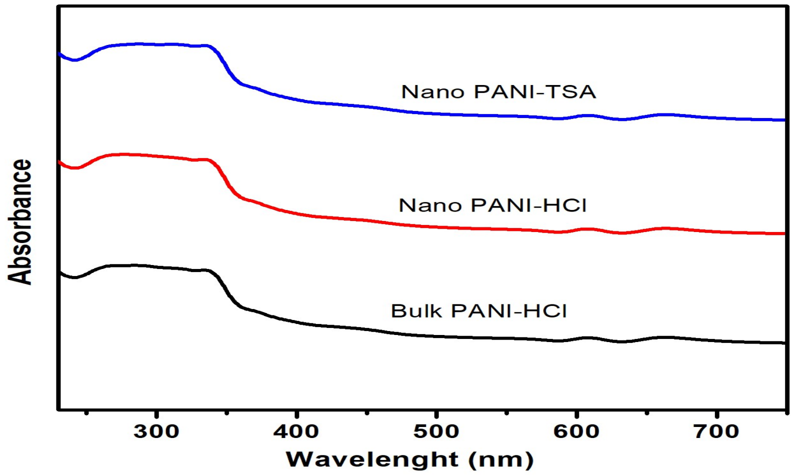

Figure 3.5. UV-Visible spectra of Bulk PANI-HCl, Nano PANI-HCl and Nano PANI-TSA.

Electronic absorption of conducting polymers is useful in investigating the oxidation and doping state of the polymer. The UV-Visible spectra of PANI namely, bulk PANI-HCl, nano PANI-HCl and nano PANI-TSA are shown in Figure 3.5. Two absorption bands at 277–288 nm and 608–663 nm were obtained for all the three samples. The band at 277–288 nm is due to π-π^* transitions in the benzenoid rings of polymer backbone while the band at 608–663 nm is due to exciton absorption of quinoid rings (n–π^*) (inter-band charge transfer associated with excitation of benzoid (HOMO) to quinoid (LUMO) moieties) and a small shoulder-like band at 335 nm attributable to the formation of polaronic/bipolaronic transitions resulting in protonation of the polymer, indicating that the resulting PANIs are in the doped state [6, 9, 16-24]. The continuous absorption peak at 780-790 nm shows free carrier tail, confirming the presence of conducting emeraldine salt phase of the polymer [6, 15, 16, 18, 22]. The slight difference in the absorption bands observed for the three PANI samples might be due to the molecular interaction of dopants with imine nitrogen of PANI [24] coupled with the difference in dimension of the particles resulting in the slight shift in absorption values. The bulk PANI with comparatively larger particles as seen in SEM micrograph which may induce more specular reflection, hence lower absorption and vice versa. This could also influence the conductivity of the samples.

3.3.1.6 Thermogravimetric analysis (TGA) of Polyaniline

The thermogravimetric analysis (TGA) of PANI-(bulk PANI-HCl, nano PANI-HCl and nano PANI-TSA) respectively was conducted to ascertain their thermal stability characteristics (Figure 3.6).

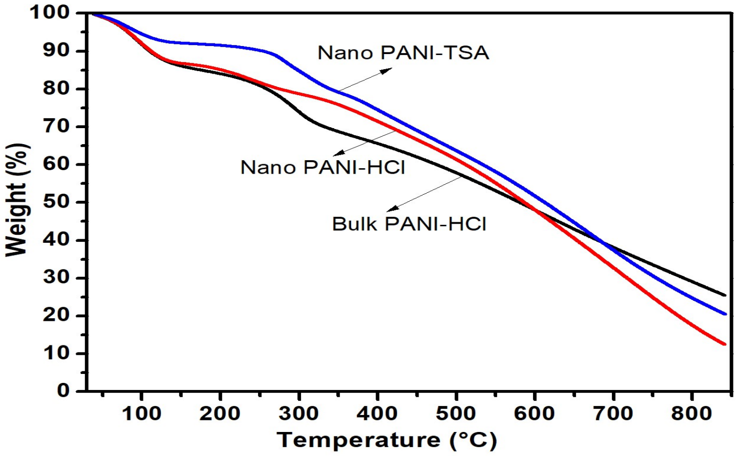

Figure 3.6. TGA curves of Bulk PANI-HCl, Nano PANI-HCl and Nano PANI-TSA.

Figure 3.6 shows the TGA thermogram of PANI (bulk PANI-HCl, nano PANI-HCl and nano PANI-TSA). In the first step, approximately 10%, 10%, and 6% weight loss is observed for bulk PANI-HCl, nano PANI-HCl and nano PANI-TSA respectively at the temperature up to 105°C. This is attributed to loss of water molecules and unreacted organic monomers [13, 18, 25] from the PANI structure. The second weight loss of about 17%, 14% and 9% is seen respectively for bulk PANI-HCl, nano PANI-HCl and nano PANI-TSA at 220°C and it may be due to evaporation of dopant acids in PANI samples. The third step of weight loss was observed between 500 °C and 800 °C with 42%, 38%, 36% weight loss and 29%, 18%, 25% residues respectively. This possibly represents the oxidative degradation of the PANIs which could be an indication of chemical structure decomposition [26]. However, nano PANI-TSA showed higher thermal stability up to 700 °C with main weight loss due to oxidative degradation of PANI occurring over a wide temperature range of 350 - 650 °C.

3.3.2 Characterization of Polyaniline-MWCNT composite

3.3.2.1 Scanning Electron Microscopy (SEM)

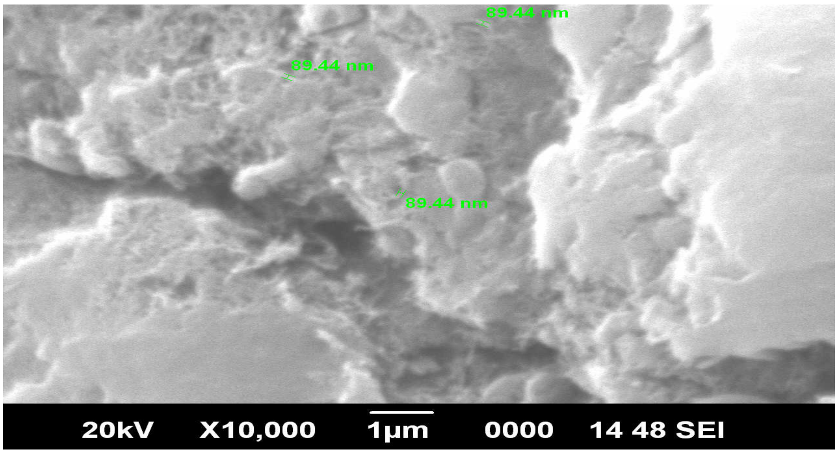

Figure 3.7a. SEM micrograph of PANI-pristine CNT composite

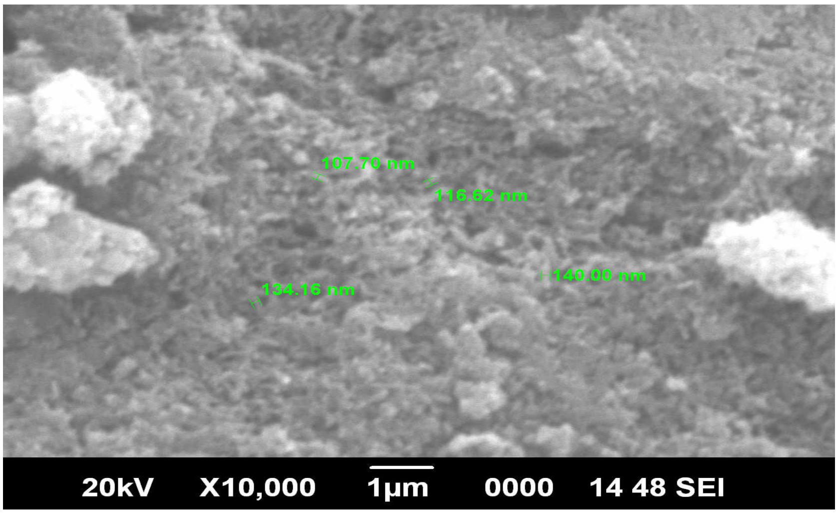

Figure 3.7b. SEM micrograph of PANI-ACNT composite

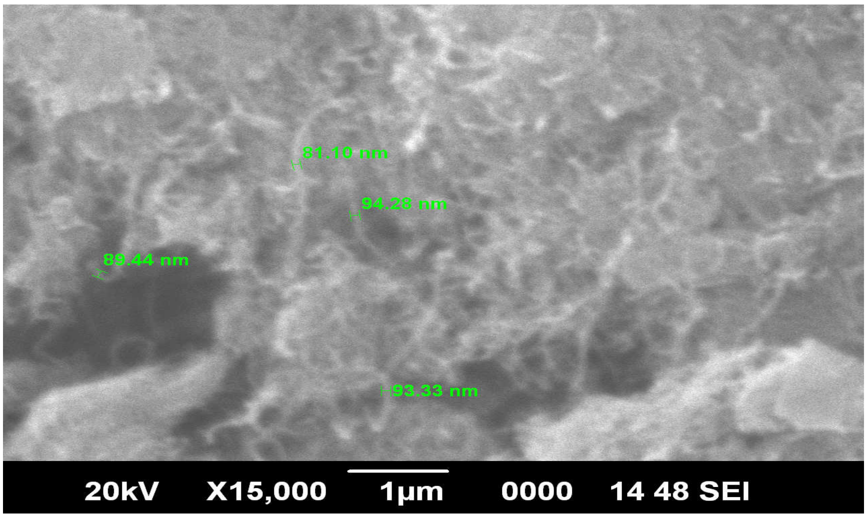

Figure 3.7c. SEM micrograph of PANI-CCNT composite

The SEM micrographs of PANI- (pristine CNT, ACNT and CCNT) samples are presented in Figures 3.7a, 3.7b and 3.7c. It is clear from the figures that the coiled rod like and fibrous structures of MWNTs are well dispersed in the PANI matrix. PANI macromolecules are uniformly distributed on the surface of MWNTs forming a tubular shell of the composites [27]. However, Figure 3.7a (PANI- pristine CNT) shows agglomerations of PANI which may be due to its weak interaction with polyaniline compared to ACNT and CCNT.

3.3.2.2 Transmission Electron Microscopy (TEM)

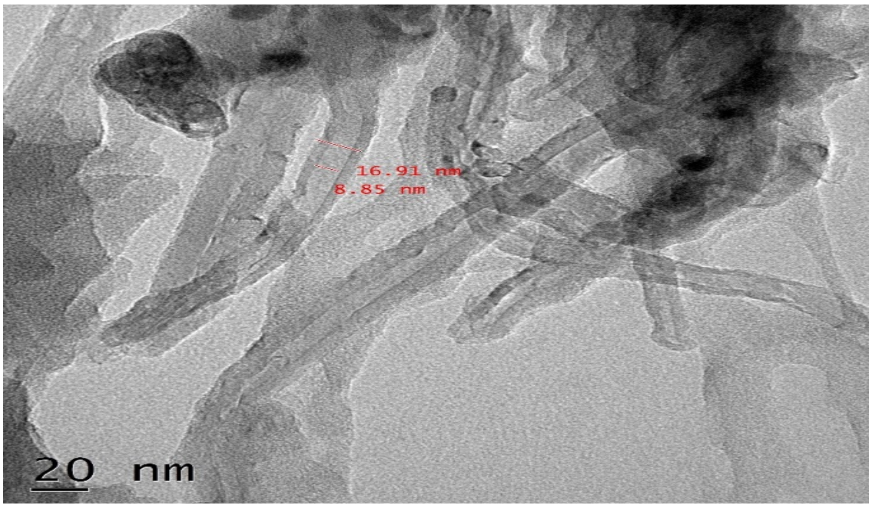

Figure 3.8a. TEM micrograph of PANI-pristine CNT

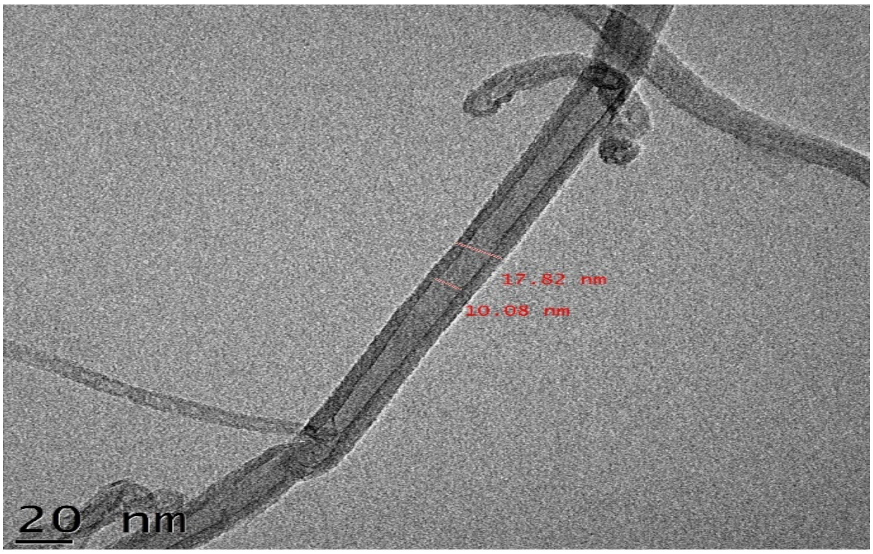

Figure 3.8b. TEM micrograph of PANI-ACNT

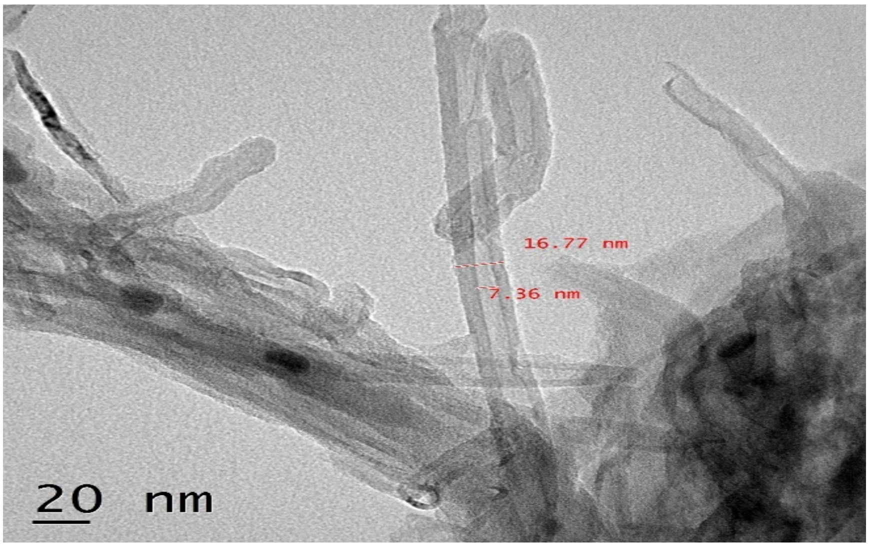

Figure 3.8c. TEM micrograph of PANI-CCNT

The TEM micrographs of PANI (pristine CNT, ACNT and CCNT) composites are shown in Figures 3.8a, 3.8b and 3.8c respectively. The TEM images reveal that a uniform layer of PANI is formed on MWNTs' surfaces resulting in the enlargement of diameters to the range of 8 to 20 nanometers. Also the TEM images shows that a marginal shortening of fibre lengths due to a possible stripping of the sides of the MWCNTs fibres during sonication in aqueous solution of the dopant acid resulting in breakages and separation of the entangled fibres [28]. This disentanglement in the fibrous tubes tends to form a stable dispersion in water especially in the case of functionalized MWCNTs forming alignment which display a new interwoven fibrous structure which may give remarkable rise to conductive passways and lead to high conductivity [29]. Since ACNT and CCNT are functionalized and can be well dispersed in the dopant solution compared to pristine CNT, a thick and uniform shell was formed on the surfaces of ACNT and CCNT as clearly observed in Figures 3.8b and 3.8c. Besides, the phenyl amino groups on the surface of ACNT is capable of initiating polymerization, the concentration of the monomeric species would be higher on the surface and hence, could lead to the formation of a thicker and more uniform coating of PANI on the surface of ACNT in the polymerization process [16, 28-32].

3.3.2.3 Fourier Transform Infrared (FTIR) Spectroscopy

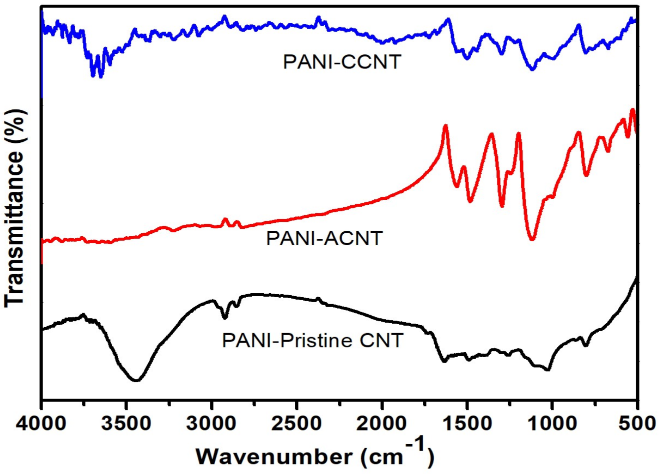

Figure 3.9. FTIR spectra of PANI-Pristine CNT, ACNT and CCNT

Figure 3.9 shows the FTIR spectra of PANI-MWCNTs - (pristine CNT, ACNT and CCNT) nanocomposites. FTIR analysis helps to determine the interactions of PANI with MWCNTs in the nanocomposites. The quinoid and benzenoid ring in the band of PANI at 1557 cm^{-1} and 1477 cm^{-1} is shifted to 1623 cm^{-1} and 1561 cm^{-1}, 1564 cm^{-1} and 1488 cm^{-1}, 1483 cm^{-1}, and 1503 cm^{-1} in the spectra of PANI - pristine CNT, PANI-ACNT and PANI-CCNT nanocomposites respectively. The shifting of the band confirms the interactions of the MWCNTs with the quinoid ring of PANI. The intensity of some of the signals in the nanocomposites were diminished compared to the pure PANI. The reason of decreased intensity is presumed to the adsorption of unreacted aniline monomer onto the surface of the MWCNTs limiting the growth of polymer chains around the nanotubes [13]. This constrained motion of the polymer chains and adsorption of monomeric aniline may limit the modes of vibration in PANI. Also, in acid solution, the NH_2 groups get protonated and becomes $+NH_3$ making the surface of the nanotubes positively charged. This in turn helps in achieving easy dispersion of CNTs in the nanocomposite due to mutual repulsion of positively charged PANI coated nanotubes [33].

3.3.2.4 X-Ray Diffractometry (XRD)

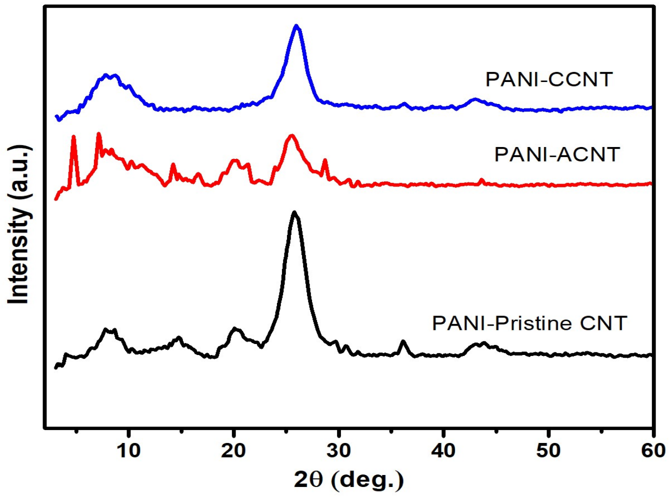

Figure 3.10. XRD profiles of PANI-Pristine CNT, ACNT and CCNT

Figure 3.10. Shows the XRD pattern of PANI-MWCNTs (pristine CNT, amine functionalized (ACNT) and carboxylic acid functionalized

(CCNT)) nanocomposites. The X-ray diffractograms of PANI–MWCNTs composites show all the peaks corresponding to PANI as well as the MWCNTs, indicating that no additional crystalline order is introduced in these composites. The diffractograms show a highly pronounced structure of the primary doped PANI (ES) superimposed in the MWCNTs peaks, showing crystalline peaks at 25° with high intensity and sharpness especially the peaks of PANI - pristine CNT and carboxylic acid functionalized (CCNT)). The appearance of diffraction peak at 25° is common in both PANI and the MWNTs, indicating that MWCNTs are dispersed in the PANI matrix [21, 25, 34, 35].

3.3.2.5 UV-Visible spectroscopy (UV-Vis)

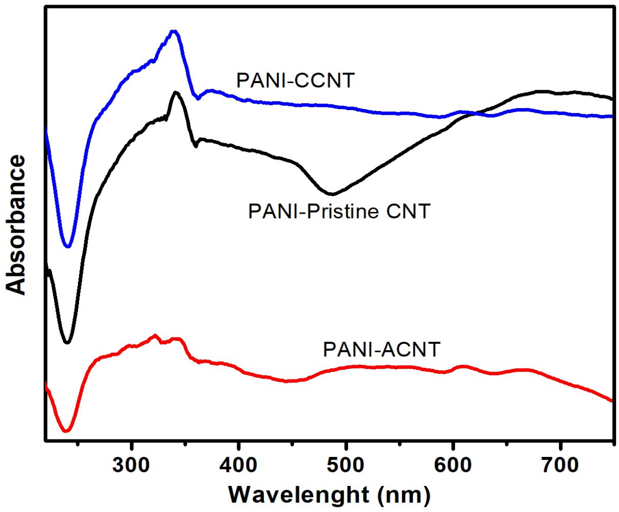

Figure 3.11. UV-Visible spectra of PANI-Pristine CNT, ACNT and CCNT

To understand the effect of insitu polymerization of aniline in the MWCNTs, UV–Vis spectroscopy was carried out on the PANI-MWCNTs.

Figure 3.11 shows the UV-Vis spectra of PANI–MWCNTs (pristine CNT, amine functionalized (ACNT) and carboxylic acid functionalized (CCNT)) nanocomposites. The absorption peak around 260 nm in the PANI spectra is shifted to higher wavelengths for the PANI-MWNCTs indicating a lower energy for the π–π^* electronic transitions [25]. The spectra of the composites exhibit both blue shift for PANI and red shift for the MWCNTs with characteristic absorption bands at 341, 322 and 341 nm respectively. The blue shift is attributed to the increased delocalization of charge carriers and charge transfer (CT) interaction between PANI and MWCNTs composites nanostructure which is believed to involve a strong interaction between aniline monomer and MWCNTs due to the presence of the π–π^* electron while the red shift is attributed to the hydrogen bond interaction between MWCNTs and the amino groups of aniline monomers enhancing charge transfer from quinoid unit of PANI to nanotubes. Such strong interaction resulting from the presence of MWCNTs in the composites ensures that the aniline monomer is adsorbed on the surface of MWCNTs, which serve as the core and self-assembly template during the formation of the tubular nanostructure [17, 20, 21, 36]. Such shifts of the π–π^* band in PANI-MWCNT composites compared to the PANIs is suggested to be due to the site-selective interaction between the quinoid ring of the PANI and CNTs. When PANI coats over the MWCNTs, the interfacial interaction between the two causes the π–π^* transition to shift to a lower wavelength while at the same time, the absorption peak due to the polaron/bipolaron transition is red shifted in PANI-MWCNT composites compared to neat PANIs. Consequently, such a hypsochromic shift of the π–π^* band is expected to result to a higher electrical conductivity for the PANI-MWCNT composites compared to the neat PANI [20].

3.3.2.6 Thermogravimetric Analysis (TGA)

The thermogravimetric analysis (TGA) of PANI-(pristine CNT, ACNT and CCNT) nanocomposites respectively was conducted to ascertain their thermal stability characteristics (Figures 3.12).

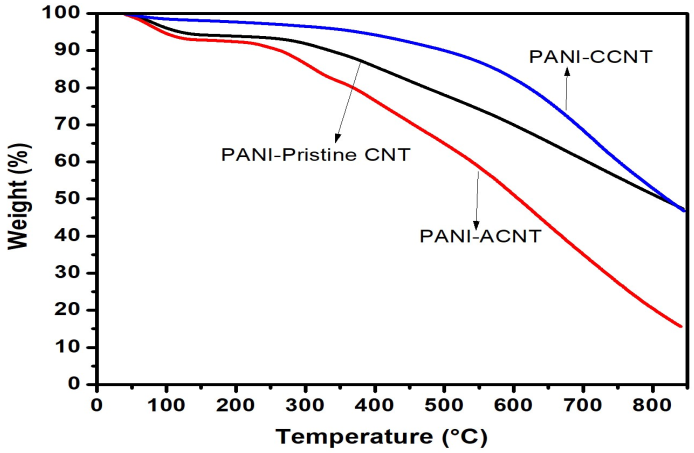

Figure 3.12. TGA curves of PANI-Pristine CNT, ACNT and CCNT

Figure 3.12 shows the TGA thermogram of PANI-MWCNTs (pristine CNT, ACNT and CCNT) composites. This analysis is to determine the effect of MWCNTs on the thermal stability of PANI and verse-versa. In the first step, approximately 5%, 8%, and 1% weight loss respectively for PANI- pristine CNT, PANI-ACNT and PANI-CCNT at the temperature up to 105°C is attributed to the loss of water molecules and unreacted organic monomers from the PANI-MWCNTs composite structure. The second weight loss of about 7%, 11% and 3% respectively at 220°C may be due to evaporation of dopant acids and low molecular weight oligomer in the PANI composites [13, 37]. The third step of weight loss usually referred to as oxidative degradation and decomposition temperature at between 500°C and 800°C has 21%, 35%, 10% and 51%, 21%, 53% weight loss and residues respectively for the three composites. The weight loss at all stage is much less for PANI-MWCNT nanocomposites compared to that of pure PANIs (bulk PANI-HCl, nano PANI-HCl and nano PANI-TSA) in Figure 3.4. These degradation patterns of PANI-MWCNT composites indicates the superior thermal stability which was due to the ordered structure of MWCNTs [38, 39].

3.3.3 Conductivity Measurements

The electrical conductivity of pelletized bulk PANI-HCl, nano PANI-HCl and nano PANI-TSA is measured using Keithley nanovoltmeter. The conductivity of bulk PANI-HCl, nano PANI-HCl and nano PANI-TSA are found to be 0.127, 0.478 and 0.824 S/cm^{-1} respectively. The increase in electrical conductivity of nano PANI-HCl and nano PANI-TSA may be due to the less particle size and high crystallinity compared to that of bulk PANI. The higher conductivity for TSA doped PANI may due to a stronger intermolecular interaction between aniline and counteranion molecules when TSA is incorporated [40-44]. This will facilitate the formation of a resonating structure thereby activating electron flow in the form of polaron over the whole structure of the polymer chain. Also, the sulfur content of the TSA dopant anions may have contributed to the molecular interactions resulting in higher conductivity [42-45].

Table 3.1. DC conductivity of PANI-(pristine CNT, ACNT and CCNT) composites as a function of weight ratio of PANI.

Ratio of MWCNTs in 200mg of PANI	Conductivity (S/cm)		
	Pristine CNT	**ACNT**	**CCNT**
1:0.25	0.85	1.37	0.55
1:0.50	0.64	0.97	0.94
1:0.75	0.85	0.76	0.91
1:1	1.14	0.42	4.17
1:1.25	0.80	0.31	1.86
1:1.50	1.66	0.18	1.48

The conductivity of PANI-MWCNTs (pristine CNT, ACNT and CCNT) as a function of weight ratio of MWCNTs is presented in Table 3.1. The conductivity of the composites is greatly improved by the introduction of MWCNTs in the PANI compared to neat PANI. The composites exhibited an order of magnitude increase in electrical conductivity with increase of the CNT content up to at a ratio 1:1. A remarkable increase in the conductivity (4.2 S/cm) was obtained for PANI-CCNT composite. The increase in conductivity of the composites may be due to the doping capability of carbon nanotubes where the nanotubes tends to compete with sulfonic ion. MWNTs may serve as conducting bridges between scattered islands of PANI, thereby boosting charge delocalization [42-46]. The improved crystallinity of PANI with the addition of MWNT is another possible reason for the increase in conductivity across the PANI-WMCNTs composites. However, it is observed that the composites containing functionalized MWCNTs (carboxylic acid and amine) were more stable and regular in the conductivity values compared to the pristine CNT.

3.4 Conclusion

The preparation of PANI/MWCNT composites was successfully performed by in situ polymerization method. The incorporation of MWCNT in the PANI matrix was confirmed by (UV–Vis), FTIR, SEM, TEM, TGA and XRD studies. SEM and TEM images confirmed that, in all of the PANI-MWCNT samples, the polymers were coated over the CNTs. UV–Vis spectra supported the presence of quinoid and benzoid rings; however, the lower intensity of the exciton absorption band of the quinoid rings supported the dominance of the benzoid ring. FTIR analysis revealed the formation of PANI and the change in polymer structure due to the introduction of CNTs in the polymer matrix. Thermal analysis shows enhanced thermal stability of polyaniline. TGA provided evidence for better thermal stability in the different PANI-MWCNT composites. The formation of hybrid materials was confirmed by XRD analysis as the X-ray peaks became sharper and peak broadening occurred because of the superimposition of the peaks of the CNTs and polymers. The polymerization of PANI with MWCNT causes strong interfacial interactions between PANI and MWCNT crystallites, also suggested by FT–IR and XRD studies, thereby changing the molecular conformation of PANI from compact structure to an expanded structure. The electrical-transport properties of the samples were measured at room temperature. The maximum conductivity was found in the PANI CCNT composite at ratio 1:1. Among the compositions investigated, this composition may be used as the best electronic conductor.

There is a visible enhancement in the conductivity of composites of PANI up as the MWCNT concentration increases.

Reference

[1] Shirakawa H, Lewis EJ, MacDiarmid AG, Chiang CK and Heeger AJ, 1977. Synthesis of electrically conducting organic polymers: halogen derivatives of polyacetylene (CH)x. J Chem Soc, Chem Comm, 16 578-580.

[2] Ameen S, Akhtar SM, Song M and Shin HS, 2013. Solar cells - research and application perspectives. In Arturo Morales-Acevedo (Eds) Metal oxide nanomaterials, conducting polymers and their nanocomposites for solar energy. InTech, p 203-259.

[3] Palaniappan S and John A, 2008. Polyaniline materials by emulsion polymerization pathway. Prog Polym Sci, 33 732-758.

[4] Bakhishi AK and Bhalla G, 2004. Electrically conducting polymers: Materials of the twenty-first century. J Sci and Ind Res, 63 715-728.

[5] Stejskal J and Gilbert RG, 2002. Polyaniline: preparation of a conducting polymer. Pure Appl Chem, 74 (5) 857-867.

[6] Rafeeq SN and Khalaf WZ, 2015. Preparation, characterization and electrical conductivity of doped polyaniline with (HCL and P-TSA). Eng Technol J, 33 (7) Part B 1220-1231.

[7] Yongfang Li, 2015. Organic optoelectronic materials, Yongfang Li (ed.), Springer International Publishing Switzerland, Lecture Notes in Chemistry 91, 23-50, doi:10.1007/978-3-319-16862-3.

[8] Yuan B, Yu L, Sheng L, An K and Zhao X, 2012. Comparison of electromagnetic interference shielding properties between single-wall carbon nanotube and graphene sheet/polyaniline composites. J Phys D: Appl Phys, 45 (23) 1-6.

[9] Abdullah ET, Hassan SM and Ahmed RS, 2016. Electrical properties of polyaniline/functionalized multi walled carbon nanotubes nanocomposite. Int J Current Eng Technol, 6 (2) 617-621.

[10] Iijima S, 1991. Helical microtubules of graphitic carbon. Nature, 354 56-58.

[11] Gogotsi Y, Naguib N, and Libera JA, 2002. In situ chemical experiments in carbon nanotubes. Chem Phys Letts, 365 354-360.

[12] Mathew H, Punnackal VS, Kuriakose S, Kumari BS and Manuel A, 2013. Synthesis and electrical characterization of polyaniline-multiwalled carbon nanotube composites with different dopants. Int J Sci Res Publication, 3 (8) 1-10.

[13] Kumar A, Kumar V, Kumar M and Awasthi K, 2017. Synthesis and characterization of hybrid PANI/MWCNT nanocomposites for EMI applications. Polym Compos, 1-11, doi:10.1002/pc.24418.

[14] Abdullah ET, Ahmed RS, Hassan SM and Naje AN, 2015. Synthesis and characterization of PANI and polyaniline/multi walled carbon nanotube composite. Int J Application Innovation Eng Mgt, 4 (9) 130-134.

[15] Ratheesh R and Viswanathan K, 2014. Chemical polymerization of aniline using para-toluene sulphonic acid. IOSR J Appli Phys, 6 (1) 1-9.

[16] Bachhav SG and Patil DR, 2015. Synthesis and characterization of polyaniline-multiwalled carbon nanotube nanocomposites and its electrical percolation behavior. Amer J Mater Sci, 5 (4) 90-95.

[17] Wu T-M and Lin Y-W, 2006. Doped polyaniline/multi-walled carbon nanotube composites: preparation, characterization and properties. Polymer, 47 (10) 3576-3582.

[18] Gajendran P and Saraswathi R, 2008. Polyaniline-carbon nanotube composites. Pure Appl Chem, 80 (11) 2377-2395.

[19] Chakraborty G, Gupta K, Rana D and Meikap AK, 2012. Effect of multiwalled carbon nanotubes on electrical conductivity and magnetoconductivity of polyaniline. Adv Nat Sci: Nanosci Nanotechnol. 3 (3) 1-8.

[20] Johny EJ, Ramakrishnan S, Rangarajan M and Kothurkar NK, 2013. Effect of different carbon fillers and dopant acids on electrical properties of polyaniline nanocomposites. Bull Mater Sci, 36 (1) 37-44.

[21] Calamba K, Ringor C, Pascua C and Miyazawa K, 2014. Pleated surface morphology of C60 fullerene nanowhiskers incorporated by polyaniline in N-methyl-2-pyrrolidone. Fullerenes, Nanotubes and Carbon Nanostructures, 23 (8) 709-714.

[22] Kulkarni MV and Kale BB, 2012. Development of optical pH sensor using conducting polyaniline-wrapped multiwalled carbon nanotubes (PANI-MWCNTs) nanocomposite. IMCS 2012 - The 14th International Meeting on Chemical Sensors, 934-937, doi:10.5162/IMCS2012/P1.3.2.

[23] Babu VJ, Vempati S and Ramakrishna S, 2013. Conducting polyaniline-electrical charge transportation. Mater Sci and Applications, 4 1-10.

[24] Khalid M, Tumelero MA, Brandt IS, Zoldan VC, Acuna JJS, and Pasa AA, 2013. Electrical conductivity studies of polyaniline nanotubes doped with different sulfonic acids. Indian J Mat Sci, 2013 1-7, doi.org/10.1155/2013/718304.

[25] Yılmaz F and Kuqukyavuz Z, 2009. Conducting polymer composites of multiwalled carbon nanotube filled doped polyaniline. J Appl Polym Sci, 111 680-684.

[26] Zhang J, Shi C, Ji T, Wu G and Kou K, 2014. Preparation and microwave absorbing characteristics of multi-walled carbon nanotube/chiral-polyaniline composites. Open J Polym Chem, 4 62-72.

[27] Choudhury A and Kar P, 2011. Doping effect of carboxylic acid group functionalized multi-walled carbon nanotube on polyaniline. Composites: Part B, 42 1641–1647.

[28] Shahnawaza S, Sohrabi B and Najafib M, 2014. The investigation of functionalization role in multi-walled carbon nanotubes dispersion by surfactants. The 18th International Electronic Conference on Synthetic Organic Chemistry, October 2014; 1-7, DOI: 10.3390/ecsoc-18-f002.

[29] Lu KL, Lago RM, Chen YK, Green MLH, Harris PJF and Tsang SC, 1996. Mechanical damage of carbon nanotubes by ultrasound. Carbon, 34 (6) 814-816.

[30] He BL, Dong B, Wang W and Li HL, 2009. Performance of polyaniline/multi-walled carbon nanotubes composites as cathode for rechargeable lithium batteries. Mater Chem Phys, 114 (1) 371-375.

[31] Thomassin J-M, Jerome C, Pardoen T, Bailly C, Huynen I and Detrembleur C, 2013. Polymer/carbon based composites as electromagnetic interference (EMI) shielding materials. Mater Sci and Eng R: Reports, 74 (7), 211-232.

[32] Zhao Y, Wu W, Chen J, Zou H, Hu L, and Chu G, 2012. Preparation of polyaniline/multiwalled carbon nanotubes nanocomposites by high gravity chemical oxidative polymerization. Ind Eng Chem Res, 51 3811-3818.

[33] Cui L, Yu J, Lv Y, Li G, Zhou S, 2013. Doped polyaniline/multiwalled carbon nanotube composites: preparation and characterization. Polym Comps, 34 (7) 1119-1125.

[34] Mogre P, Ganachari SV, Yaradoddi JS, Banapurmath NN, Hunashyal AM and Shettar AS, 2018. Synthesis and characterization studies of polyaniline nano fibres. Adv Mater Proceedings, 3 (3) 178-180.

[35] Haider AJ, Mohammed MR and Ahmed DS, 2014. Preparation and characterization of multi walled carbon naotubes/Ag nanoparticles hybrid materials. Int J Sci & Eng Res 5 (3) 255-260.

[36] Tomova A, Gentile G, Grozdanov A, Errico ME, Paunovic P, Avella M and Dimitrov AT, 2016. Functionalization and characterization of MWCNT produced by different methods. ACTA Phys Pol A, 129 (3) 405-408, doi: 10.12693/APhysPolA.129.405.

[37] Elsayed AH, Mohy-Eldin MS, Elsyed AM, A. H. Abo-Elazm AH, Younes EM and Motaweh HA, 2011. Synthesis and properties of polyaniline/ferrites nanocomposites. Int J Electrochem Sci, 6 206-221.

[38] Ghatak S, Chakraborty G, Meikap AK, Woods T, Babu R and Blau WJ, 2011. Synthesis and characterization of polyaniline/carbon nanotube composites. J Appl Polym Sci, 119 (2) 1016-1025.

[39] David T, Mathad JK, Padmavathi T and Vanaja A, 2014. Part A: Synthesis of polyaniline and carboxylic acid functionalized SWCNT composites for electromagnetic interference shielding coatings. Polym, 55 (22) 5665-5672.

[40] Das NC, Yamazaki S, Hikosaka M, Chaki TK, Khastgir D and Chakraborty A, 2005. Electrical conductivity and electromagnetic interference shielding effectiveness of polyaniline ethylene vinyl acetate composites. Polym Int 54 256-259.

[41] Chutia P and Kumar A 2014. Electrical, optical and dielectric properties of HCl doped polyaniline nanorods. Physica B, 436 200-207.

[42] Ajekwene KK and Thomas Kurian, 2018. Bulk and nano-structured polyaniline: synthesis, characterization, thermal behaviour and dc conductivity. Int J Res Advent Technolo, 6 (9) 2385-2391.

[43] Ajekwene KK, Jelmy EJ and Thomas Kurian, 2018. Preparation, characterization, thermal behaviour and dc conductivity of nano-structured polyaniline doped with HCL or TSA: a comparative analysis. J Emerging Technologies Inn Res, 5 (9) 284-288.

[44] Ajekwene KK, Jelmy EJ and Thomas Kurian, 2018. Preparation, characterization, thermal behaviour and dc conductivity of nanopolyaniline and polyaniline-multi walled carbon nanotube nanocomposites. J Emerging Technologies Inn Res, 5 (9) 374-388.

[45] Xiao Wang, Sudip Ray, Marija Gizdavic-Nikolaidis and Allan J Easteal 2012. The effects of dopant acids on structure and properties of poly(o-methoxyaniline). J Polym Sci Part A: Polym Chem, 50 353-361.

[46] Silva WM, Ribeiro H, Seara LM, Calado HDR, Ferlauto AS, Paniago RM, Leite CF and Silva GG, 2012. Surface properties of oxidized and aminated multi-walled carbon nanotubes. J Brazilian Chem Soc, 23 (6) 1078-1086.

…..◆…..

Chapter 4

IONOMER-POLYANILINE BINARY COMPOSITES: PREPARATION, PROPERTIES AND APPLICATIONS

Contents

Modification of polymeric materials by means of blending is a way to obtain products with high performance for specific and tailored applications. The present chapter reports the design and development of poly(ethylene-methacrylic acid copolymer) neutralized with zinc salt (EMAAZn) or sodium salt (EMAANa) and polyaniline (PANI: bulk PANI-HCl, nano PANI-HCl and nano PANI-TSA) binary composite films, with the aim of modifying EMAAZn or EMAANa to achieve high electromagnetic interference (EMI) shielding effectiveness (SE). EMAAZn/PANI and EMAANa/PANI binary composites are prepared in solution by dissolving EMAAZn or EMAANa in a solvent mixture of toluene/1-butanol (90:10) at 65 °C and mixing PANI in it. These binary composites are characterized and evaluated by FTIR, UV-Visible spectroscopy, XRD spectroscopy and thermogravimetric analysis (TGA). The electrical conductivity of the PANI, EMAAZn/PANI and EMAANa/PANI composites are measured by conventional four-probe method. The EMI shielding effectiveness is studied using a wave-guide coupled to an Agilent Synthesized Sweeper 8375A and a Hewlett-Packard spectrum analyzer 7000 in the X band frequency range (8-12 GHz). FTIR indicates a π-π and hydrogen bonding interaction between PANI and EMAAZn, enabling the PANI to be adsorbed on the ionomer. The results of electrical conductivity measurements and EMI SE demonstrates that a good synergism was established between PANI and EMAAZn or EMAANa substrate.

4.1 Introduction

It is well known that polymer materials (thermoplastics, thermosets, elastomers, etc.) possess good melt strength to bind PANI particles together in order to make it processable without compromising its conductivity and other properties of the polymer. One of the ways to achieve these benefits lies in the exfoliation of PANI into the polymer matrix to generate high aspect ratio particles [1-5]. Due consideration has to be given to a commercially important class of thermoplastic polymer such as ionomers, which consists of random copolymers of ethylene and methacrylic acid where some of the acid groups are neutralized to form metal salts. Characteristically, the methacrylic acid content of these polymers is low (<15 mol %) and the degree of neutralization ranges from 20 to 80% [6, 7]. This results in amorphous and crystalline phases along with ionic clusters in the polymer structure thereby improving the toughness, melt viscosity, clarity and adhesion properties of the polymer [8-14]. In this regard, ethylene/methacrylic acid ionomers have a distinct advantage over the base polyolefin, such as low-density polyethylene (LDPE). Ionomers are polymers containing hydrophobic backbone chains and a small amount of ionic salt groups attached on either the backbones, side chains or on backbone terminals thereby possessing polar groups which make it hydrophilic also. These polar salt groups form ionic aggregations such as mulitplets and clusters making the nonpolar chains to group together and the polar ionic groups to attract and cling to each other [15]. This allows thermoplastic ionomers to act in a way similar to that of crosslinked polymers or block copolymers [11, 16]. The ionic attractions that results strongly affect the polymer properties which dramatically increase the mechanical properties such as modulus, tensile strength, impact resistance and stiffness [15]. Based on these properties, ionomers are commonly used in commercial and industrial fields including electrodialysis, electrolysis, solid polymer electrolyte for batteries, potentiometric sensors, membranes for water treatment, solution recycling, filtering, proton exchange membranes for fuel cells, packaging, coatings, optics, medical and biological fields as sensors, membranes and dental restorative materials [17]. Mechanical and electrical properties of polymers are significantly influenced by the presence of fillers. Mixing thermoplastics with the electroconductive PANI, besides an increase of electroconductivity, lead to an increase of modulus and tensile strength accompanied by a decrease of deformability resulting in lower elongation at break and diminished toughness of the material [18].

Applications of polyaniline (PANI) in electrical and electronic devices, chemical and biological sensors, batteries, electrochromic displays, electronic devices, field effect transistors, electrochemical sensors, electromagnetic interference shielding materials, etc., has been sufficiently documented [2, 4, 19-24]. However, the insolubility of the doped form, poor mechanical and thermal properties and low processability of PANI have hindered its industrial applications [25-34]. To overcome these problems, PANI-thermoplastics composites / blends are prepared through direct polymerization within a matrix polymer, melt processing and dry mixing such as extrusion, injection or compression moulding and solution processing methods such as casting or spraying by using a suitable solvent and mixing the dispersion with a solution of a matrix polymer [3, 35-39]. This could extend their applications in electromagnetic shielding, antistatic charge dissipation, printed circuit boards for electronics applications, corrosion protection of metals such as iron, etc. [40]. The presence of the pendant ionic groups and the polar methacrylic acid groups in these ionomers potentially creates favorable interactions between the polymer and the PANI, resulting in a much more exfoliated morphology compared to composites prepared from LDPE and other forms [12, 41-43]. The modified PANI composites possess good electrical conductivity, good film properties and processability [1-5, 44, 45].

The present chapter reports the preparation, characterization, thermal behaviour, DC conductivity and EMI shielding effectiveness of EMAAZn-PANI binary composites as Part A and EMAANa-PANI binary composites as Part B. PANI obtained via chemical oxidative polymerization of aniline is blended with the ionomers through a novel solution blending method to obtain good conductivity and film forming strength.

Part A

Studies on Zinc Ionomer-Polyaniline Binary Composites

This part reports the design and development of poly(ethylene-methacrylic acid copolymer) neutralized with zinc salt (EMAAZn) and polyaniline (PANI: bulk PANI-HCl, nano PANI-HCl and nano PANI-TSA) binary composite films, with the aim of modifying EMAAZn in order to achieve improved electrical conductivity and high electromagnetic interference (EMI) shielding effectiveness (SE). EMAAZn-PANI binary composites were prepared in solution by dissolving EMAAZn in solvent using a solvent mixture of toluene/1-butanol (90:10) at 65 °C and mixing PANI in it. These binary composites were characterized and evaluated by FTIR, UV-Vis spectroscopy, XRD spectroscopy, thermogravimetric analysis (TGA). The electrical conductivity of the PANI, EMAAZn-PANI binary composites were measured by conventional four-probe method. The EMI shielding effectiveness was studied using a wave-guide coupled to an Agilent Synthesized Sweeper 8375A and a Hewlett-Packard spectrum analyzer 7000 in the X band frequency range (8-12 GHz).

4A.1 Experimental Methods

4A.1.1 Preparation of Ionomer-Polyaniline Composites

The ionomer (EMAAZn) was dissolved in a mixture of toluene: 1-butanol solvents at a ratio of 90:10 at 65°C. Varying weights (0.1g, 0.3g, 0.5g, 0.7g, 1.0g, 1.2g, 1.5g and 2.0g) of the as prepared three types of PANI (bulk PANI-HCl, nano PANI-HCl and nano PANI-TSA) were mixed thoroughly by magnetic stirring in the ionomer solution for the preparation of polyaniline-ionomer binary composites.

A constant weight percentage (1.0g of ionomer in 100ml solvent mixture) each of the ionomers was used in all the composite blends. The dissolved solution of ionomer/PANI composites were allowed to evaporate to get a solid film in a petri dish and dried in vacuum oven at 50°C for 24 hours.

4A.1.2 Characterization and Instrumental Analysis

The microstructure of the samples was examined by Fourier transform infrared (FTIR) spectroscopy using a Thermo Nicolet Avatar 370 FTIR spectrometer. The compositional state of the samples was determined using X-Ray Powder Diffractometry (XRD - Bruker AXS D8). The optical absorption by the sample in the UV and visible region was measured with Varian Cary 5000 UV-Visible spectrophotometer in the spectral range 225-1000 nm. Thermo gravimetric analysis (TGA) was performed on a Perkin Elmer STA 6000 thermogravimetric analyzer to determine decomposition, transition temperatures and thermal stabilities of the samples. The electrical properties of the PANI samples were measured by four probe technique (D.C conductivity) using sensitive digital electrometer type Keithley Agilent 616. EMI shielding measurements was performed using a wave-guide coupled to an Agilent Synthesized Sweeper 8375A and a Hewlett-Packard spectrum analyzer 7000 in the X band frequency range (8-12 GHz).

4A.2 Results and discussions

4A.2.1 Fourier Transform Infrared (FTIR) Spectroscopy

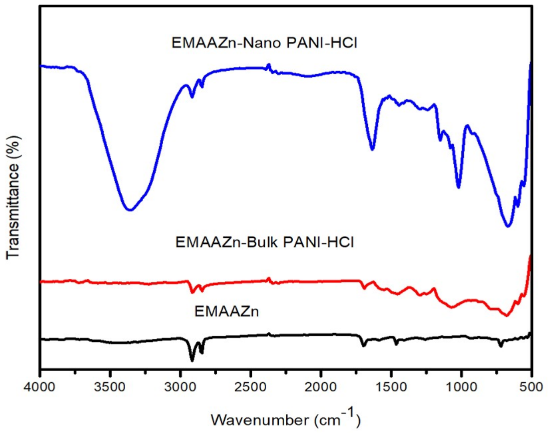

Figure 4.1a. FTIR spectra of EMAAZn and EMAAZn-Bulk PANI-HCl and Nano PANI-HCl binary composites.

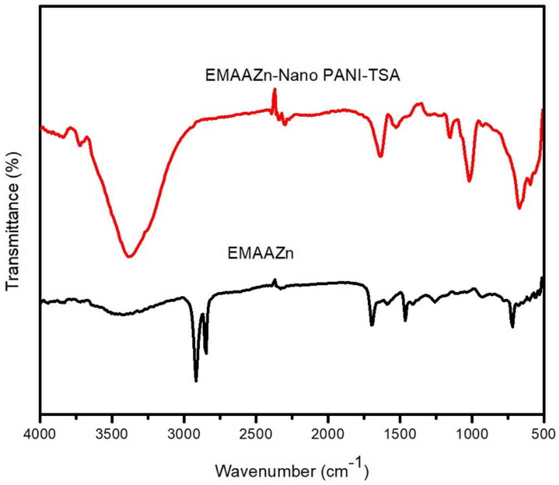

Figure 4.1b. FTIR spectra of EMAAZn and EMAAZn-Nano PANI-TSA binary composites.

Figure 4.1a shows the FTIR spectra of EMAAZn and EMAAZn-PANI (bulk PANI-HCl and nano PANI-HCl) binary composites. Figure 4.1b shows the FTIR spectra of EMAAZn and EMAAZn-Nano PANI-TSA binary composites. The region of 1500-1750 cm^{-1} bands observed in all samples as shown in Figures 4.1a and 4.1b is ascribed to the asymmetric stretching vibrations of carboxylate groups [46, 47]. The COO- of EMAAZn consist of a peak at 1460 cm^{-1}, a small peak at 1691 cm^{-1} and two shoulder peaks at 2900 cm^{-1} and 2840 cm^{-1} which is different from the peaks in the composites especially in ionomer/TSA doped nanopolyaniline composite. These differences is attributable to the changes in the local environment exerted by the neutralizing cations (Zn^{2+}) in the blend. This is an indication that interactions exist between the EMAAZn-PANI thereby forming a new structure in the ionic aggregates [46, 49]. The spectrum of the film obtained after mixing of PANI with EMAAZn, presents all the bands of EMAAZn and PANI.

4A.2.2 X-Ray Diffractometry (XRD)

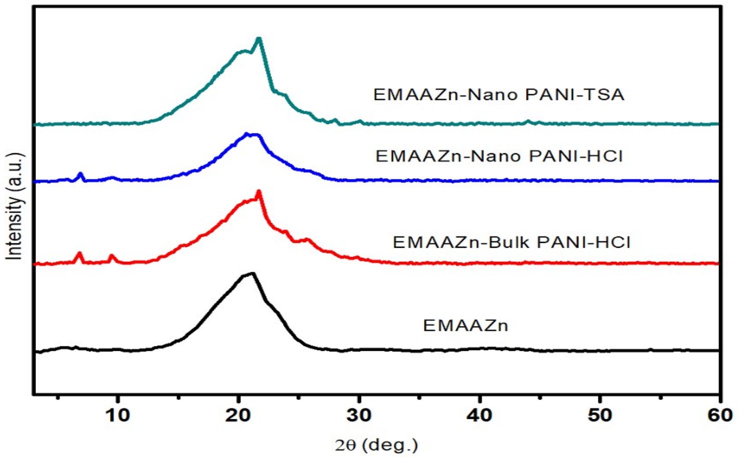

Figure 4.2. XRD profiles of Bulk PANI-HCl, Nano PANI-HCl and Nano EMAAZn binary composites.

Figure 4.2 represents the XRD of EMAAZn-PANI (bulk PANI-HCl, nano PANI-HCl and nano PANI-TSA) binary composites. The EMAA-Zn pattern shows a single broad peak at around 2 θ = 21° indicating that the material is semi crystalline in nature. This peak is called an ionic peak and it is attributed to the aggregation of ionic groups such as COO-Zn in the ionomer [41, 46, 50]. This sharp peak around 2θ =21° in the neat Zinc ionomer is very prominent in all the three PANI-Zn ionomer binary composites. The diffraction pattern of EMAAZn -PANI doped with hydrochloric acid (bulk PANI-HCl and nano PANI-HCl) showed similar sharp peaks at 2θ equal to 21°, 23° and 25°. The diffraction pattern of the toluene sulphonic acid (TSA) doped PANI (nano PANI-TSA)-zinc salt ionomer is observed to have sharp bands at 2θ equal to 21°, 23°, 27°, 30° and 44°. The peaks observed at 21° and a shoulder peak at 23° correspond to the presence of polyethylene crystallites in the EMAA ionomer [5, 7]. These observations are consistent with the degree of polyethylene crystallinity [51, 52].

4A.2.3 UV-Visible spectroscopy (UV-Vis)

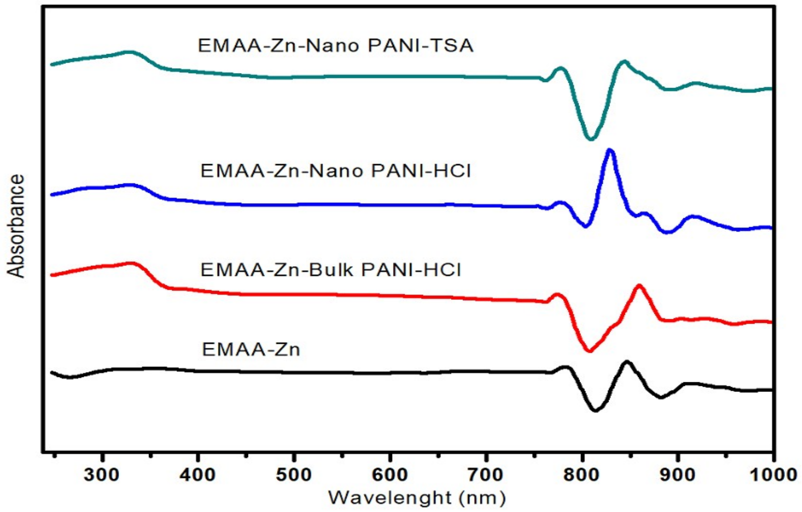

Figure 4.3. UV-Visible spectra of Bulk PANI-HCl, Nano PANI-HCl and Nano PANI-TSA-EMAA-Zn binary composites.

The UV-Visible spectra of PANI (bulk PANI-HCl, nano PANI-HCl and nano PANI-TSA)-EMAAZn binary composites were shown in Figure 4.3. Absorption bands observed in the EMAAZn are all present in the composites. The shift observed in the EMAAZn from 915 nm to 930, 991 and 995 nm in EMAAZn-PANI (bulk PANI-HCl, nano PANI-HCl and nano PANI-TSA) respectively is attributable to the introduction of PANI in the composites. This might be due to exfoliation and homogeneous interaction between EMAAZn and PANI. However, the red shift observed in absorption peaks at 991 nm and 995 nm observed in composites of EMAAZn-nano PANI (nano PANI-HCl and nano PANI-TSA) might be due to the dimensions of the particle size of the PANI in the blends. Based on the UV-visible spectroscopic analysis as seen in the absorption bands, it can be observed that the composite films have lower UV transmission compared to the EMAAZn. Therefore, they can reasonably shield from UV radiation and hence, could be suitable for UV resistant applications. The visible light transparency of all the composite films are as well lower than that for neat ionomer at the near IR and visible region; therefore, are expected to be resistant to the UV radiation [40, 48].

4A.2.4 Thermogravimetric analysis (TGA)

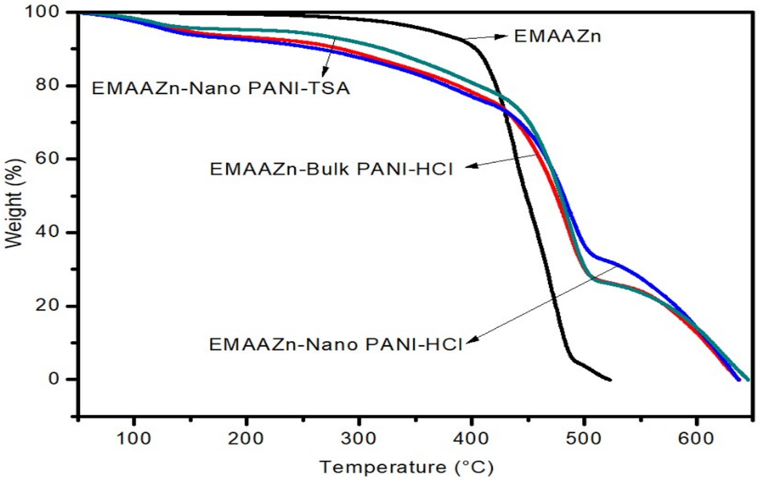

Figure 4.4. TGA curves of EMAAZn-Bulk PANI-HCl, Nano PANI-HCl and Nano PANI-TSA binary composites

Figure 4.4 shows the TGA thermogram of EMAAZn and EMAAZn-PANI (bulk PANI-HCl, nano PANI-HCl and nano PANI-TSA) binary composites. The EMAAZn exhibits two major decompositions. The initial weight loss of 8% is observed at 200 ^{O}C to 430 °C for the ionomer [53, 54]. This is due to the moisture removal and dequaternization at Zn+ site. The second weight loss of 95% is observed at 430 °C – 488 °C. The weight loss occurring in this stage may be due to scission in zinc ionic aggregate linkage of the monomeric units of ionomer. Complete rupture of the ionomer is observed at around 520 °C. The composites shows a typical three stage decomposition. The initial weight loss of 6%, 5% and 4% is observed for EMAAZn-bulk PANI-HCl, EMAAZn-nano PANI-HCl and EMAAZn-nano PANI-TSA composites respectively at 150 °C due to the removal of moisture. The weight loss in the stage two is about 28% each for (EMAAZn-bulk PANI-HCl and EMAAZn-nano PANI-HCl) composites and about 24% for (EMAAZn-nano PANI-TSA) composite at 430 °C. It may be due to the scission in amide linkage of both monomeric units of ionomer and it is found to be around 73% each for EMAAZn-bulk PANI-HCl and EMAAZn-nano PANI-TSA) composites and 67% for EMAAZn-nano PANI-HCl) at 510 °C. The decomposition temperature showed that the stability of ionomer increased with the introduction of PANI in the blends owing to the reduction in segmental mobility.

4A.2.5 Conductivity Measurements

Table 4.1 shows the electrical conductivity of the EMAAZn-PANI (bulk PANI-HCl, nano PANI-HCl and nano PANI-TSA) binary composites as a function of weight concentration of PANI in the composites. Zinc ionomer (EMAAZn) is an insulating thermoplastic material whose electrical conductivity lies around 10^{-17}-10^{-18} Scm^{-1} at room temperature [55].

Table 4.1. DC conductivity of EMAAZn-PANI (bulk PANI-HCl, nano PANI-HCl and nano PANI-TSA) binary composites as a function of weight ratio of PANI of 1.0g of EMAA-Zn

Weight of PANI (g)	**Conductivity (S/cm) of EMAAZn- PANI**		
	Bulk PANI-HCl	**Nano PANI-HCl**	**Nano PANI-TSA**
0.1	$3.43E^{-4}$	4.66E-4	4.76E-4
0.3	$3.71E^{-4}$	4.78E-4	4.92E-4
0.5	$3.31E^{-4}$	4.73E-4	4.97E-4
0.7	$3.53E^{-4}$	4.74E-4	1.15E-3
1.0	8.2E-4	1.86E-3	3.45E-3
1.2	$2.53E^{-4}$	3.52E-4	5.21E-4
1.5	$1.25E^{-4}$	2.24E-4	4.16E-4
2.0	$1.78E^{-4}$	3.34E-4	3.80E-4

The electrical conductivity as a function of PANI content in the composites with EMAAZn is presented in Table 4.1. The conductivity of EMAAZn ionomer increased from insulator level to semiconductor range on the addition of even 0.1 g of PANI. The conductivity gradually increases with increase in amount of PANI, possibly owing to the quality of intermolecular interactions between PANI and EMAAZn causing a possible good and homogenous conductive network. A percolation threshold is observed at 1:1 PANI-ionomer for all the three composites (EMAAZn-bulk PANI-HCl, EMAAZn-nano PANI-HCl and EMAAZn-nano PANI-TSA), which exhibit a conductivity jump in the percolation region. Beyond the percolation region, the conductivity level slowly decreases with the PANI content owing to the absence of a continuous network of PANI due to agglomeration. The results showed that the interaction between the macromolecules of PANI and EMAAZn in their composites, particularly those of EMAAZn-nano PANI-HCl and EMAAZn-nano PANI-TSA are stronger due to high surface area of nano PANI than in composite of EMAAZn-bulk PANI-HCl, thus resulting in a better compatibility and higher electrical conductivity. This is most pronounced in the composites of EMAAZn-nano PANI-TSA with the highest values of conductivity. It may be due to the influence of the intermolecular interactions and chemical interactions between aniline [56, 57] and counteranion molecules of TSA during polymerization of polyaniline thereby forming a stronger and stable bipolaron responsible for electronic oxidation (protonation) of the polymer. The positive charges localized in -NH groups during protonation enable the bipolaron to move along the chain without the need for protons to hop and thereby giving rise to higher electronic conductivity [38, 58-60].

4A.2.6 Electromagnetic Interference (EMI) Shielding Effectiveness (SE)

The use of conducting polymers as microwave absorbers and electromagnetic interference shielding materials have attracted increased attention due to their good electrical conductivity, processability, light weight and non-corrosiveness especially when blended with polymer matrix [61-63]. The shielding effectiveness of the conducting composites of EMAAZn-PANI binary composites prepared by solution blending of EMAAZn is measured using a Vector Network Analyzer. The values of the shielding effectiveness at 8.5 GHz measured for the different loading levels of the different PANIs in the EMAAZn matrix are shown in Table 4A.2

Table 4.2. Shielding Efficiency of EMAAZn-PANI (bulk PANI-HCl, nano PANI-HCl and nano PANI-TSA) binary composites as a function of weight ratio of PANI in 1.0g of EMAA-Zn at 8.5 GHz
Zinc ionomer alone: SE = -0.2874 dB

Weight of PANI (g)	Shielding Efficiency (dB) of EMAAZn-PANI		
	Bulk PANI-HCl	Nano PANI-HCl	Nano PANI-TSA
1.0	-10.0	-12.9	-13.9
1.2	-13.5	-14.7	-20.2
1.5	-15.7	-15.7	-21.9
2.0	-15.2	-18.2	-26.1

The results indicate that the shielding effectiveness increases with the increase of PANI concentration in the composites. The measured value of EMI SE of the neat EMAAZn film is 0.2874 dB and did not exhibit EMI shielding efficiency. The shielding effectiveness of the composites (shown in Table 4.2) is increased with increase in PANI content. Comparing the shielding efficiency of the various composites, the higher shielding effectiveness is achieved in the EMAAZn-nano PANI-TSA composite which shows the highest attenuation value of -26.1 dB at the baseline frequency of 8.5 GHz. Filler content loading and thereby electrical conductivity are the very important parameters with respect to electromagnetic interference (EMI) shielding effectiveness (SE). Materials which could be useful for EMI shielding applications are normally expected to have a minimum of -20dB attenuation. At this minimum value of shielding more than 99% of the incident wave is attenuated ensuring that electronic equipment does not generate or it is not affected by electromagnetic interference [64]. The values of attenuation obtained in this work are lower in EMAAZn-PANI (bulk PANI-HCl and nano PANI-HCl) than the minimum of attenuation that ensures safety. From the results it is clear that the increase in weight fraction of PANI can increase the EMI shielding efficiency to more than -20dB. However, values of attenuation in the EMAAZn-nano PANI-TSA (1.2g, 1.5g and 2.0g) composites shows well above the minimum requirement and therefore, it can be useful as effective EMI shielding material. The variation of EMI shielding effectiveness at various frequencies (8.0-12 GHz) is measured for the different loading levels of PANI-TSA in EMAAZn matrix are shown in Figure 4.5.

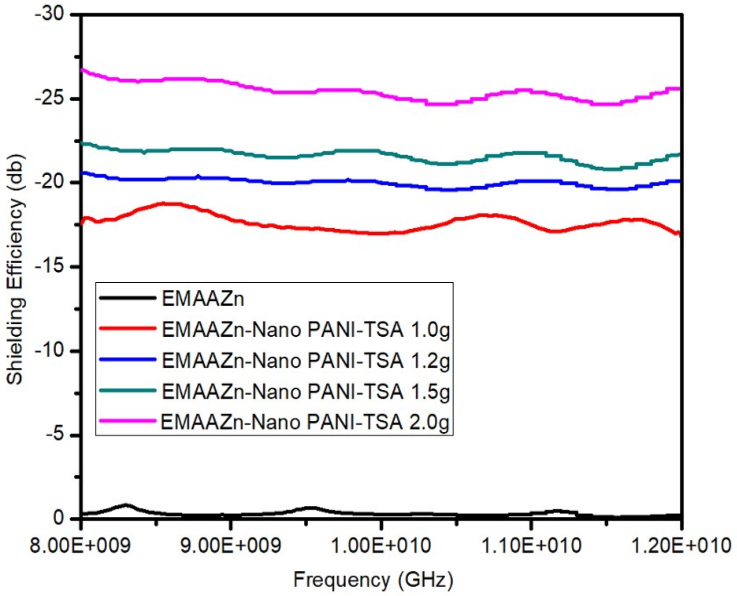

Figure 4.5. Shielding Efficiency of EMAAZn-PANI nano PANI-TSA) binary blends as a function of weight ratio of PANI in 1.0g of EMAA-Zn at 8.5 GHz

The EMI shielding effectiveness is almost similar at varying frequencies indicating the material is useful at all frequencies of the X-band (8 GHz to 12 GHz).

Part B

Studies on Sodium Ionomer-Polyaniline Binary Composites

Part B reports the fabrication of poly(ethylene-methacrylic acid copolymer) neutralized with sodium salt (EMAANa) and polyaniline (PANI: bulk PANI-HCl, nano PANI-HCl and nano PANI-TSA) binary composite films, with the aim of modifying EMAANa in order to achieve improved electrical conductivity and high electromagnetic interference (EMI) shielding effectiveness (SE).

4B.1 Experimental Methods

4B.1.1 Preparation of Sodium Salt Ionomer-Polyaniline Binary Composites

The ionomer-polyaniline composite is prepared by following the same procedure as described in PART A with sodium salt of poly(ethylene-co-methacrylic acid) (EMAANa)) as ionomer instead of EMAAZn ionomer.

4B.1.2 Characterization and Instrumental Analysis

The characterization was done using the same methods as detailed in PART A.

4B.2 Results and discussions

4B.2.1 Fourier Transform Infrared (FTIR) Spectroscopy

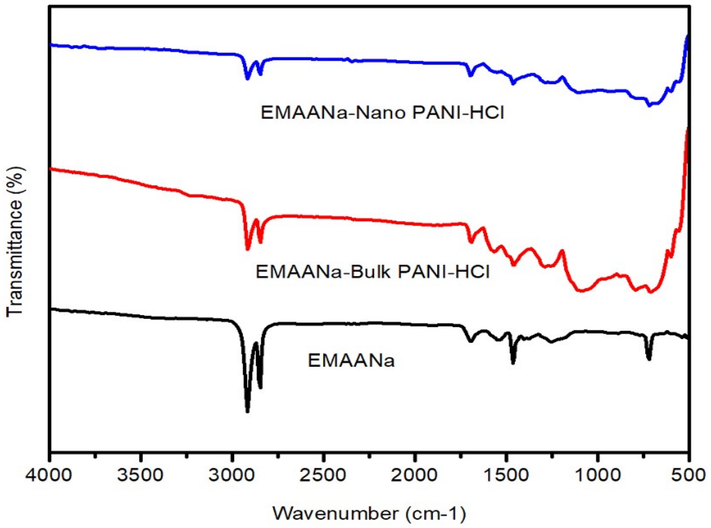

Figure 4.6a. FTIR spectra of EMAANa and EMAANa-Bulk PANI-HCl and Nano PANI-HCl binary composites.

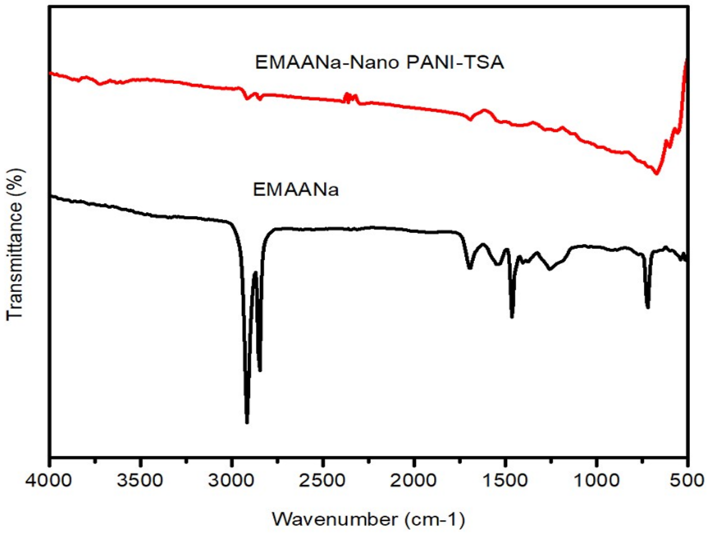

Figure 4.6b. FTIR spectra of EMAANa and EMAANa-Nano PANI-TSA binary composites.

Figure 4.6a shows the FTIR spectra of EMAANa and EMAANa-PANI (bulk PANI-HCl and nano PANI-HCl) binary composites. Figure 4.6b shows the FTIR spectra of EMAANa and EMAANa-PANI-TSA composite. The analysis of the spectra of the ionomer (EMAANa) shows a sharp band at 722 cm^{-1} is caused by methylene rocking in the pendant backbone. The 1250 cm^{-1} broad peak is attributed to C-O stretching vibrations of COOH groups. The band around 1500 cm^{-1} is due to CO_2^- groups. The peak with a wavelength of 1697 cm^{-1} is due to C=O stretching vibrations [46, 65-67]. The sharp peaks with high intensity observed in the spectra of EMAANa became broad and weak in composites with the different PANIs as shown in the Figure 4.6. These differences reflect changes in the local environment of the neutralizing cations Na+ with the PANI, indicating that EMAANa-PANI forms a new structure in the ionic aggregates. The spectrum of the film obtained after blending of PANI with EMAANa, presents all the bands of EMAANa (Figure 4.6a and b) and PANI (Figure 3.3). However, as reported previously in Figure 4.1b, these bands are not prominent in the EMAANa-PANI-TSA composite (Figure 4.6b).

4B.2.2 X-Ray Diffractometry (XRD)

Figure 4.7 represents the XRD of EMAANa-PANI (bulk PANI-HCl, nano PANI-HCl and nano PANI-TSA) binary blends. The EMAANa pattern shows a single broad peak at around $2\theta = 21°$ indicating that the material is semi crystalline in nature. This peak is known as ionic peak and is attributed to the aggregation of ionic groups in the ionomer resulting in a strong ionic interactions of the metal salts in the ordered structure of the ionic salt groups (ionic crystallites) [13, 46]. A second small shoulder-like peak located at 2θ =24° corresponds to the presence of the crystalline polyethylene crystallites in the EMAA ionomer [7, 68].

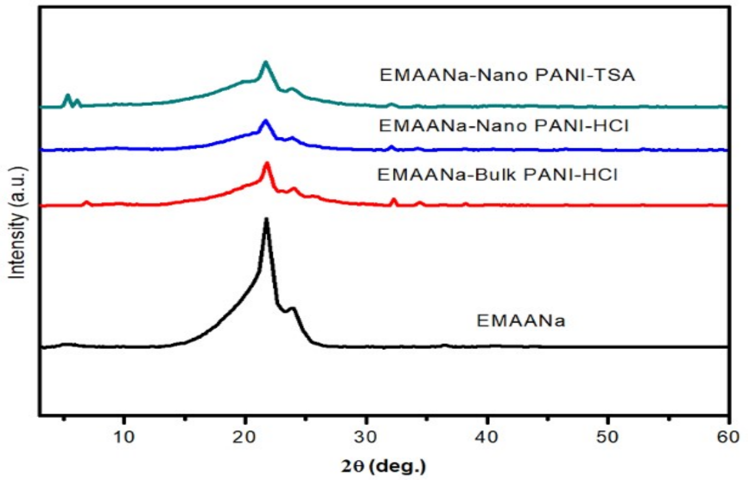

Figure 4.7. XRD profiles of EMAANa-Bulk PANI-HCl, Nano PANI-HCl and Nano PANI-TSA binary composites

This characteristics is also reflected in the composites. The diffraction pattern of sodium salt ionomer-PANI doped with hydrochloric acid doped (bulk PANI-HCl and nano PANI-HCl) shows sharp peaks at 2θ equal to 7°, 21°, 24° 26°, 32°, 35° and 38°for bulk PANI-HCl and 2θ equal to 21°, 24°, 32°, 34° and 38° for nano PANI-HCl. The diffraction pattern of the toluene sulphonic acid (TSA) doped PANI (nano PANI-TSA)-EMAANa is observed to have sharp bands at 2θ equal to 5°, 6°, 21°, 24°, 32°, and 40°. These observations are consistent with the degree of polyethylene crystallinity [69, 70] and the XRD pattern of doped PANI. The peaks observed for the composites are found to be relatively weaker and broader than the neat EMAANa suggesting the extent of intercalation and exfoliation of PANI in EMAANa and indicating a better compatibility between the hydrophobic and the hydrophilic phases in the ionomer blends.

4B.2.3 UV-Visible spectroscopy (UV-Vis)

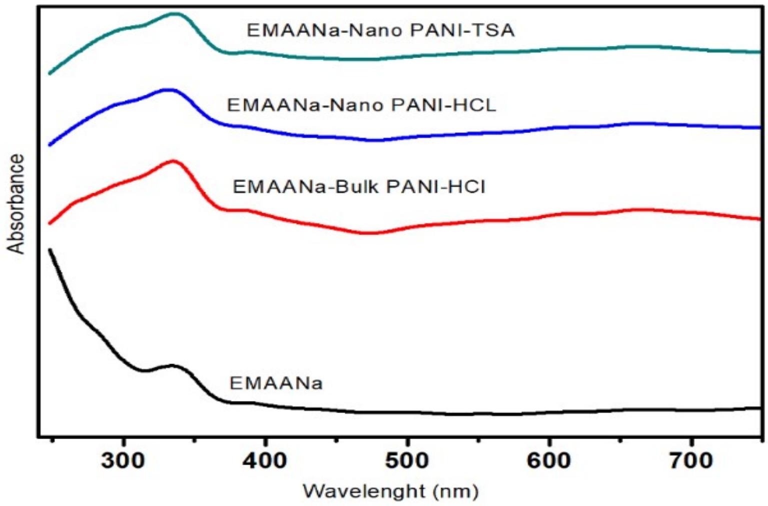

Figure 4.8. UV-Visible spectra of EMAANa-Bulk PANI-HCl, Nano PANI-HCl and Nano PANI-TSA binary composites

The UV-Visible spectra of EMAANa and EMAANa-PANI (bulk PANI-HCl, nano PANI-HCl and nano PANI-TSA) binary composites are shown in Figure 4.8. Absorption band at 335 nm, is observed for Na ionomer (EMAANa) and the three composites of EMAANa-PANI (bulk PANI-HCl, nano PANI-HCl and nano PANI-TSA). Two main absorption bands at 277-288 nm and 608-663 nm in all three PANIs (Figure 3.3 chapter 3) are not visible in the binary composites. This might be due to exfoliation and homogeneous interaction between ionomer and PANI. Based on the UV-visible spectroscopic analysis as shown in the absorption bands, it is observed that the composite films have lower UV transmission compared to what is observed in EMAAZn-PANI composites studied in Part A. Therefore, it can shield better from UV radiation and hence, it could be suitable for UV resistant applications.

4B.2.4 Thermogravimetric analysis (TGA)

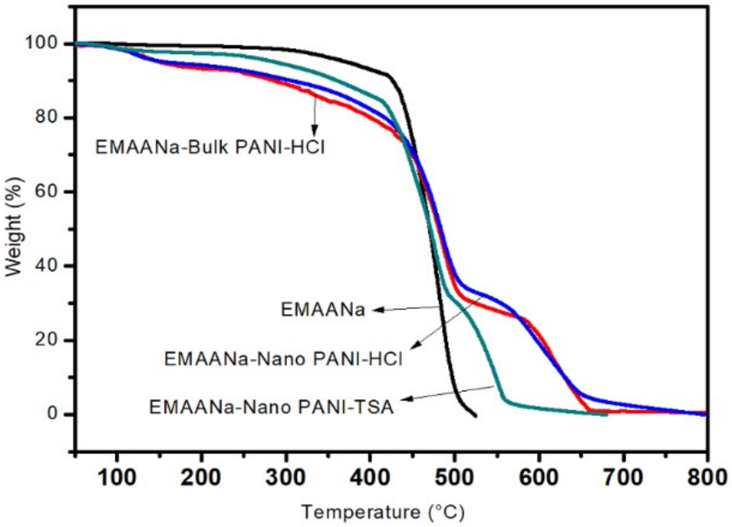

Figure 4.9. TGA curves of EMAANa-Bulk PANI-HCl, Nano PANI-HCl and Nano PANI-TSA binary composites

Figure 4.9 shows the TGA thermogram of ionomer (EMAANa)-PANI (bulk PANI-HCl, nano PANI-HCl and nano PANI-TSA) binary composites. The ionomer (EMAANa) shows first weight loss (10%) due to the loss of the methacrylic acid at the temperature range of 300°C to 420°C. The second observed weight loss which is the thermal decomposition of the ionomer (decomposition temperature) resulted in a sharp increase of weight loss of about 96% is observed between 420°C to 500°C with a residue of 4%. This is attributable to loss of the methacrylate back-bone apparently due to the scission in ionic aggregate linkage of the monomeric units of ionomer [53, 53b, 54]. These decomposition patterns changed with the composites which retarded the degradation of the molecules of the ionomer at higher temperatures. Similar results is obtained with EMAAZn as reported previously in PART A. The improved decomposition temperature showed that the stability of ionomer increased with the introduction of PANI in the blends owing to the reduction in segmental mobility.

4B.2.5 Conductivity Measurements

In chapter 3 (3.5), the electrical conductivity of pelletized bulk PANI-HCl, nano PANI-HCl and nano PANI-TSA are reported to be 0.127, 0.478 and 0.824 S/cm^{-1} respectively with nano PANI-HCl and nano PANI-TSA possessing higher conductivity values compared to bulk PANI-HCl. These difference in the electrical conductivities of PANI samples is attributed to the less particle size and higher crystallinity [71]. The PANI samples are solution blended at various loading values with constant weight of Na ionomer (EMAANa). The same trend of conductivity differences as in the case of EMAAZn is also manifested in the composites of EMAANa as shown in Table 4.3.

Table 4.3. DC electrical conductivity of ionomer (EMAANa)-PANI (bulk PANI-HCl, nano PANI-HCl and nano PANI-TSA) binary blends as a function of weight ratio of PANI of 1.0g of EMAA-Na.

Weight of PANI (g)	Conductivity (S/cm) of EMAANa- PANI		
	Bulk PANI-HCl	Nano PANI-HCl	Nano PANI-TSA
0.1	5.41E-4	6.33E-4	6.73E-4
0.3	5.38E-4	6.62E-4	1.91E-3
0.5	5.63E-4	7.37E-4	3.25E-3
0.7	5.74E-4	2.15E-3	4.27E-3
1.0	9.86E-4	2.75E-3	5.45E-3
1.2	5.52E-4	1.21E-3	4.31E-3
1.5	5.34E-4	1.16E-3	5.36E-3
2.0	5.25E-4	9.65E-4	4.81E-3

The electrical conductivity of the various composites increased in the order: EMAANa-bulk PANI-HCl<EMAANa-nano PANI-HCl<EMAANa-nano PANI-TSA. The gradual increases in conductivity with the content of PANI observed for all the composites is attributed to the difference of intermolecular interactions between PANI and EMAANa causing a possible good and homogenous conductive network. The incidence of percolation threshold (the inflexion point on the dependence of electrical conductivity on filler concentration) occurred at 1:1 EMAANa-PANI similar to the results reported in PART A with composite series (Table 4.1), where conductivity increase sharply and reached a peak value at 1:1 composition and then reduced. However, in comparison with the conductivity values obtained for the EMAAZn based composites, the EMAANa based composites shows higher conductivity values. This may be due to the difference in the electrochemical activity state of the metallic salts present in the ionomers (zinc and sodium). Most metals are electropositive in nature and the metal atoms lose electrons in chemical reactions to form cations. The more reactive a metal, the greater tendency it has to form a positive ion in a chemical reaction; thereby, making it a good conductor of heat and electricity. In this case, sodium is higher than zinc in the electrochemical series, hence would be more ionic resulting in the stronger ionic interactions of the metal salts in the ordered structure of ionic salt groups (ionic crystallites)and would likely show better conductivity. The results shows that EMAANa-nano PANI-HCl and EMAANa-nano PANI-TSA has better conductivity values with EMAANa-nano PANI-TSA having the highest electrical conductivity compared to EMAANa-bulk PANI-HCl [3, 56, 57, 71] for reasons discussed in PART A.

4B.2.6 Electromagnetic Interference (EMI) Shielding Effectiveness (SE)

The uses of conducting polymers as microwave absorbers and electromagnetic interference shielding materials have attracted increased attention due to their good electrical conductivity, processability, light weight and non-corrosiveness especially when blended with polymer matrix. [61-63].The shielding effectiveness of the conducting composites of EMAANa-PANI binary composites prepared by solution blending of EMAANa and PANI was measured. The values of the shielding effectiveness at 8.5 GHz is measured for the loading 1:1, 1:1.2, 1:1.5 and 1:2 PANI in the ionomer matrix are shown in Table 4.4.

Table 4.4. Shielding effectiveness of EMAANa-PANI (bulk PANI-HCl, nano PANI-HCl and nano PANI-TSA) binary composites as a function of weight ratio of PANI in 1.0g of EMAA-Na at 8.5 GHz. EMAANa: SE = -0.3197dB

Weight of PANI (g)	Shielding Efficiency (dB) of EMAANa-PANI		
	Bulk PANI-HCl	Nano PANI-HCl	Nano PANI-TSA
1.0	-11.2	-12.8	-18.7
1.2	-16.5	-17.7	-22.2
1.5	-18.7	-18.7	-24.9
2.0	-19.2	-21.2	-29.1

The results indicate that the shielding effectiveness generally increased with the incorporation of PANI in the composites as neat ionomer film exhibited very low EMI shielding efficiency of 0.3197 dB. The composites containing 1:2 weight ratio of EMAANa-bulk PANI-HCl shows shielding effectiveness of -19.2 dB while the shielding effectiveness of composites containing same grams of nano PANI-HCl in 1g EMAANa shows shielding efficiency of around -21.2. In the same measure, the SE of nano PANI-TSA in 1g EMAANa showed shielding effectiveness of -29.1 dB. As reported earlier in PART A (Table 4A.2), EMAANa-nano PANI-TSA shows better shielding effectiveness compared to its EMAANa-nano PANI-HCl and EMAANa-bulk PANI-HCl counterparts. From the values obtained in Table 4.4 maintaining the same PANI content loading as in Table 4.2, EMAANa-PANI composites are slightly better than EMAAZn-PANI for EMI shielding. The variation of EMI shielding effectiveness with varying frequencies at X- band (8.0-12 GHz) measured for the different loading levels of the different PANI-TSA in the EMAANa matrix are shown in Figure 4.10.

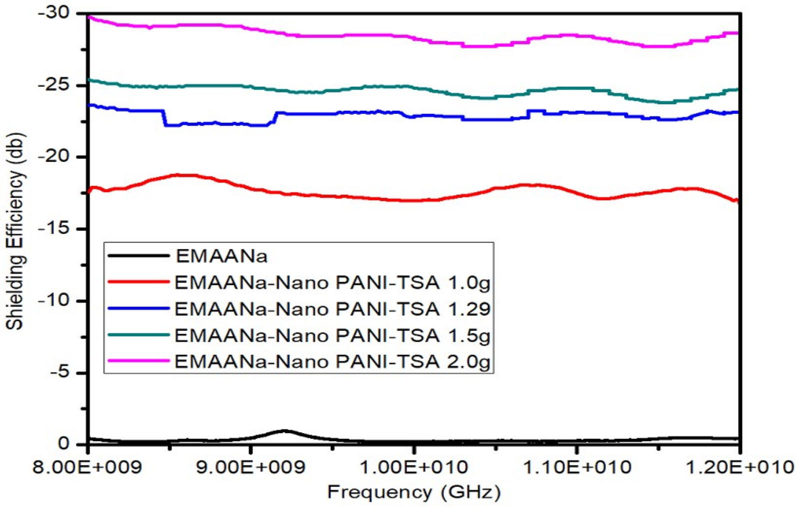

Figure 4.10. Shielding Efficiency of EMAANa-PANI nano PANI-TSA) binary blends as a function of weight ratio of PANI in 1.0g of EMAA-Zn at 8.5 GHz

Electrical conductivity and or filler content loading are very important parameters with respect to electromagnetic interference (EMI) shielding effectiveness (SE). While conductivity requires connectivity, EMI shielding requires only conductive particles to interact and impede the radiations [71]. Figure 4.10 indicates that the EMAANa-nano PANI-TSA composite shows almost same values of -28 dB at frequencies of 8 GHz, 9 GHz, 10 GHz, 11 GHZ and 12 GHz and hence this composite is suitable for EMI shielding applications at all frequencies of X-band.

4.2 Conclusions

The ionomers (EMAAZn or EMAANa) matrix could be successfully and effectively dissolved in the solvent blend of toluene and 1-butanol at 65°C. The composites of EMAAZn or EMAANa and PANI could be prepared by mixing the ionomer solution with PANI. The enhancement of the electrical conductivity and electromagnetic interference (EMI) shielding effectiveness (SE) of EMAAZn or EMAANa matrices upon mixing with PANI clearly indicates the successful introduction of PANI into matrices by solution mixing. Results of UV-visible spectroscopic analyses establish lower UV transmission in the binary composite films compared to the neat matrices (EMAAZn or EMAANa). Therefore composite films could be used for UV shielding applications. The decomposition pattern of the ionomer matrices (EMAAZn or EMAANa) changed on mixing with PANI, which tend to retard the degradation of the molecules of the pure matrices at higher temperatures. The improvement in the decomposition temperature of the composites shows that the stability of neat matrices (EMAAZn or EMAANa) is increased with the introduction of PANI, owing to the reduction in segmental mobility. The results of DC electrical conductivity show that the composites containing nano PANI-TSA has higher conductivity compared to the nano PANI-HCl and bulk PANI-HCl based composites. This indicates that PANI in nano dimension are more conducting than in bulk form. The conductivity was in the order EMAA-bulk PANI-HCl < EMAA-nano PANI-HCl < EMAA-nano PANI-TSA for both sodium ionomer and zinc ionomer. Among the polymer composites studied, the highest electrical conductivity values was obtained for 1:1 EMAA-nano PANI-TSA composite. The electromagnetic interference (EMI) shielding effectiveness (SE) of the EMAA-PANI binary composites also showed the highest value in EMAA-nano PANI-TSA composite. The values of attenuation obtained in the EMAA-bulk PANI-HCl and EMAA-nano PANI-HCl composites are lower than the minimum attenuation that ensures the safety of electronic gadgets. EMAANa-PANI binary composites show better electrical conductivity and EMI shielding effectiveness compared to EMAAZn-PANI binary composite. The EMAA-nano PANI-TSA composites are a promising material for EMI shielding. The composite films may be utilized for static charge dissipation, lightweight devices and effective EMI shielding or microwave absorption materials. The results obtained revealed that the solution blending is an effective way to improve the processability of electrically conducting polyaniline as well as to improve the thermal, electrical and EMI SE properties of EMAAZn or EMAANa.

Reference

[1] Subrahmanyam AR, Geetha V, Kumar A, Alakanandana A and Siva KJ, 2012. Mechanical and electrical conductivity studies of PANI-PVA and PANI-PEO blends. Int J Mater Sci, 2 (1) 27-30.

[2] Castillo-Ortega MM, Encinas JC, Rodriguez DE, Olayo R, 2001. Preparation and characterization of electroconductive polypyrrole-thermoplastic composites. J Appl Polym Sci, 81 1498-1506.

[3] Castillo-Ortega MM, Rodriguez DE, Encinas JC, Plascencia M, Mendez-Velarde FA, Olayo R, 2002. Conductometric uric acid and urea biosensor prepared from electroconductive polyaniline-poly (n-butylmethacrylate) composites. Sens Actuat B, 85 19-25.

[4] Castillo-Ortega MM, Del Castillo-Castro T, Encinas JC, Perez-Tello M, De Paoli M-A and Olayo R, 2003. Electrically conducting polyaniline-PBMA composite films obtained by extrusion. J Appl Polym Sci, 89 179-183.

[5] Gazotti Jr WA, Casalbore-Miceli G, Mitzakoff S, Geri A, Gallazzi MC and De Paoli MA, 1999. Conductive polymer blends as electrochromic materials. Electrochimica Acta, 44 1965-1971.

[6] Eisenberg A and Joon-Kim J-S, 1998. Introduction to Ionomers. Wiley Interscience, New York, p 327.

[7] Shah RK and Paul DR, 2006. Comparison of nanocomposites prepared from sodium, zinc, and lithium ionomers of ethylene/methacrylic acid copolymers. Macromol, 39 3327-3336.

[8] Jerome R and Mazurek M, 1997. In Tant MRM, Kenneth A, Wilkes GL (eds) Ionomers. Blackie Academic and Professional: London, p 3-40.

[9] Hasegawa N, Kawakado M, Usuki A and Okada A, 1998. Preparation and mechanical properties of polypropylene-clay hybrids using a maleic anhydride-modified polypropylene oligomer. J Appl Polym, 67 (1) 87-92.

[10] Shah R K, 2006. Polymer-layered silicate nanocomposites by melt processing, PhD Thesis, The University of Texas at Austin.

[11] Mathias LJ. www.pslc.ws/macrog/Polymer Science Learning Center/ ionomer. Accessed 2 June, 2018.

[12] Tant M and Wilkes GL, 1987. Viscoelastic behavior of ionomers in bulk and solution, in structure and properties of ionomers, Pineri M and Eisenberg A (Eds.), Reidel, Dordrecht, NATO ASI Series, p. 191-226.

[13] Schlick S, 1996. Ionomers: characterization, theory and applications. Boca Raton, Florida: CRC Press LLC.

[14] Samuel J, Xavier T and Kurian T, 2000. Ionomers. Prog Rubber Plast Technol, 16 (1) 1-15.

[15] Hirasawa E, Yamamoto Y, Tadano K and Yano S, 1991. Effect of metal cation type on the structure and properties of ethylene lonomers. J Appl Polym Sci, 42 351-362.

[16] Nandi A, Gupta DG and Banthia AK, 2002. Sulfonated polybutadiene random ionomer as stabilizer for colloidal copper nanoparticles. Colloids and Surfaces A: Physicochem Eng Aspects, 197 119-124.

[17] Capek I, 2005. Nature and properties of ionomer assemblies II. Adv Colloid Interface Sci, 118 73-112.

[18] Chodak I and Krupa I, 1999. Percolation effect and mechanical behavior of carbon black filled polyethylene. J Mater Sci Lett, 18 1457-1459.

[19] Carinhana Jr D, Faez R, Nogueira AF and De Paoli MA, 2001, Photoelectrochemical properties of PANI-DBSA/EPDM blends. Synth Met, 121 1569-1570.

[20] Koul S, Chandra R and Dhawan SK, 2001. Conducting polyaniline composite: a reusable sensor material for aqueous ammonia. Sens Actuat B, 75 151-159.

[21] Gao J, Sansinena JM and Wang HL, 2003. Chemical vapor driven polyaniline sensor/actuators. Synth Met, 135 809-810.

[22] Gerard M, Chaubey A and Malhotra BD, 2002. Application of conducting polymers to biosensors. Biosens Bioelect, 17 (5) 345-359.

[23] Falcao EHL and Azevedo WM, 2002. Polyaniline-poly(vinyl alcohol) composite as an optical recording material. Synth Met, 128 149-154.

[24] Faez R, Martin IM and De Paoli MA, 2001. Microwave properties of EPDM/PANI-DBSA blends. Synth Met, 119 435-436.

[25] Shirakawa H, Lewis EJ, MacDiarmid AG, Chiang CK and Heeger AJ, 1977. Synthesis of electrically conducting organic polymers: halogen derivatives of polyacetylene (CH)x. J Chem Soc, Chem Comm, 16 578-580.

[26] Das TK and Prusty S, 2012. Review on conducting polymers and their applications. Polym-Plast Technol Eng, 51 14 1487-1500.

[27] Kar P, 2013. Doping in conjugated polymers, in polymer science and plastic engineering. John Wiley and Sons, p 176.

[28] Ajekwene KK, John H and Kurian T, 2017. Progress in preparation, processing and applications of conducting polymer-ionomer blends. Int J Res Sci Innov, IV IX 23-31.

[29] Palaniappan S and John A, 2008. Polyaniline materials by emulsion polymerization pathway. Prog Polym Sci, 33 732-758.

[30] Bakhishi AK and Bhalla G, 2004. Electrically conducting polymers: Materials of the twenty-first century. J Sci and Ind Res, 63 715-728.

[31] Stejskal J and Gilbert RG, 2002. Polyaniline: preparation of a conducting polymer. Pure Appl Chem, 74 (5) 857-867.

[32] Rafeeq SN and Khalaf WZ, 2015. Preparation, characterization and electrical conductivity of doped polyaniline with (HCL and P-TSA). Eng Technol J, 33 (7) Part B 1220-1231.

[33] Yongfang Li, 2015. Organic optoelectronic materials, Yongfang Li (ed.), Springer International Publishing Switzerland, Lecture Notes in Chemistry 91, 23-50.

[34] Inzelt G, 2002. Conducting Polymers: A new era in electrochemistry, Springer-Verlag Berlin Heidelberg, Monographs in electrochemistry book series, p 123-148.

[35] Su SJ and Kuramoto N, 2000. Synthesis of processable polyaniline complexed with anionic surfactant and its conducting blends in aqueous and organic system. Synth Met, 108 121-126.

[36] Barbero C, Salavagione HJ, Acevedo DF, Grummelli DE, Garay F and Planes GA, 2004. Novel synthetic methods to produce functionalized conducting polymers I. Polyanilines. Electrochim Acta, 49 3671-3686.

[37] Yang JP, Planes RJ, Pron A and Nechtschein M, 1998. Preparation of low density polyethylene-based polyaniline conducting polymer composites with low percolation threshold via extrusion. Synth Met, 93 169-173.

[38] Wang Y, Xie H, Cai Y and Guo J, 1997. Synthesis and properties of polyaniline/sodium and zinc ionomer composites. Polym J, 9 875-880.

[39] Xie HQ, Pu QL and Xie D, 2004. Preparation of conductive polyaniline-sulfonated EPDM ionomer composites from in situ emulsion polymerization and study of their properties. J Appl Polym Sci, 93 2211-2217.

[40] Morgan H and Foot PJS, 2001. The effects of composition and processing variables on the properties of thermoplastic polyaniline blends and composites. J Mater Sci, 36 5369 -5377.

[41] Barber GD, Calhoun B H and Moore RB, 2005. Poly(ethylene terephthalate) ionomer based clay nanocomposites produced via melt extrusion. Polym, 46 6706-6714.

[42] Chisholm BJ, Moore RB, Barber G, Khouri F, Hempstead A, Larsen M, Olson E, Kelley J, Balch G and Caraher J, 2002. Nanocomposites derived from sulfonated poly(butylene terephthalate). J Macromol, 35 5508-5516.

[43] Start PR and Mauritz KA, 2003. Surlyn/silicate nanocomposite materials via a polymer in situ sol–gel process: Morphology. J Polym Sci, Part B: Polym Phys, 41 1563-1571.

[44] Ameen S, Akhtar SM, Song M and Shin HS, 2013. Solar cells - research and application perspectives. In Arturo Morales-Acevedo (eds) Metal oxide nanomaterials, conducting polymers and their nanocomposites for solar energy. InTech, p 203-259.

[45] Olabisi O and Adewale K, 2015. Handbook of thermoplastics. 2nd Edition, CRC Press, doi: 10.1201/b19190-1.

[46] Kutsumizu S, Hara H, Tachino H, Shimabayashi K and Yano S, 1999. Infrared spectroscopic study of the binary blends of sodium and zinc salt ionomers produced from poly(ethylene-co-methacrylic acid). Macromol, 32 6340-6347.

[47] MacKnight WJ, McKenna LW, Read BE and Stein RS, 1968. Properties of ethylene-methacrylic acid copolymers and their sodium salts: infrared studies. J Phy Chem, 72 1122-1126.

[48] Seethamraju S, Ramamurthy PC and Madras G, 2014. Performance of an ionomer blend-nanocomposite as an effective gas barrier material for organic devices. RSC Adv, 4 11176-11187.

[49] Scaffaro R, Re GL, Dispenza C, Sabatino MA and Armelao L, 2011. A new route for the preparation of flexible skin–core poly(ethylene-co-acrylic acid)/polyaniline functional hybrids. React Funct Polym, 71, 1177-1186.

[50] Pineri M and Eisenberg A, 1987. Structure and properties of ionomers. NATO ASI Series C, Mathematical and Phy Sci D. Reidel: Dordrecht, The Netherlands, 198, p 581.

[51] Kutsumizu S, Tadano K, Matsuda Y, Goto M, Tachino H, Hara H, Hirasawa E, Tagawa H, Muroga Y and Yano S, 2000. Investigation of microphase separation and thermal properties of noncrystalline ethylene ionomers. 2. IR, DSC, and dielectric characterization. Macromol, 33, 9044-9053.

[52] Ray S, Easteal AJ, Cooney RP and Edmonds NR, 2009. Structure and properties of melt-processed PVDF/PMMA/polyaniline blends. Mater Chem Phys, 113 829-838.

[53] Pazhanisamy P and Reddy BSR, Synthesis and characterization of methacrylamidopropyltrimethylammonium chloride and N-substituted acrylamide ionomers. eXPRESS Polym Lett, 1 (11) 740-747.

(b) Darryl D. DesMarteau, Li-Mei Jin and Stephen Creager, 2008. Perfluorinated ionomers containing the bis(perfluoroalkyl)phosphonic acid. The 2008 Annual Meeting Philadelphia, PA. https://aiche.confex.com /aiche/2008/techprogram/P138238.HTM.

[54] Dun Li and Sur GS, 2013. Comparison of poly(ethylene-co-acrylic acid) loaded Zn^{2+}-montmorillonite nanocomposites and poly(ethylene-co-acrylic acid) zinc salt. J Ind Eng Chem, 20 3122-3127.

[55] Kutsumizu S, Hashimoto Y, Hara H, Tachino H, Hirasawa E and Yano S, 1994. DC conduction properties of a model ethylene-methacrylic acid ionomer. Macromol, 27 (7) 1781-1787.

[56] Zilberman M, Siegmann A and Narkis M, 2000. Conductivity and structure of melt-processed polyaniline binary and ternary blends. Polym Adv Technol, 11 20-26.

[57] Terlemezyan L, Mihailov M, and Ivanova B, 1992. Electrically conductive polymer blends comprising polyaniline. Polym Bull, 29 283-287.

[58] Inoue M, Castillo-Ortega MM and Inoue MB, 1997. Polyaniline toluenesulfonates: X-ray diffraction and electrical conductivity. J.M.S.-Pure Appl Chem, A34 (8) 1493-1497.

[59] Das NC, Yamazaki S, Hikosaka M, Chaki TK, Khastgir D and Chakraborty A, 2005. Electrical conductivity and electromagnetic interference shielding effectiveness of polyaniline ethylene vinyl acetate composites. Polym Int, 54 256-259.

[60] Chutia P and Kumar A 2014. Electrical, optical and dielectric properties of HCl doped polyaniline nanorods. Physica B, 436 200-207.

[61] Wang Y, 2014. Microwave absorbing materials based on polyaniline composites: A review. Int J Mater Res, 105 (1) 3-12.

[62] Thomassin JM, Jerome C, Pardoen T, Bailly C, Huynen I, Detrembleur C 2013. Polymer/carbon based composites as electromagnetic interference (EMI) shielding materials. Materials Science and Engineering: R: Report, 74 211-232.

[63] John H, Thomas RM, Jacob J, Mathew KT and Joseph R, 2007. Conducting polyaniline composites as microwave absorbers. Polym Comp, 28 588-592.

[64] Schmitz DP, Ecco LG, Dul S, Pereira ECL, Soares BG, Barra GMO and Pegoretti A, 2018. Electromagnetic interference shielding effectiveness of ABS carbon-based composites manufactured via fused deposition modelling. Mater Today Comm, 15 70–80.

[65] Painter PC, Brozoski BA and Coleman MM, 1982. FTIR studies of calcium and sodium ionomers derived from an ethylene-methacrylic acid and copolymer. J Polym Sci, Polym Phys Edition, 20 (6) 1069-1080.

[66] Reynolds PJ, 2012. A surlyn® ionomer as a self-healing and self-sensing composite. MRes Thesis, Department of Metallurgy and Materials, University of Birmingham, UK.

[67] Joanna M, Ramos JM, De M Cruza MT, Costa Jr AC, Versiane O and Tellez Soto CA, 2011. Fourier transform infrared spectrum: vibrational assignments using density functional theory and natural bond orbital analysis of the bis(guanido acetate) nickel (II) complex. Science Asia, 37 247-255.

[68] Gazotti Jr WA Jr, Casalbore-Miceli G, Mitzakoff S, Geri A, Gallazzi MC and De Paoli MA, 1999. Conductive polymer blends as electrochromic materials. Electrochimica Acta, 44 1965-1971

[69] Kutsumizu S, Tadano K, Matsuda Y, Goto M, Tachino H, Hara H, Hirasawa E, Tagawa H, Muroga Y and Yano S, 2000. Investigation of microphase separation and thermal properties of noncrystalline ethylene ionomers. 2. IR, DSC, and dielectric characterization. Macromol, 33, 9044-9053.

[70] Ray S, Easteal AJ, Cooney RP and Edmonds NR, 2009. Structure and properties of melt-processed PVDF/PMMA/polyaniline blends. Mater Chem Phys, 113 829-838.

[71] Ajekwene KK, Jelmy EJ and Thomas Kurian, 2018. Sodium salt of polyethylene-co-methacrylic acid ionomer/polyaniline binary blends for EMI shielding applications. PIER C, 88 207–218.

* * *

Chapter 5

IONOMER-POLYANILINE-MULTI WALLED CARBON NANOTUBES HYBRID COMPOSITES: SYNTHESIS, PROPERTIES AND APPLICATIONS

Contents

Composites made up of conducting fillers dispersed in an insulating and flexible polymer matrix are generally used in electronics sensors, electromagnetic shielding and anti-static devices applications. In this chapter, conducting composites based on EMAAZn or EMAANa matrices for electrical and EMI shielding applications is reported. MWCNTs were chosen as conductive filler due to its excellent electronic structure and growing industrial usage. Prior to exploring the influence of MWCNTs on the electrical properties and EMI shielding of composites containing EMAAZn or EMAANa matrices, studies were carried out on EMAAZn/PANI and EMAANa/PANI binary composites (chapter 4, PART A and PART B) to obtain a general understanding from the electrical and EMI shielding behaviors of EMAAZn or EMAANa matrices as a function of MWCNTs content. PANI:MWCNT composite was prepared by varying the weight percentages (25%, 50%, 75%, 100%, 125%, and 150%) of the MWCNTs (Pristine CNT, amine functionalized CNT (ACNT) and carboxylic acid functionalized CNT (CCNT)) through in-situ polymerization technique. The PANI coated MWCNTs nanocomposites were mixed with the ionomer (EMAAZn or EMAANa) matrices to fabricate electrically conducting hybrid composite films (EMAAZn-PANI-MWCNTs or EMAANa-PANI-MWCNTs) at a ratio of 1:1 using a solution mixing method with toluene and 1-butanol as solvents at 65°C. The conducting hybrid composites were characterized using XRD, UV-Vis and TGA. The electrical conductivity and microwave absorption / reflection characteristics of the fabricated hybrid composites were also studied. The results of four-probe electrical conductivity measurements and EMI SE over the X-band (8 - 12 GHz) showed that the electrical conductivity and EMI shielding properties rose with MWCNTs content. The increase in electrical conductivity with MWCNT loading was attributed to the formation of conductive paths across the composite. Increase in EMI shielding with MWCNT content was related to a greater number of interacting roving charges. These hybrid composites are found to have potential applications in the areas of electromagnetic interference (EMI) shielding and electrostatic dissipation (ESD).

5.1 Introduction

The growth in the application of electrical and electronic devices across a broad spectrum of military, industrial, commercial and consumer sectors such as wireless device systems, navigation, air space technology, military installations, etc. has resulted in the rapid proliferation of electronic devices ranging from simple to sophisticated. The consequence has created a peculiar form of pollution known as noise or electromagnetic interference (EMI). EMI can cause serious harm to the effective performance of electrical and electronic devices as well as various life forms, including human beings. And so, there is a greater need for the effective shielding of electronic devices from the adverse effects of EMI noise with effective shielding materials [1, 2, 3]. Materials for this purpose are prepared by adding ferrites, carbon black or other conducting fillers in a polymeric matrix. Conventionally, EMI shielding techniques focused on metallic materials and their composites, which effectively reflect the electromagnetic waves. Metals have good mechanical strength but have the disadvantages of higher density [4], easy corrosion and uneconomic processability. Additionally, it is difficult to retain a uniform distribution of the metal filler throughout the matrix in which it is mixed during its composites fabrication. This could results in deficiency of the metallic filler in corners, edges and surfaces which tends to result in gaps in the shield composite materials causing disconnection in the conducting path and leakages of the radiation and thus diminishing the conductivity and effectiveness of the shield [5, 6]. Hence, the need for conducting polymers that displays several characteristics of organic polymers such as lightweight, lower cost, resistance to corrosion and chemical attack, flexibility and greater workability as well [7-11].

Among the conducting polymers, polyaniline (PANI) and PANI based materials have been researched most comprehensively for the reason that they possess easier and inexpensive preparation methods, good environmental stability in both doped and undoped forms, excellent physical and chemical properties and high conductivity [7-9, 12]. But the main limitations of PANI is that it requires a large amount of protons attached to the polymer to be electrically conducting, it is a very poor conductor when the pH is greater than 5, therefore PANI tends to experience loss of conductivity in neutral and high pH environment [13], highly unstable even at moderate temperatures (>100 °C) [14]. Therefore, there is the need to further expand the application possibilities of conducting PANI in order to meet the requirements of present day sophisticated technologies if their conductivity, chemical and thermal stability can be enhanced to a certain extent. Such a situation needs materials with fixed conductivity and opaque to microwaves. Conducting fillers can offer an attractive solution for this. In this regard, CNTs based composites can provide a vital role due to its conductivity, non-corrosiveness, nominal processing cost and its thermal and environmental stability resulting in technological and commercial applications [1].

Incorporation of CNTs in PANI and or polymer matrix to make composites, has been intensively studied [1, 5, 6, 15-40]. This is attributable to the unique structure of CNT which promotes several outstanding properties including thermal stability and in particular electrical conductivity. This act of incorporating CNTs into PANI or polymer matrix in the form of composites could extend the applications of CNTs itself, PANI and polymer matrices such as in electrostatic discharge (ESD) and electromagnetic interference (EMI) shielding materials.

It is important to note that the high aspect ratio, the strong Van-der Waals attractions of CNTs and their insolubility in most of the available solvents as well as the incompatibility with various polymer matrices can result in its poor dispersions [17-19]. The poor dispersion may result in strong agglomeration in the polymer matrix which in turn could contribute to the poor electrical conductivity and EMI shielding efficiency of the composites [20-22]. This is a major drawback which is challenging for a lot of composites applications, since the polymer matrix is an effective barrier capable of preventing the exchange of electrons between the CNT encapsulates. Attempts have been made to overcome this limitation by adding secondary fillers such as conducting polymers into the composites thereby generating new conducting hybrid filler-filler pathways [19, 23-25]. Conducting polymers which possess tunable conductivity, non-transparency to EM radiations and dispersibility/solubility in common solvents [15, 16, 17, 19, 26-34] can reduce CNT aggregation and at the same time preserve its intrinsic properties. An electrically conducting polymer matrix has the added advantage of being able to electrically connect the filler units that do not touch one another, thereby enhancing the connectivity. In this way, polymer-matrix composites containing CNTs and conducting polymers may become attractive for shielding due to their processability which CNTs and/or conducting polymers does not possess. In addition, polymer-matrix composites are attractive in their low density to compliment. Polyaniline/carbon nanotubes (PANI/CNTs) based composites have been widely explored in which the charge-transfer activities between the two components leads to considerable improvement in conductivity [41] and, chemical and thermal stability. PANI/CNTs nanocomposites are prepared either through grafting PANI macromolecules on the CNTs or through in situ polymerization of aniline monomer in CNT dispersion. Despite this improved electrical conductivity, chemical and thermal stability due to the introduction of CNT to boost the mentioned limitations, PANI/CNT composites however, possess poor mechanical properties such as strength and processability due to stiffness of their backbone and insolubility in the common organic solvents. Thus, the unique combination of electronic and mechanical properties of the composites with conventional polymers to form a hybrid composites seems to have great promise for many applications. The mixing of polymers has become commercially and technologically more important than the synthesis of homopolymers and copolymers in the last decade. Blending allows for creating new materials with specific properties for the desired application at low cost [42]. Since the conducting polycomposites are stable and retain the mechanical properties of the host polymer, films can be fabricated by solvent evaporation or by melt-processing for use in anti-static applications, for electromagnetic shielding, microwave absorption devices, etc.

This chapter presents the preparation of hybrid composites of EMAAZn or EMAANa with PANI and MWCNT for electrical and EMI shielding applications. PANI was synthesized and characterized as explained in chapter 3. PANI-MWCNT composites were prepared by insitu polymerization of aniline monomer in the presence of MWCNT (pristine CNT, amine functionalized CNT (ACNT) and carboxylic acid functionalized CNT (CCNT)) using TSA as dopant and APS as oxidant. Hybrid composite films of EMAAZn-PANI-MWCNT and EMAANa-PANI-MWCNT respectively were fabricated by solution mixing in blend of solvents (toluene (90%)/ 1-butanol (10%)) at 65°C. The electrical properties and EMI shielding effectiveness characteristics of the conducting hybrid composites were evaluated.

Part A

Zinc salt of poly(ethylene-co-methacrylic acid) ionomer-polyaniline-multi walled carbon nanotubes hybrid composites: preparation, evaluation and applications.

5A.1 Experimental Methods

5A.1.1 Preparation of EMAAZn-PANI-MWCNT Hybrid Composites

The Hybrid Composites of EMAAZn-PANI-MWCNT were prepared by solution mixing of the ionomers (EMAAZn) with the previously synthesized PANI-MWCNT (pristine CNT, ACNT and CCNT) composites in a mixing ratio of 1:1 (EMAAZn : PANI-MWCNT). The EMAAZn was first dissolved in a solvent mixture of 90:10 (toluene/1-butanol) at 65°C and then mixed thoroughly with PANI-MWCNT to obtain the hybrid composites. The solution of EMAAZn-PANI-MWCNT were allowed to evaporate to a solid film in a petri dish and dried in vacuum oven at 50°C for 24 hours.

5A.1.2 Characterization and Instrumental Analysis

Fourier transform infrared (FTIR) spectra of samples were recorded using a Thermo Nicolet Avatar 370 FTIR spectrometer. The compositional state of the samples was determined using X-Ray Powder Diffractometry (XRD) using Bruker AXS D8. The electronic transitions in the samples were determined by measuring the absorptions in the UV and visible regions using UV-Visible spectroscopy (Varian Cary 5000). Thermo gravimetric analysis (TGA) was performed on a Perkin Elmer STA 6000 thermogravimetric analyzer to determine decomposition and thermal stabilities of the samples.

DC electrical conductivity measurements were done by four-probe method using Keithley 616 sensitive digital electrometer at room temperature. EMI shielding measurements were performed using a wave-guide coupled to an Agilent Synthesized Sweeper 8375A and a Hewlett-Packard spectrum analyzer 7000 in the X band frequency range (8-12 GHz).

5A.2 Results and Discussions

5A.2.1 X-Ray Diffractometry (XRD)

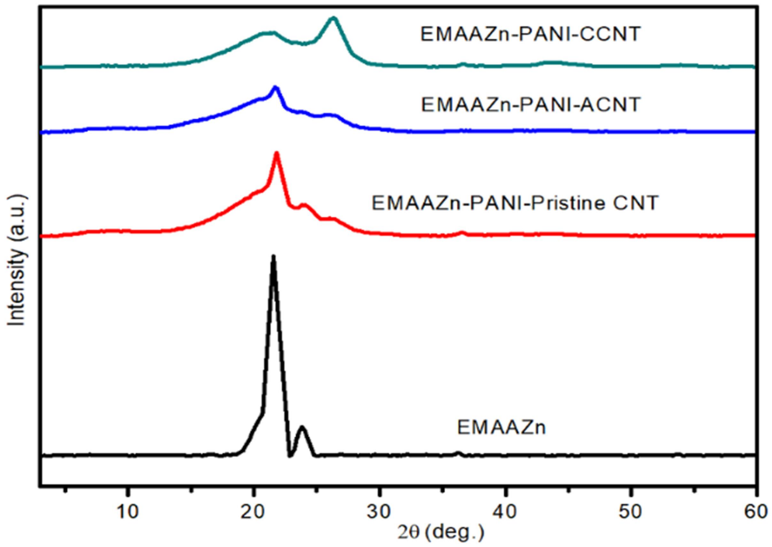

Figure 5.1. XRD profiles of EMAAZn-PANI-Multi Walled CNT (pristine CNT, ACNT and CCNT) hybrid composites.

As reported earlier in chapter 3, acid treatment of MWCNT brings about enhanced negative charges on its surface which improved the interaction between PANI and MWCNT nanoparticles thereby achieving good disentanglement. Figure 5A.1 shows the XRD PANI-MWCNTs (pristine CNT, ACNT and CCNT)-EMAAZn hybrid composites. The X-ray diffractograms of EMAAZn-PANI-MWCNT composites show all the peaks corresponding to PANI as well as the MWCNTs, with sharp peak at around 21° observed for the ionomer matrices (EMAAZn). The appearance of diffraction peak at 26° in the (3) composite indicates a red shift from 25° which is common in both PANI and the MWCNTs (Figures 3.2, 3.8 and 3.14), indicating that MWCNTs and PANIs are dispersed in the ionomer matrices. It is observed that the diffraction peak in the pattern of the ionomer became weak in the XRD pattern of exfoliated blends especially those containing ACNT and CCNT, indicating a high degree of exfoliation and the presence of PANI and MWCNT. In the XRD pattern of EMAAZn/PANI/MWCNT mixture, there is obvious peaks weakening observed, indicating the blend components were exfoliated due to the presence of large electrostatic interaction between the EMAAZn and PANI-MWCNTs nanoparticles [43].

5A.2.2 UV-Visible spectroscopy (UV-Vis)

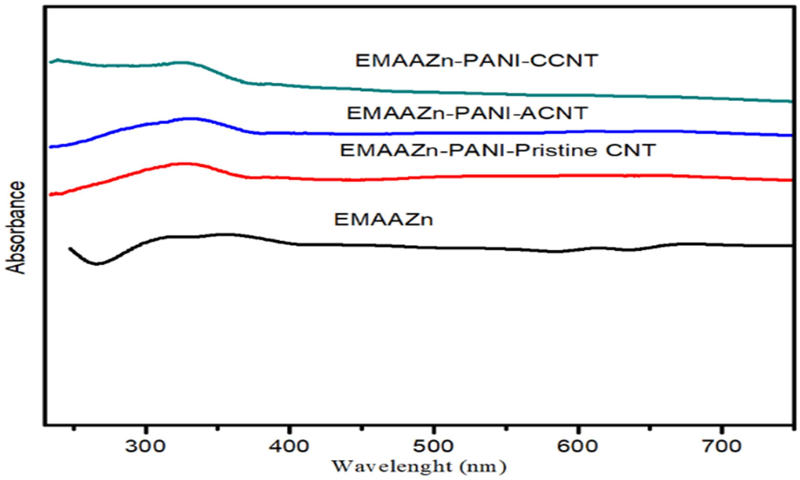

Figure 5.2. UV-Visible spectra of EMAAZn-PANI-Multi Walled CNT (pristine CNT, ACNT and CCNT) hybrid composites

Figures 5.2 shows the UV-Vis spectra of PANI-MWCNTs (pristine CNT, ACNT and CCNT)-EMAAZn hybrid composites. The peaks at 326 nm, 331 nm, 325 nm were assigned for PANI–MWCNTs (pristine CNT, ACNT and CCNT)-EMAAZn composites respectively. The peaks due to PANI and MWCNTs as observed in Figures 3.5, 3.11 and 3.17 became very faint to the point that it is absorbed by the ionomer matrices probably due to the strong interaction between PANI and MWCNTs composites with the ionomer matrices.

5A.2.3 Thermogravimetric Analysis (TGA)

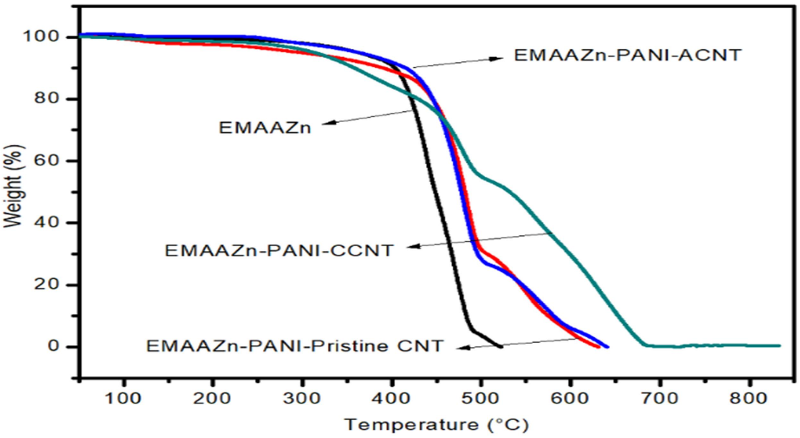

Figure 5.3. TGA curves of EMAAZn-PANI-Multi Walled CNT (pristine CNT, ACNT and CCNT) hybrid composites

Figure 5.3 shows the TGA thermogram of EMAAZn-PANI-MWCNTs (pristine CNT, ACNT and CCNT) hybrid composites. When the PANI-CNT composite was prepared and blended with EMAAZn in a hybrid composite, the composites decomposition temperature increased compared to EMAAZn-PANI binary blends (Figure 4.4). This effect is obviously due to the presence of MWCNT which tends to acts as an additive for thermal stabilization. As the temperature increases, the weight loss of the EMAAZn-PANI-MWCNTs composites decreased. When the temperature was approximately 500 °C, the mass of EMAAZn was almost zero and at 520 °C the entire mass had completely decomposed, leaving no residue. The EMAAZn-PANI-MWCNTs hybrid composites left some heat-resistant parts even at temperature beyond 520 °C. Therefore, the weight values of EMAAZn, EMAAZn-PANI-pristine CNT, EMAAZn-PANI- ACNT and EMAAZn-PANI-CCNT at 520 °C were 0.02%, 28%, 25% and 52%, respectively. Improved physical and chemical interactions between thermally stable MWCNTs and the polymer is reported to slow down the thermal degradation of the composites [45, 46]. Apart from this, the formation of a perfect network due to good dispersion of MWCNTs can act as an obstacle to the escape of degradation products from the matrix of the polymer. High thermal conductivity of the MWCNTs [46] also play a major role in enhancing thermal stability by dissipating heat more rapidly from the composites. The sample EMAAZn-PANI-CCNT composite showed superior thermal stability due to its better exfoliation into EMAAZn.

5A.2.4 Conductivity Measurements

Understanding the conduction mechanism will helps to determine the applications of conducting polymer composites at various conducting filler loading concentrations. The electrical conductivity of the nano EMAAZn-PANI-multi walled CNT (Pristine CNT, ACNT and CCNT) hybrid composites with various weight percentages of MWCNTs were reported in Table 5.1.

Table 5.1. Electrical conductivity of PANI-multi walled CNT (Pristine CNT, ACNT and CCNT) as a function of weight ratio of PANI-MWCNTs in EMAAZn hybrid composites.

Weight % of MWCNT in 0.2mg PANI	Conductivity (S/cm) of EMAAZn/PANI-MWCNT (1g:1g)		
	EMAAZn-PANI-Pristine CNT	**EMAAZn-PANI-ACNT**	**EMAAZn-PANI-CCNT**
25 (50mg)	0.027	0.057	0.026
50 (100mg)	0.063	0.028	0.037
75 (150mg)	0.035	0.039	0.045
100 (200mg)	0.051	0.015	0.195
125 (250mg)	0.034	0.013	0.068
150 (300mg)	0.075	0.011	0.075

In Table 5.1, the electrical conductivity of EMAAZn-PANI-multi walled CNT (pristine CNT, ACNT and CCNT) respectively as a function of weight ratio of CNTs in PANI. It is observed that the conductivities in the hybrid composites were much improved compared to the binary composites of EMAAZn-PANI as recorded in Table 4.1. This is attributed to the introduction of MWCNTs. The higher the concentration of MWCNTs in polymers, the lower is the gap width and the higher is the chance that electrons will pass through the barrier. By increasing MWCNT concentration, the gaps between the conductor materials (MWCNTs) decrease. When the mean particle-particle distance is close enough, the insulating gaps between the conducting fillers becomes narrower, giving rise to very high field strength. This high field strength provides free electrons sufficient energy to cross the insulative gap. High conductivity is the result of transport processes within the polymer host matrix [47]. The hybrid composites (EMAAZn-PANI-pristine CNT and

EMAAZn-PANI-ACNT) did not show a typical percolation phenomenon as their conductivities are not consistent with conditions of percolation mechanism as reported in table 5.1. For EMAAZn-PANI-pristine CNT, the conductivity was found to be irregular with increase in the concentration of MWCNT content. This is attributed to its unfunctionalized state. For EMAAZn-PANI-ACNT, the conductivities were decreasing as the weight concentration increased. The possible reason is the fact that the phenyl amino groups on the surface of ACNT is capable of initiating polymerization, thereby increasing the concentration of the monomeric species on the surface and hence, could lead to the formation of a thicker and more uniform coating of PANI on the surface of ACNT in the polymerization process [48-50]. This scenario can lead to the formation of more agglomerated and bulky PANI above the required PANI volume in the PANI-MWCNT composites. The bulky PANI formed is capable of increasing the MWCNT-MWCNT distance there by reducing the conducting network formation of MWCNT.

However, the results of EMAAZn-PANI-CCNT showed typical percolation phenomenon. The results can be divided into three regions: pre percolation region - low concentration (1:0.27-0.75), percolation region (1:1) and post percolation region (1:1.25-1.50) – high concentration of PANI-MWCNTs. In the pre percolation region, the MWCNT-MWCNT particles is assumed to be far from each other and the conductance is restricted by the polymer matrix because the MWCNT concentration is very low and there is very large insulating gaps between the MWCNT particles. Therefore, the possibility that electrons are transferred from one MWCNT particles to another is very low. The higher the concentration of

MWCNTs in polymers, the lower is the gap width and the higher is the chance that electrons will pass the barrier. The MWCNTs and the insulating gap between the polymer molecules, could be modeled as a capacitor [19, 51, 52]. By increasing MWCNT concentration, the particle-particle distance between the conductor materials (MWCNTs) decrease. In narrow insulating gaps between conducting fillers, very high field strength may develop which is higher than the macroscopic voltage [53, 54]. This high field strength provides free electrons sufficient energy to cross the insulating gap. By increasing filler loading further, the filler particles get closer and eventually at percolation threshold, the first network forms which lets the current pass through. In the second region, where percolation occurs (at ratio 1:1) of EMAAZn/PANI-CCNT, the free electrons in conducting filler will play the role of charge carriers more prominently due to direct contact between particles of MWCNTs. After percolation, increasing the conductive filler content alters the conductivity only marginally. The third region is the region known as post percolation; in this region, two effects govern the conductivity: the restriction resistance of contact spots and tunneling resistance between separated particles [45, 55-58]. A considerable amount of current dissipates at the contact spots between the conductive fillers, therefore, the restriction resistance that restricts conductivity increase due to large number of contact spots and the conductivity begins to decrease.

From the foregoing, the hybrid composites containing EMAAZn-PANI-MWCNTs are better conductors compared to the binary composites containing EMAAZn/PANI and would perform better in electrical applications such as capacitors, sensors, etc. even at lower concentration of loading.

5A.2.5 Electromagnetic Interference (EMI) Shielding Effectiveness (SE)

The uses of conducting polymers as microwave absorbers and electromagnetic interference shielding materials have attracted increased attention due to their good electrical conductivity, processability, light weight and non-corrosiveness especially when blended with nanocomponents such as CNTs. [10, 58]. The shielding effectiveness of the conducting hybrid composites of PANI-MWCNTs-EMAAZn prepared by solution blending was measured between 8.0 – 12 GHz as shown in Figure 5.4.

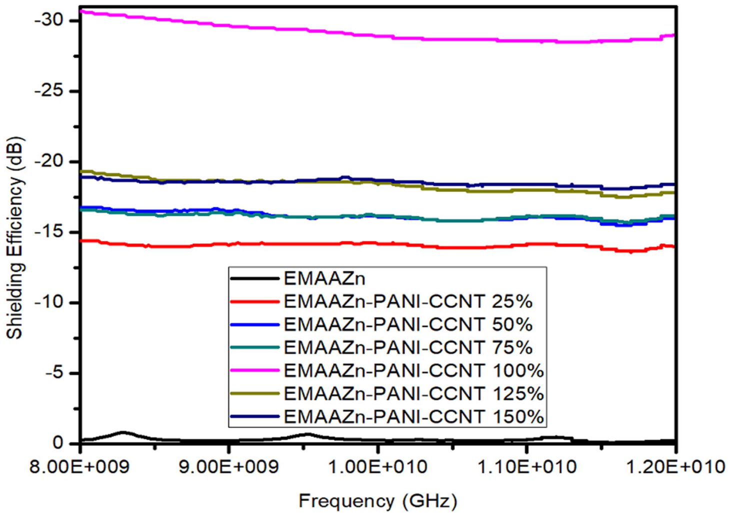

Figure 5.4. EMI SE of EMAAZn-PANI-CCNT) hybrid composites

The values of the shielding effectiveness at 8.5 GHz measured for the different loading ratios of the different MWCNTs in the PANI-MWCNT composites in the EMAAZn matrix are shown in Table 5.2.

Table 5.2. Shielding Efficiency of EMAAZn-PANI-MWCNTs (pristine CNT, ACNT and CCNT) at 8.5 GHz.

Shielding Materials	Amount (%)	SE (dB)
EMAAZn-PANI-Pristine CNT	25	-11.5308
	50	-11.8906
	75	-13.8850
	100	-18.3308
	125	-12.7001
	150	-13.4036
EMAAZn-PANI-ACNT	25	-10.6108
	50	-13.9044
	75	-13.4666
	100	-14.7538
	125	-14.9398
	150	-16.4230
EMAAZn-PANI-CCNT	25	-14.0449
	50	-16.6990
	75	-16.2834
	100	**-30.1054**
	125	-18.5996
	150	-18.8524

Table 5.2 shows the average values of EMI SE of EMAAZn-PANI-MWCNTs hybrid composites as a function of MWCNT concentration over the X-band frequency range. As shown in the table, EMI SE increases with MWCNT concentration. The increase in EMI SE by increase in MWCNT content is due to formation of more networks of conducting composites of PANI-MWCNTs thereby making way for free electrons in the hybrid composite materials that can interact with incoming electromagnetic wave. The increase in MWCNTs concentration also results in the increase in conductivity. Consequently, it can be said

that increase in EMI SE is due to increase in conductivity. However, it is worthy to note that while conductivity requires connectivity, EMI SE does not [27, 44, 59-64]. EMI SE increases with increase in the bulk of conducting filler that interact with the incoming electromagnetic wave. The EMAAZn-PANI-CCNT hybrid composites had higher average SE values compared to the EMAAZn-PANI-MWCNTs (pristine CNT and ACNT) ternary blends at the same content of MWCNTs in the PANI-MWCNT composites. When the MWCNTs content in the PANI-MWCNT composites was 1:1 ratio, the average SE values of EMAAZn-PANI-MWCNTs (pristine CNT, ACNT and CCNT) hybrid composites were 12.8 dB, 14.8 dB and 30 dB respectively. As the MWCNTs content increases, the average EMI SE of the hybrid composites increased marginally unlike the DC electrical conductivity that witnessed reduction as MWCNT contents increase above 1:1 (Table 5.1). These results implies that the EMI SE was improved from results obtained after introducing the MWCNTs in the composites with the exception of EMAAZn-PANI-pristine CNT when compared with results from the EMAAZn-PANI binary composites obtained at the same blending ratio in Table 4A.2. Therefore, the improvement of EMI SE is attributed to the increase of electrical conductivity [66].

Part B

Enhanced electromagnetic interference shielding effectiveness of polyaniline functionalized carbon nanotubes filled sodium ionomer hybrid composites

5B.1 Experimental Methods

5B.1.1 Preparation of EMAANa-PANI-MWCNT Hybrid Composites

The same procedure as in PART A with ionomer (sodium salt of poly(ethylene-co-methacrylic acid) (EMAANa)) was repeated keeping all other components the same.

5B.1.2.2 Characterization and Instrumental Analysis

Thermo gravimetric analysis (TGA) was performed on a Perkin Elmer STA 6000 thermogravimetric analyzer to determine decomposition and thermal stabilities of the samples. DC electrical conductivity measurements were done by four-probe method using Keithley 616 sensitive digital electrometer at room temperature. EMI shielding measurements were performed using a wave-guide coupled to an Agilent Synthesized Sweeper 8375A and a Hewlett-Packard spectrum analyzer 7000 in the X band frequency range (8-12 GHz).

5B.2 Results and discussions

5B.2.1 Thermogravimetric Analysis (TGA)

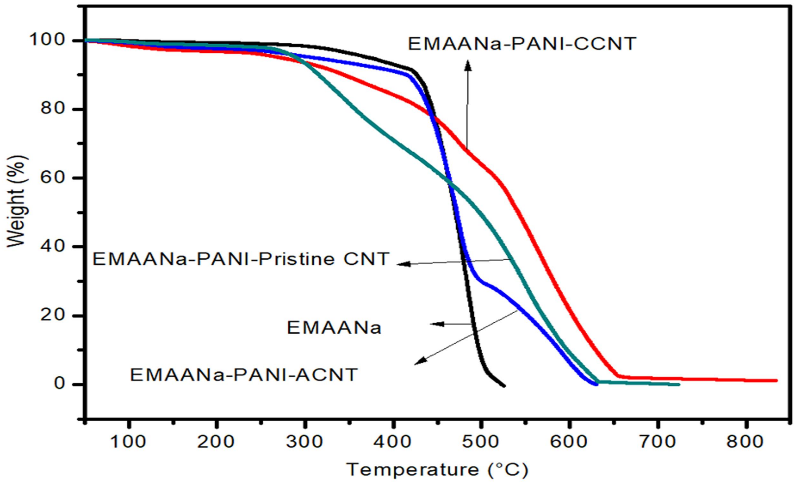

Figure 5.5. TGA curves of EMAANa-PANI-Multi Walled CNT (pristine CNT, ACNT and CCNT) hybrid composites

The TGA results (Figure 5.5) of the pure EMAANa and EMAANa-PANI-MWCNTs hybrid composites, respectively, shows that both have almost same stability up to 268 ^{O}C. Afterwards, curves of EMAANa-PANI-pristine CNT and EMAANa-PANI-CCNT shows abrupt acceleration of mass loss up to 42% and 26% respectively at 460 ^{O}C. On the other hand, EMAANa and EMAANa-PANI-ACNT show good stability up to 420 ^{O}C. After 420 ^{O}C, both EMAANa and EMAANa-PANI-ACNT show a sharp weight loss. The loss for EMAANa continued and degraded completely at 520 ^{O}C while EMAANa-PANI-ACNT deteriorated to 70% and degraded completely at 630 ^{O}C. At 630 ^{O}C, EMAANa-PANI-pristine CNT deteriorated up to 98% with 2% residue and EMAANa-PANI-CCNT deteriorated to 90% with 10% residue and at 660 ^{O}C, 2% residue.

The data clearly reveal that the thermal stability of EMAANa is less than EMAANa-PANI-MWCNTs hybrid composites (weight loss initiation temperature shifts to higher temperature). A larger effect is observed for EMAANa-PANI-CCNT. This behaviour can be attributed to the formation of an apparent shielding nanotube network which is destroyed on increasing the temperature up to a limit value [29, 35, 38, 65]. The stabilizing effect of MWCNTs can be also ascribed to the interfacial interaction between the PANI-MWCNT and EMAANa increasing the activation energy of degradation and to retarding the degradation at the surface of the samples owing to the better heat distribution within the heat conductive MWCNTs-containing samples.

5B.2.2 Conductivity Measurements

Electrical conductivity is a property that can theoretically be used to illustrate or investigate the quality of network formation of the component filler or conducting fillers dispersion in the polymer matrix of a composite. The electrical conductivity of a composite rises with increasing conducting filler loading. When a continuous interconnect network of electrically conducting fillers is formed, it provides a conducting pathway through which the polymer material at a proper conducting filler~~s~~ concentration undergoes a sudden transition from being an insulator to a conductor; the electrical conductivity rises by some orders of magnitude. The concentration at which the transition takes place is called electrical percolation threshold which is defined or predicated on the filler contents, filler morphology, the aspect ratio, particles size, structure, filler–matrix and filler–filler interactions altogether determining to the state of dispersion [22]. Figure 5.5 shows the effect of MWCNTs loading in the insitu polymerization of PANI-MWCNTs composites on the electrical conductivity of EMAANa-PANI-MWCNTs (pristine CNT, ACNT and CCNT)) hybrid composites.

Table 5.3. Electrical conductivity of EMAANa-PANI-MWCNTs (pristine CNT, ACNT and CCNT) as a function of weight ratio of MWCNTs in PANI-MWCNT composites.

Weight of MWCNT in 200mg PANI	Conductivity (S/cm) of EMAANa/PANI-MWCNT (1g:1g)		
	EMAANa-PANI-Pristine CNT	EMAANa-PANI-ACNT	EMAANa-PANI-CCNT
25% (50mg)	0.043	0.05	0.03
50% (100mg)	0.032	0.04	0.05
75% (150mg)	0.043	0.05	0.04
100% (200mg)	0.057	0.02	0.21
125% (250mg)	0.040	0.02	0.16
150% (300mg)	0.083	0.01	0.17

In Table 5.3, the electrical conductivity of PANI-multi walled CNT (pristine CNT), amine functionalized (ACNT) and carboxylic acid functionalized (CCNT)) respectively as a function of weight ratio of the MWCNTs in sodium salt ionomer (EMAANa) hybrid composites were presented. Increase in conductivity was observed for the hybrid composites compared to the binary composites as recorded in Table 4.1. Notably, when the addition amount of PANI-MWCNTs composites in EMAANa (Table 5.3) was the same as PANI in EMAANa Table 4.3, the EMAANa-PANI-MWCNT displayed a higher conductivity in comparison with EMAANa-PANI. For instance, at (1:1), electrical conductivity for EMAANa-PANI-TSA binary composite was $3.45E^{-3}$ S/cm while the electrical conductivity of EMAANa-PANI-MWCNTs (Pristine CNT, ACNT and CCNT) hybrid composites were 0.057, 0.02 and 0.21 S/cm respectively. These results suggested that the enhanced electrical conductivity is related to the incorporation of MWCNTs in PANI for the EMAANa-PANI-MWCNT hybrid composites preparation. Also the electrical conductivities of EMAANa-PANI-MWCNTs (Table 5.3) were found to be higher compared to the EMAAZn-PANI-MWCNTs samples in Table 5.1. Reason is also attributable to earlier report in chapter 4 based on the reactivity of the two metal salts (Na^{2+} and Zn) used in the neutralization reactions during the synthesis of the ionomers (EMAAZn and EMAANa).

Apparently two main factors influenced the electrical conductivities of the composites: MWCNTs type (in terms of functionalization) and MWCNTs loading used in the PANI-MWCNTs all of which influenced the interactions of PANI-MWCNTs and EMAANa. The overall results clearly confirm that choice of the MWCNTs type might be the most effective way to improve the conductivity of the hybrid composites. Likewise, a combination of MWCNTs type and loading are found to have improved conductivity relatively at MWCNT concentrations below or above 1:1. This means that increased MWCNTs loading increases the relative conductivity of the composites except for EMAANa-PANI-ACNT whose conductivities were observed to decrease with increasing MWCNT loading. Due to the same reason proposed previously in chapter 5A. For EMAANa-PANI-pristine CNT, the electrical conductivity was erratic as depicted in the table probably to its non functionalization. For EMAANa-PANI-CCNT, it is observed that the MWCNT type influenced the conductivity than the MWCNT loading where conductivity increased with MWCNT loading up to 1:1 and started to decrease with further increase in MWCNT loading. This is apparent in the saturated conductivities above the 1:1 loading where conductivity experienced a decline, hence was independent of MWCNT loading. This indicates that once the conducting networks were extensively formed with the MWCNT, conductivities either starts to decline, remain the same or may increase marginally. Clearly, the MWCNTs type and to some extent MWCNTs loading influenced the relative conductivity of the hybrid composites by the level of networks formed in the EMAANa matrix. This might be the reason for the different optimal conductivities of the EMAANa mixed with various MWCNTs types: PANI-pristine CNT, PANI-ACNT and PANI-CCNT composites. The higher conductivity of the EMAANa matrix with PANI-CCNT composite than PANI-pristine CNT and PANI-ACNT is due to the bridging effects of CCNT.

5B.2.3 Electromagnetic Interference (EMI) Shielding Effectiveness (SE)

Electromagnetic interference (EMI), is a disorder caused by an external source that affects an electrical device through an electromagnetic induction, electrostatic coupling or conduction. The disorder may reduce the performance of the device or even stop it from working. Electromagnetic shielding is the act of reducing the electromagnetic field in a space by blocking the field with barriers made of conducting or magnetic materials [66, 67]. In practical terms, shielding is used to prevent electromagnetic waves to escape from a noisy system or prevent them to enter sensitive systems. In this study, the EMI shielding effectiveness of EMAANa-PANI-MWCNTs (pristine CNT, ACNT and CCNT) hybrid composites was measured using an HP 8510 vector network analyzer. The frequency was scanned from 8.0 to 12.0 GHz (X band) and data taken within the frequency range.

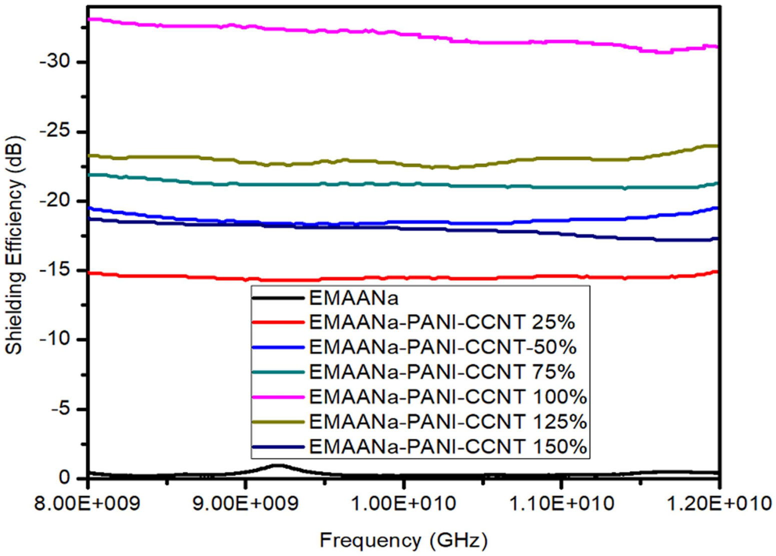

Figure 5.6. EMI SE of EMAANa-PANI-CCNT) hybrid composites

It was observed that the shielding effectiveness of each of the composites was almost independent of the frequency in the measured frequency region. For this reason, in order to do a concise comparison between samples of the composites being studied, a frequency of 8.5 GHz was considered for this analysis. Table 5.6 shows the variation of the EMI shielding effectiveness at the frequency of 8.5 GHz for EMAANa-PANI-MWCNTs (pristine CNT, ACNT and CCNT) composites with various MWCNTs loadings.

Table 5.4. Shielding Efficiency of EMAANa-PANI-MWCNTs (pristine CNT, ACNT and CCNT) at 8.5 GHz.

Shielding Materials	Amount (%)	SE (dB)
Na Ionomer PANI-OCNT	25	-11.0983
	50	-13.0797
	75	-14.6051
	100	-18.7884
	125	-18.1812
	150	-18.6243
Na Ionomer PANI-ACNT	25	-17.7025
	50	-15.8938
	75	-16.1190
	100	-17.0069
	125	-17.4678
	150	-17.9185
Na Ionomer PANI-CCNT	25	-14.5714
	50	-18.7963
	75	-21.5260
	100	**-32.6251**
	125	-23.3233
	150	-18.5451

The results show that the EMI shielding effectiveness of the hybrid EMAANa-PANI-MWCNT composites increased with increasing content of MWCNT in the PANI-MWCNT composites. This increment of the EMI shielding effectiveness is attributed mainly to the formation of conducting interconnected PANI-MWCNTs networks in the insulating EMAANa matrix. The increase in MWCNTs loading increases the number of interconnections in the EMAANa-PANI-MWCNT composite that will interact with the incident radiation resulting to the higher shielding effectiveness.

Conductivity is a consequence of conductive network formation in the insulating matrix such as EMAANa. Generally, higher loading levels are required for effective interception of incoming EM radiation and to achieve good microwave reduction efficiencies [1, 2, 24], hence, the shielding effectiveness of a conducting composite EMAANa-PANI-MWCNTs is related to its conductivity. This conductive network is distributed uniformly in the polymer matrix which interacts with electromagnetic waves and contributes to the EMI shielding effectiveness. Therefore, variation in the shielding effectiveness (Table 5.4) against conductivity can be correlated with the change in conductivity (Table 5.3) of EMAANa-PANI-MWCNT composites against MWCNT loading in PANI-MWCNT composites. The Table 5.4 also provides the comparable EMI shielding effectiveness of the three hybrid composites - EMAANa-PANI-pristine CNT, EMAANa-PANI-ACNT and EMAANa-PANI-CCNT of this study at the same content. As shown in the same Table, there is a significant difference in the efficiency of the different MWCNTs in influencing shielding effectiveness in the composites. For example, the EMAANa-PANI-CCNT composite at ratio 1:1 of PANI-MWCNT exhibited a higher shielding effectiveness of 32 dB compared to 23 dB and 18 dB for the EMAANa-PANI-ACNT and EMAANa-PANI-pristine composites respectively at the same PANI-MWCNTs loading. Reason was previously reported in chapter 5A.

Carbon nanotubes possess much smaller diameters and larger aspect ratios with higher electrical conductivities as compared to PANI. The smaller size of the carbon nanotubes may provide a larger surface area. Therefore, the number of conductive interconnected nanotubes increases. And the larger aspect ratio of carbon nanotubes also helps to form a comprehensively continuous networks that can facilitate electron transport in the EMAANa-PANI-MWCNT composite. From the foregoing, comparing with the EMAANa-PANI binary composite (Table 4.4) at the same loading, the EMAANa-PANI-MWCNT hybrid composites are more effective in providing EMI shielding. Higher conductivity means more conductive paths within the polymer matrix. Therefore, larger surface area of conductive MWCNTs contributes to shielding. Based on this, it can be said that the higher the conductivity of the blend the higher the EMI SE.

The EMI SE of pure polymer matrix is usually very negligible and ineffective in any shielding application [59, 68]. However, the EMI SE of EMAAZn matrix (-0.29 dB) used in chapter 6 varied from EMAANa matrix (-0.47 dB) used in this chapter under discussion. The EMI SE of EMAANa-PANI-MWCNTs composites exhibited a higher shielding effectiveness of 32 dB compared to 30 dB for the EMAAZn-PANI-MWCNTs hybrid composites at the same PANI-MWCNTs loading. Therefore, it can be said that the EMI SE is influenced by the polymer type as well which could be the reason the results in Table 5.4 are relatively higher than those of Table 5.2. This maybe due to the different metal salts in the polymer matrices as previously reported in the electrical conductivity. Based on that, we can rightly say that the higher the conductivity of the composites, the higher will be the EMI SE. Higher conductivity means more conductive paths within the polymer matrix [39].

However, the level of shielding effectiveness attained by the composites (11-32 dB) may be adequate for shielding applications. According to Markham, [69] the required EMI SE of notebooks and desktop computer enclosures is between 15 and 20 dB and cell phone 70-90 dB.

5.2 Conclusion

PANI-MWCNT nanocomposites could be incorporated into the ionomer (EMAAZn or EMAANa) matrices by solution mixing method using a solvent mixture of 90:10 (toluene/1-butanol) at 65°C. Incorporation of the PANI-MWCNT nanocomposites results in the improvement of the electrical conductivity of the ionomer matrices. The results showed that the hybrid composites displayed good electromagnetic interference shielding effectiveness. At ratio 1:1 of MWCNT with PANI, the EMI SE and electrical conductivity of the hybrid composites with CCNT were higher than those of the ACNT > pristine CNT composites. The higher EMI SE and electrical conductivity can be ascribed to the higher conducting networks established within PANI-MWCNT and the polymer matrix, thereby enhancing the composite's EMI SE and electrical conductivity. The EMAANa-PANI-MWCNT hybrid composites exhibited much higher electrical conductivity and better EMI SE compared to EMAAZn-PANI-MWCNT hybrid composites. The results of DC electrical conductivity show that the hybrid composites containing PANI-CCNT has higher conductivity compared to the PANI-ACNT and PANI-

Pristine CNT based hybrid composites. The EMI SE and DC conductivity was in the order EMAA-PANI-CCNT > EMAA- PANI-ACNT > EMAA-PANI-Pristine CNT for both sodium ionomer and zinc ionomer. Among the polymer composites studied, the highest electrical conductivity values was obtained for 1:1 EMAA-PANI-CCNT hybrid composites. The electromagnetic interference (EMI) shielding effectiveness (SE) of the EMAA-PANI hybrid composites also showed the highest value in EMAA-PANI-CCNT hybrid composite. The higher thermal properties, EMI SE and electrical conductivity of the hybrid composites was influenced by strong interactions of MWCNTs type and loading compared to results obtained from EMAA-PANI binary composites in chapter 4. The prepared composites can find applications where better thermal resistance, EMI SE and conducting properties are required. The EMI SE obtained are very promising for some EMI shielding applications such as laptop and desktop computers shielding and could be utilized effectively as EMI shielding materials in X-band region. This work provides a promising novel methodology to fabricate flexible and lightweight microwave shields based on EMAAZn-PANI-MWCNT and EMAANa-PANI-MWCNT hybrid composites.

Reference

[1] John H, Thomas RM, Jacob J, Mathew KT and Joseph R, 2007. Conducting polyaniline composites as microwave absorbers. Polym Comp, 28 588-592.

[2] Geetha S, Kumar KKS, Rao CRK, Vijayan M and Trivedi DC, 2009. EMI Shielding: Methods and Materials-A review. J Appl Polym Sci, 112 2073-2086.

[3] Tantawy HR, Aston DE, Smith JR and Young JL, 2013. Comparison of electromagnetic shielding with polyaniline nanopowders produced in solvent-limited conditions. ACS Appl. Mater Interfaces, 5 4648-4658.

[4] Faez R, Martin IM, De Paoli M-A and Rezende MC, 2001. Microwave properties of EPDM/PANI-DBSA blends. Synth Metals, 119 (1) 435-436.

[5] Chung DDL, 2001. Electromagnetic interference shielding effectiveness of carbon materials. Carbon, 39 279-285.

[6] Shacklette LW, Colaneri NF, Kulkarni VG and Wessling B, 1992. EMI Shielding of Intrinsically Conductive Polymers. J Vinyl Technol, 14 (2) 118-122.

[7] Ameen S, Akhtar SM, Song M and Shin HS, 2013. Solar cells - research and application perspectives. In Arturo Morales-Acevedo (Eds) Metal oxide nanomaterials, conducting polymers and their nanocomposites for solar energy. InTech, p 203-259.

[8] Palaniappan S and John A, 2008. Polyaniline materials by emulsion polymerization pathway. Prog Polym Sci, 33 732-758.

[9] Bakhishi AK and Bhalla G, 2004. Electrically conducting polymers: Materials of the twenty-first century. J Sci and Ind Res, 63 715-728.

[10] Stejskal J and Gilbert RG, 2002. Polyaniline: preparation of a conducting polymer. Pure Appl Chem, 74 (5) 857-867.

[11] Rafeeq SN and Khalaf WZ, 2015. Preparation, characterization and electrical conductivity of doped polyaniline with (HCL and P-TSA). Eng Technol J, 33 (7) Part B 1220-1231.

[12] Wang Y, 2014. Microwave absorbing materials based on polyaniline composites: A review. Int J Mater Res, 105 (1) 3-12.

[13] Song E and Choi J-W, 2013. Conducting polyaniline nanowire and its applications in chemiresistive sensing. Nanomater, 3 (3) 498–523.

[14] Cardoso MJR, Lima MFS and Lenz DM, 2007. Polyaniline synthesized with functionalized sulfonic acids for blends manufacture. Mater Res, 10 (4) 425-429.

[15] Saini P, Choudhary V, Singh BP, Mathur RB and Dhawan SK, 2011. Enhanced microwave absorption behavior of polyaniline-CNT/polystyrene blend in 12.4–18.0 GHz range. Synth Met, 161 1522-1526.

[16] Saini P, Choudhary V, Vijayan N and Kotnala RK, 2012. Improved electromagnetic interference shielding response of poly (aniline)-coated fabrics containing dielectric and magnetic nanoparticles. J Phys Chem C, 116 13403-13412.

[17] Blanchet GB, Fincher CR and Gao F, 2003. Polyaniline nanotube composites: a high-resolution printable conductor. Appl Phys Lett, 82 1290-1292.

[18] Ramasubramaniam R, Chen J and Liu H, 2003. Homogeneous carbon nanotube/polymer composites for electrical applications. Appl Phys Lett, 83 2928-2930.

[19] Nakaramontri Y, Pichaiyut S, Wisunthorn S and Nakason C, 2017. Hybrid carbon nanotubes and conductive carbon black in natural rubber composites to enhance electrical conductivity by reducing gaps separating carbon nanotube encapsulates. Eur Polym J, 90 467-484.

[20] Nakaramontri Y, Kummerlöwe C, Nakason C and Vennemann N, 2015. Influence of modified natural rubber on properties of natural rubber-carbon nanotubes composites. Rubber Chem Technol, 88 199-218.

[21] Nakaramontri Y, Kummerlöwe C, Nakason C and Vennemann N, 2014. Effect of modified natural rubber and functionalization of carbon nanotubes on properties of natural rubber composites. Adv Mater Res 844 301-304.

[22] Nakaramontri Y, Kummerlöwe C, Nakason C and Vennemann N, 2015. The effect of surface functionalization of carbon nanotubes on the properties of natural rubber/carbon nanotube composites. Polym Comp, 36 2113-2122.

[23] Sumfleth J, Adroher XC and Schulte K, Synergistic effects in network formation and electrical properties of hybrid epoxy nanocomposites containing multiwall carbon nanotubes and carbon black. J Mater Sci, 44 3241-3247.

[24] Li C, Thostenson ET and Chou TW, 2007. Dominant role of tunneling resistance in the electrical conductivity of carbon nanotube-based composites. Appl Phys Lett, 91 223114-223117.

[25] Ma PC, Liu MY, Zhang H, Wang SQ, Wang R, Wang K, Yiu-Kei W, Ben-Zhong T, Soon-Hyung H, Kyung-Wook P and Jang-Kyo K, 2009. Enhanced electrical conductivity of nanocomposites containing hybrid fillers of carbon nanotubes and carbon black. ACS Appl Mater Interfaces, 1 1090-1096.

[26] Che RC, Peng LM, Duan XF, Chen XF and Liang XL, 2004. Microwave absorption enhancement and complex permittivity and permeability of Fe encapsulated within carbon nanotubes. Adv Mater, 16 401-405.

[27] Colaneri NF and Shacklette LW, 1992. EMI shielding measurements of conductive polymer blends. IEEE Trans Instrum Meas, 41 291-297.

[28] Joo J and Epstein AJ, 1994. Electromagnetic radiation shielding by intrinsically conducting polymers. Appl Phys Lett, 65 2278-2280.

[29] Saini P, Jalan R and Dhawan SK, 2008. Synthesis and characterization of processable polyaniline doped with novel dopant NaSIPA. J Appl Polym Sci, 108 1437-1446.

[30] Saini P, Choudhary V, Singh BP, Mathur RB and Dhawan SK, 2009. Polyaniline/MWCNT composites for microwave absorption and EMI shielding. Mater Chem Phys, 113 919-926.

[31] Ting TH, Jau YN and Yu RP, 2012. Microwave absorbing properties of polyaniline/multi-walled carbon nanotube composites with various polyaniline contents. Appl Surf Sci, 258 3184-3190.

[32] Eswaraiah V, Sankaranarayanan V and Ramaprabhu S, 2011. Inorganic nanotubes reinforced polyvinylidene fluoride composites as low-cost electromagnetic interference shielding materials. Nanoscale Res Lett, 6 137-148.

[33] Kim HM, Kim K, Lee CY, Joo J, Cho SJ, Yoon HS, Pejakovic DA, Yoo JW and Epstein AJ, 2004. Electrical conductivity and electromagnetic interference shielding of multiwalled carbon nanotube composites containing Fe catalyst. Appl Phys Lett, 84 589-591.

[34] Li Y, Chen C, Li J-T, Zhang S, Ni Y, Cai S and Huang J, 2010. Enhanced dielectric constant for efficient electromagnetic shielding based on carbon-nanotube-added styrene acrylic emulsion based composite. Nanoscale Res Lett, 5 1170-1176.

[35] Saini P, Choudhary V and Dhawan SK, 2012. Improved microwave absorption and electrostatic charge dissipation efficiencies of conducting polymer grafted fabrics prepared via in situ polymerization. Polym Adv Technol, 23 343-349.

[36] Sandler JKW, Kirk JE, Kinloch IA, Shaffer MSP and Windle AH, 2003. Ultra-low electrical percolation threshold in carbon- nanotube-epoxy composites. Polymer, 44 5893-5899.

[37] Sangermano M, Pegel S, Potschke P and Voit B, 2008. Antistatic epoxy coatings with carbon nanotubes obtained by cationic photopolymerization. Macromol Rapid Comm, 29 396-400.

[38] Singh BP, Prabha, Saini P, Gupta T, Garg P, Kumar G, Pandey I, Pandey S, Seth RK, Dhawan SK and Mathur RB, 2011. Designing of multiwalled carbon nanotubes reinforced low density polyethylene nanocomposites for suppression of electromagnetic radiation. J Nanopart Res, 13 7065-7074.

[39] Yang Y, Gupta MC, Dudley KL and Lawrence RW, 2005. Novel carbon nanotube-polystyrene foam composites for electromagnetic interference shielding. Nano Lett, 5 (11) 2131-2134.

[40] Saini P and Choudhary V, 2013. Enhanced electromagnetic interference shielding effectiveness of polyaniline functionalized carbon nanotubes filled polystyrene composites. J Nanopart Res, 15 1415-1422.

[41] Abdullah ET, Hassan SM and Ahmed RS, 2016. Electrical properties of polyaniline/functionalized multi walled carbon nanotubes nanocomposite. Int J Current Eng Technol, 6 (2) 617-621.

[42] Huang JC, 1995. EMI shielding plastics-A review. Adv Polym Technol, 14 (2) 137-150.

[43] Sun D, Chu CC, Sue HJ, 2010. Simple approach for preparation of epoxy hybrid nanocomposites based on carbon nanotubes and a model clay. Chem Mater, 22 3773-3778.

[44] Li D and Sur GS, 2013. Comparison of poly(ethylene-co-acrylic acid) loaded Zn^{2+}-montmorillonite nanocomposites and poly(ethylene-co-acrylic acid) zinc salt. J Ind Eng Chem, 20 3122-3127.

[45] Jose T, Moni G, Salini S, Ann Jess Raju AJ, George JJ and George SC, 2017. Multifunctional multi-walled carbon nanotube reinforced natural rubber nanocomposites. Ind Crops Products, 105 63–73.

[46] George N, Bipinbal PK, Bhadran B, Mathiazhagan A and Rani Joseph R, 2017. Segregated network formation of multiwalled carbon nanotubes in natural rubber through surfactant assisted latex compounding: A novel technique for multifunctional properties. Polym, 112 264-277.

[47] Yang SY, Lozano K, Lomeli A, Foltz HD and Jones R, 2005. Electromagnetic interference shielding effectiveness of carbon nanofiber/LCP composites. Comp Part A, 36 (5) 691-7.

[48] Eren O, Ucar N, Onen A, Kızıldag N, Vurur OF, Demirsoy N and Karacan I, 2014. Effect of amine-functionalized carbon nanotubes on the properties of CNT-PAN composite nanofibers. J Chem and Molecul Eng, 8 (8) 767-769.

[49] Khatake SM, Mathe VL and Joshi GM, 2015. Grafting of amine-functionalized multiwall carbon nanotubes with free acid anhydride in carboxylic acid modified epoxy. Polym-Plasts Technol Eng, 54 (8) 851-860.

[50] Bachhav SG and Patil DR, 2015. Synthesis and characterization of polyaniline-multiwalled carbon nanotube nanocomposites and its electrical percolation behavior. Amer J Mater Sci, 5 (4) 90-95.

[51] Arjmand M, 2014. Electrical Conductivity, Electromagnetic Interference Shielding and Dielectric Properties of Multi-walled Carbon Nanotube/Polymer Composites. PhD Thesis, Department of Chemical and Petroleum Engineering, University of Calgary, Calgary, Alberta.

[52] Fiuschau GFL, Yoshikawa S and Newnham RE, 1992. Resistivities of conductive composites. J Appl Phys 72 (3) 953-959.

[53] Sichel EK, Gittleman JI and Sheng P, 1978. Transport properties of the composite-material carbon-poly(vinyl chloride). Phys Rev B, 18 (10) 5712-5716.

[54] Chekanov Y, Ohnogi R, Asai S and Sumita M, 1999. Electrical properties of epoxy resin filled with carbon fibers. J Mater Sci, 34 (22) 5589-5592.

[55] Ruschau GR, Yoshikawa S and Newnham RE, 1992. Resistivities of conductive composites. J Appl Phys, 72 (3) 953-959.

[56] Thomassin JM, Jerome C, Pardoen T, Bailly C, Huynen I, Detrembleur C 2013. Polymer/carbon based composites as electromagnetic interference (EMI) shielding materials. Mater Sci Eng: R: Report, 74 211-232.

[57] George N, Chandra JCS, Mathiazhagan A and Joseph R, 2015. High performance natural rubber composites with conductive segregated network of multiwalled carbon nanotubes. Comp Sci Technol, 116 33–40.

[58] Sarvi A and Sundararaj U, Electrical permittivity and electrical conductivity of multiwall carbon nanotube-polyaniline (MWCNT-PANi) core-shell nanofibers and MWCNT-PANi/polystyrene composites. Macromol Mater Eng, 299 1013–1020.

[59] Al-Saleh MH and Sundararaj U, 2008. Electromagnetic interference (EMI) shielding effectiveness of PP/PS polymer blends containing high structure carbon black. Macromol Mater Eng, 293 (7) 621-630.

[60] Strümpler R and Glatz-Reichenbach J, 1999. Conducting polymer composites. J Electroceram, 3 (4) 329-346.

[61] Chung DDL, 2000. Materials for electromagnetic interference shielding. J Mater Eng Perf, 9 (3) 350-354.

[62] Al-Saleh MH and Sundararaj U, 2009. Electromagnetic interference shielding mechanisms of CNT/polymer composites. Carbon, 47 (7) 1738-1746.

[63] Schulz RB, Plantz VC and Brush DR. Shielding theory and practice. Electromagnetic compatibility. IEEE Trans, 30 (3) 187-201.

[64] Li J, Zhang G, Zhang H, Fan X, Zhou L, Shang Z and Shi X, 2018. Electrical conductivity and electromagnetic interference shielding of epoxy nanocomposite foams containing functionalized multi-wall carbon nanotubes. Appl Surf Sci, 428 7–16.

[65] Bikiaris D, 2010. Microstructure and properties of polypropylene/ carbon nanotube nanocomposites. Mater, 3 2884-2946.

[66] https://en.wikipedia.org/wiki/Electromagnetic_interference. Accessed on 23rd of August, 2018.

[67] Electronicsbeliever http://electronicsbeliever.com/emi-shielding-techniques/March 21, 2017. Accessed on 23rd of August, 2018.

[68] Yim Y-J, Rhee KY and Park S-J, 2016. Electromagnetic interference shielding effectiveness of nickel-plated MWCNTs/high-density polyethylene composites. Comp Part B, 98 120-125.

[69] Markham D, 2000. Shielding: quantifying the shielding requirements for portable electronic design and providing new solutions by using a combination of materials and design. Mater Design, 21 (1) 45-50.

…..ᏋᏨ…..

Chapter 6

MECHANICAL PROPERTIES OF IONOMER-PANI BINARY COMPOSITES AND IONOMER-PANI-MWCNT HYBRID COMPOSITES

Contents

This chapter presents the mechanical properties of both binary and hybrid composites of EMAAZn or EMAANa with PANI and PANI/MWCNT. PANI (bulk PANI-HCl, nano PANI-HCl and nano PANI-TSA) were synthesized and characterized as explained in chapter 3 (3.2.1 and 3.2.3). PANI-MWCNT composites were prepared by insitu polymerization of aniline monomer in the presence of MWCNT (pristine CNT, amine functionalized CNT (ACNT) and carboxylic acid functionalized CNT (CCNT)) using TSA as dopant and APS as oxidant as reported in chapter 3 (3.2.2). Binary composite films of EMAAZn-PANI and EMAANa-PANI, and hybrid composite films of EMAAZn-PANI-MWCNT and EMAANa-PANI-MWCNT were fabricated by solution mixing in a blend of solvents (toluene (90%)/ 1-butanol (10%)) at 65°C for mechanical property evaluation. The tensile properties of the conducting composites were evaluated using Shimadzu Universal Testing Machine (model AG-I).

6.1 Introduction

Ionomers has poor conductivity, poor durability of wet membranes and poor mechanical and chemical stability at elevated temperatures. These deficiencies has been reported to restrict its operating temperatures to below 100°C, thereby limiting the applications of ionomers. This has been attributed to the presence of both hydrophobic (non polar) and hydrophilic (polar) units in the polymer structure [1-6]. These limitations may be overcomed by the incorporation of fillers such as PANI, CNTs or PANI-CNT composites. Conducting polymers such as PANI possess electrical properties like that of metals and the characteristics of organic polymers such as lightweight, lower cost, resistance to corrosion and chemical attack, flexibility and greater workability [7-9]. However, they have limitations of material inconsistencies, insolubility in many organic solvents, inherent brittleness, poor mechanical properties and poor processability [10]. PANI is relatively hard to process compared with other conventional polymers and plastics. The processing of PANI is difficult, mainly due to its rigid backbone, related to its high degree of conjugation. The challenges faced in the processing of neat PANI have otherwise led to the advances in the development of PANI-based composites and blends. Carbon nanotube on the other hand possess some impressive and interesting structural, mechanical, electrical and electronic, optical, thermal and chemical characteristics, which are attributed to their small size and mass, very high aspect ratio, strong mechanical potency and high electrical and thermal conductivity. The introduction of the carbon nanotubes to PANI helps in raising of the number of charge-discharge cycles and the increase in the mechanical strength while decreasing the effects of mechanical stress.

Incorporation of CNTs into polymer matrices can potentially provide composite materials with superior material properties such as increased modulus, strength and conductivity. However, increased weight content of PANI and carbon nanotubes in the composites can deteriorate the flexible structure of the polymer and result in the heterogeneity of the composites.

In this chapter, we aimed to study the mechanical properties of solution processed ionomer-PANI binary composites and ionomer-PANI-MWCNT hybrid composites with different types of carbon nanotubes loaded at a ratio of 1:1.

6.2 Materials and Experimental Methods

6.2.1 Materials

As prepared:

Binary Composites

- EMAAZn
  EMAAZn-bulk PANI-HCl
  EMAAZn-nano PANI-HCl
  EMAAZn-nano PANI-TSA

- EMAANa
  EMAANa-bulk PANI-HCl
  EMAANa-nano PANI-HCl
  EMAANa-nano PANI-TSA

Hybrid Composites

- EMAAZn
  EMAAZn-PANI-pristine CNT
  EMAAZn-PANI-ACNT
  EMAAZn-PANI-CCNT

- EMAANa
  EMAANa-PANI-pristine CNT
  EMAANa-PANI-ACNT
  EMAANa-PANI-CCNT

Preparation of composites were carried out as per the procedure given in Section 4A.2.1, 4B.2.1, 5A.2.1 and 5B.2.1 of Chapters 4 and 5.

6.2.2 Mechanical Properties Measurements

Tensile strength, elongation at break and elastic modulus of the samples listed above were measured according to ASTM D-882 as described in chapter 2.

6.3 Results and Discussions

6.3.1 Tensile Properties

Conventionally, mechanical properties such as tensile strength of composites are evaluated by varying the filler loading in a polymer matrix (filler dependent). In this work, we have kept the filler-polymer matrix ratio constant at 1:1. We have used two different polymer matrices (EMAAZn or EMAANa), three different types of PANI (bulk PANI-HCl, nano PANI-HCl and nano PANI-TSA) and three different types of PANI-MWCNTs (PANI-pristine CNT, PANI-ACNT and PANI-CCNT) with the objective of determining the behaviour of the polymer matrices on incorporation of different fillers. While the neat polymer films have a smooth surface, the addition of fillers especially the composites containing MWCNTs, makes the surface rough and more brittle.

Table 6.1. Tensile strength and elongation at break of EMAAZn, EMAANa, EMAAZn-PANI, EMAANa-PANI binary composites, EMAAZn-PANI-MWCNT and EMAANa-PANI-MWCNT hybrid composite

Sample Name	Tensile Strength (MPa)	Elongation at break (%)	Elastic Modulus (MPa)	Modulus (300%) MPa
EMAAZn	20.1	913	103	12.4
EMAAZn-bulk PANI-HCl	14.7	11.2	287	-
EMAAZn-nano PANI-HCl	12.4	8.8	240	-
EMAAZn-nano PANI-TSA	11.0	9.6	212	-
EMAAZn-PANI-pristine CNT	9.7	11.5	206	-
EMAAZn-PANI-ACNT	6.0	13.8	250	-
EMAAZn-PANI-CCNT	8.7	11.5	198	-
EMAANa	16.1	603	47	11.8
EMAANa-bulk PANI-HCl	20.2	31.9	247	-
EMAANa-nano PANI-HCl	14.0	10.8	252	-
EMAANa-nano PANI-TSA	11.0	9.6	153	-
EMAANa-PANI-pristine CNT	9.3	8.4	197	-
EMAANa-PANI-ACNT	10.6	9.5	208	-
EMAANa-PANI-CCNT	10.1	8.1	198	-

The stress-strain curves showing the breakage behavior of the neat polymers (EMAAZn and EMAANa) and the composite films (EMAAZn-PANI (bulk PANI-HCl, nano PANI-HCl and nano PANI-TSA) binary composites and EMAANa-PANI (bulk PANI-HCl, nano PANI-HCl and nano PANI-TSA) binary composites) are shown in Figures 6.1, 6.2 and 6.3 respectively.

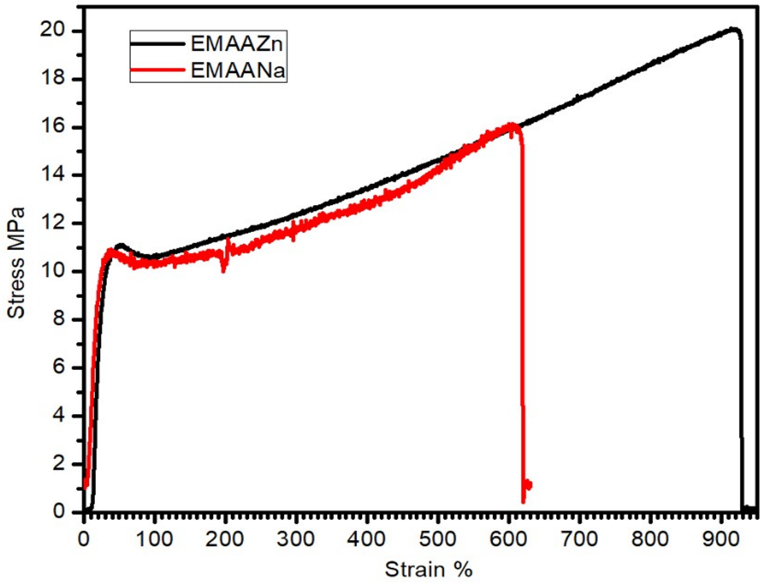

Figure 6.1. Stress strain curves of EMAAZn and EMAANa ionomers

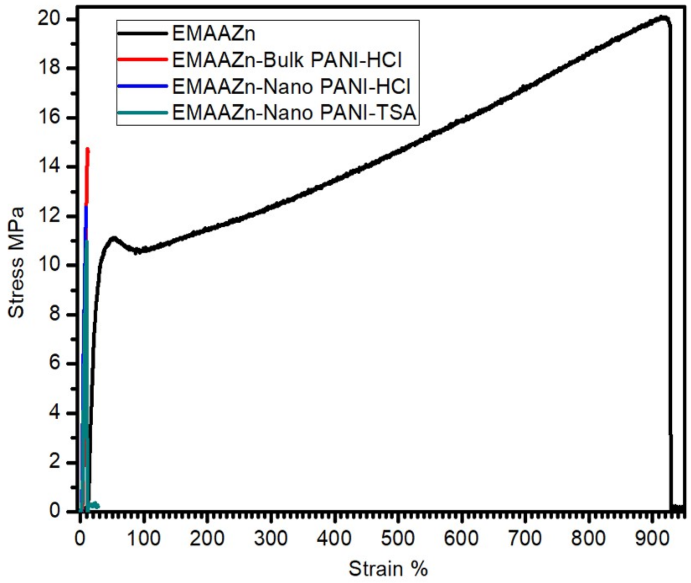

Figure 6.2. **Stress strain curves of EMAAZn and EMAAZn-PANI (bulk PANI-HCl, nano PANI-HCl and nano PANI-TSA) binary composites**

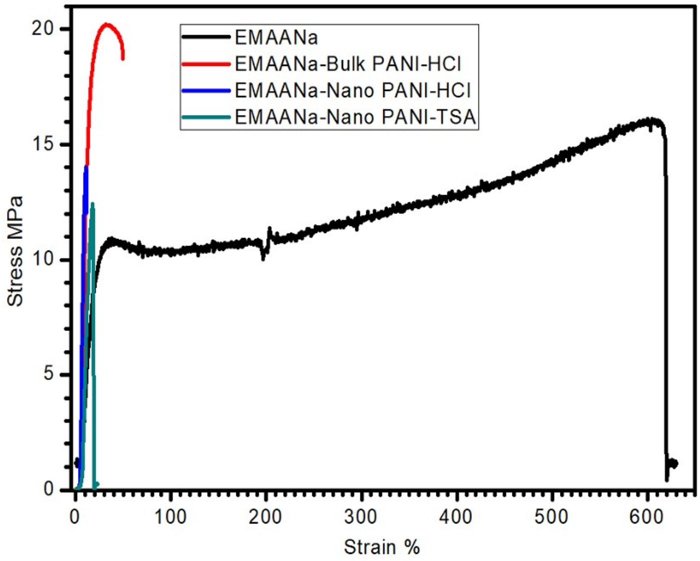

Figure 6.3. **Stress strain curves of EMAANa and EMAANa-PANI (bulk PANI-HCl, nano PANI-HCl and nano PANI-TSA) binary composites**

The neat polymers (EMAAZn or EMAANa) show strain at break of 913% and 603% with a tensile strength of 20.1 MPa and 16.1 MPa respectively. Higher strength and larger plastic deformation of EMAAZn indicate a more secured network of ionic crosslinks compared to EMAANa which keeps the macromolecular chains from sliding past one another. The sharing of bivalent Zn ions between polymer molecules in the ionomer results in effective crosslinking whereas monovalent Na ions can only impart a semblance of crosslinking through cluster association. Compared with the neat polymers, the PANI reinforced polymer matrix shows a brittle failure. The binary composites show a tensile strength of 14.8 MPa, 12.4 MPa and 11.0 MPa at strain at break of 11.2%, 8.8% and 9.6% respectively for EMAAZn-PANI (bulk PANI-HCl, nano PANI-HCl and nano PANI-TSA) while EMAANa-PANI (bulk PANI-HCl, nano PANI-HCl and nano PANI-TSA) binary composites show a behaviour of 20.2 MPa, 14.0 MPa and 11.0 MPa at a strain of 31.9%, 10.8% and 9.6% respectively (Figs. 6.1 and 6.2 respectively). The addition of PANI impart more rigidity to the ionomer as evident from the increased modulus in all cases. However tensile strength of the PANI composites has been reduced in the case of EMAAZn matrix. This may be due to the interference of PANI in the crosslinking process facilitated by the bivalent Zn ions. This may result in slipping of ionomer molecules on the application of a tensile force leading to reduced strength and elongation at break. Apart from this the agglomerations of PANI within the matrix may also trigger premature failure by acting as stress concentration points. Nanosized PANI, which has an inherent tendency for agglomeration, shows lower tensile strength compared to bulk PANI. Nano PANI doped with TSA has lower polarity attributed to the type of counter ion compared to HCl doped PANI. The reduced polarity makes the dispersion of PANI in the polar phase of ionomer matrix more difficult, leading to agglomeration in the nonpolar phase and subsequent lowering of tensile properties. In the case of EMAANa, since the physical crosslinks are formed by the association of similar ions, the effect of PANI may not be as severe compared to that in EMAAZn. On the contrary PANI may act as a binder between the ionic clusters forming a stiffening network within the ionomer matrix leading to higher tensile strength. As in the case of EMAAZn composites, nano PANI-HCl and nano PANI-TSA may form agglomerations in the matrix resulting in lower tensile strength.

However, upon the introduction of carbon nanotube into PANI (using insitu polymerization at 1:1 ratio of PANI-MWCNTs followed by incorporation into the ionomers (EMAAZn or EMAANa) at 1:1 ratio), the ionomer-PANI-MWCNT hybrid composites show a brittle fracture with slightly different strain to failure behavior compared with the binary composites at the same loading ratio. Figures 6.4 and 6.5 show the stress-strain behaviour of EMAAZn-PANI-MWCNT (Pristine CNT, ACNT and CCNT) and EMAANa-PANI-MWCNT (Pristine CNT, ACNT and CCNT) hybrid composites respectively.

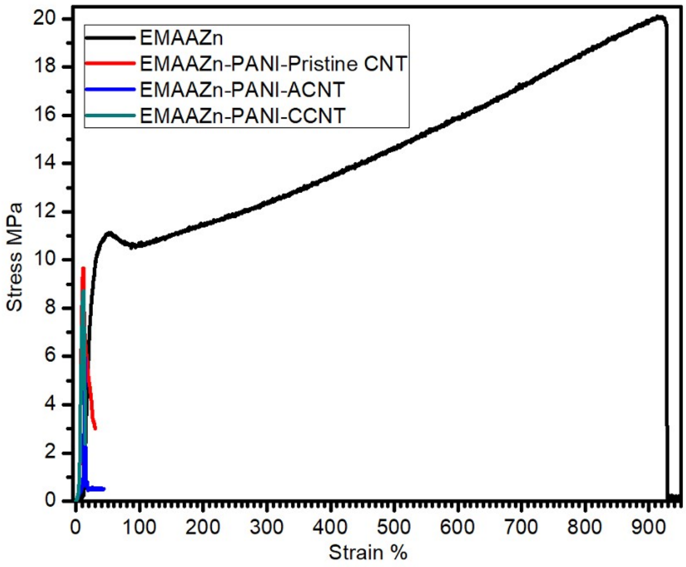

Figure 6.4. **Stress strain curves of EMAAZn and EMAAZn-PANI-MWCNT (pristine CNT, ACNT and CCNT) hybrid composites**

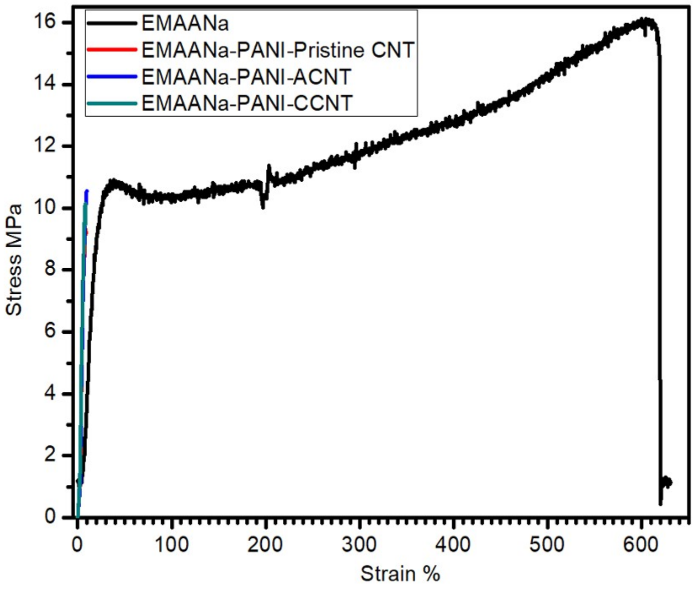

Figure 6.5. **Stress strain curves of EMAANa and EMAANa-PANI-MWCNT (pristine CNT, ACNT and CCNT) hybrid composites**

The hybrid composites show tensile strength of 9.7 MPa, 6.0 MPa and 8.7 MPa at strain of 11.5%, 13.8% and 11.5% respectively for Pristine CNT, ACNT and CCNT variants of EMAAZn-PANI-MWCNT hybrid composites while EMAANa-PANI-MWCNT (Pristine CNT, ACNT and CCNT) hybrid composites show tensile strength of 9.3 MPa, 10.6 MPa and 10.1 MPa at strains of 8.4%, 9.5% and 8.1% respectively. EMAAZn hybrid composites show a slightly higher plastic deformation while in the case of EMAANa hybrid composites deformation is slightly lower compared to the binary composites suggesting that MWCNTs impart different fracture toughness to the composites depending on the matrix polymer.

Contrary to conventions and expectations of tensile strength enhancement, no improvement in tensile strength of the composites was observed especially for the composites containing MWCNTs. In fact, for all samples, tensile strength was less than that of the neat polymer. Jia et al. in their work [11] reported a decrease in tensile strength of MWCNT-PMMA composites from about 55 MPa in the neat polymer to about 20 MPa in the composites prepared using untreated CNTs and an in situ polymerization process. In the present studies, the decrease in tensile strength of ionomer-PANI-MWCNT hybrid composites suggests weak filler-polymer interface and/or a poor dispersion. It is well known that the interphase between fillers and polymer matrix plays a key role in the stress transfer and defines an important design criteria. A uniform dispersion and a good interfacial bonding are crucial for load transfer to the PANIs and CNTs across the PANI-ionomer or PANI-MWCNT-ionomer interface [12]. Aggregation can reduce the reinforcing effect of the fillers, which expresses as a reduction in strength of the composite. Fillers such as MWCNTs possess high aspect ratio hence high surface tension that can cause filler aggregations. This can cause lower filler-matrix interfacial area, weakening the bonding between the matrix and filler which leads to poor load transfer to the fillers. Consequently, while the fillers are able to impart stiffness to the composite structure they are not able to impart the expected strength to the polymer matrix. During the in-situ polymerization of aniline layers of PANI are formed around the MWCNTs. These PANI layers interfere with the effective dispersion of MWCNTs in the ionomer matrix causing agglomeration of the filler which results in stress concentration and premature failure. Amino modified MWCNT surface may accumulate more PANI layers during polymerization, on account of the similarity in the surface functional group with that of aniline. This inhibit the CNT-matrix interaction more effectively leading to further reduction in tensile strength. The slippage of PANI layers on application of tensile force may be the reason for higher elongation in the case of EMAAZn-PANI-MWCNT composites. In the case of EMAANa hybrid composites, the association of similar ions may be capable of holding the PANI layers without slippage, stiffening the matrix and thus providing composites with higher tensile strength and lower strain at break. It should be noted that while EMAAZn-PANI-MWCNT composite registers a decrease in tensile strength up to 70% compared to the neat polymer (EMAAZn-PANI-ACNT) for the same fillers EMAANa loses only 34% of its strength. Also, the polymer matrix (ionomer) is a polar and non polar polymer, which might cause phase separation in the mix especially during cooling after solution mixing. This phase separation may attract polar fillers more towards the polar phase thus creating an inhomogeneous distribution of fillers within the composites and consequent uneven stress distribution, resulting in lower mechanical properties. Figures 6.6 – 6.11 represents the tensile strength and elongation at break and elastic modulus of EMAAZn, EMAANa, EMAAZn-PANI, EMAANa-PANI binary composites, EMAAZn-PANI-MWCNT and EMAANa-PANI-MWCNT hybrid composites.

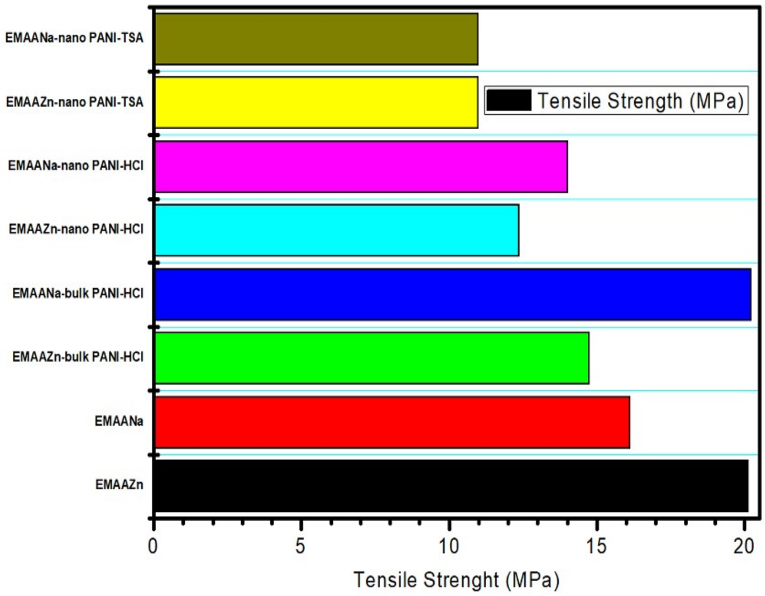

Figure 6.6. **Tensile of EMAAZn, EMAANa, EMAAZn-Bulk PANI-HCl, EMAANa-Bulk PANI-HCl, EMAAZn-Nano PANI-HCl, EMAANa-Nano PANI-HCl, EMAAZn-Nano PANI-TSA and EMAANa-Nano PANI-TSA**

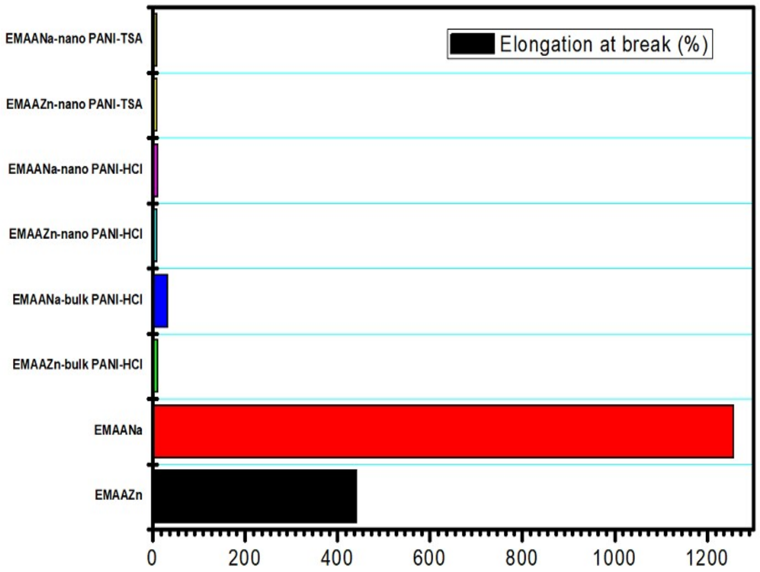

Figure 6.7. Elongation of EMAAZn, EMAANa, EMAAZn-Bulk PANI-HCl, EMAANa-Bulk PANI-HCl, EMAAZn-Nano PANI-HCl, EMAANa-Nano PANI-HCl, EMAAZn-Nano PANI-TSA and EMAANa-Nano PANI-TSA

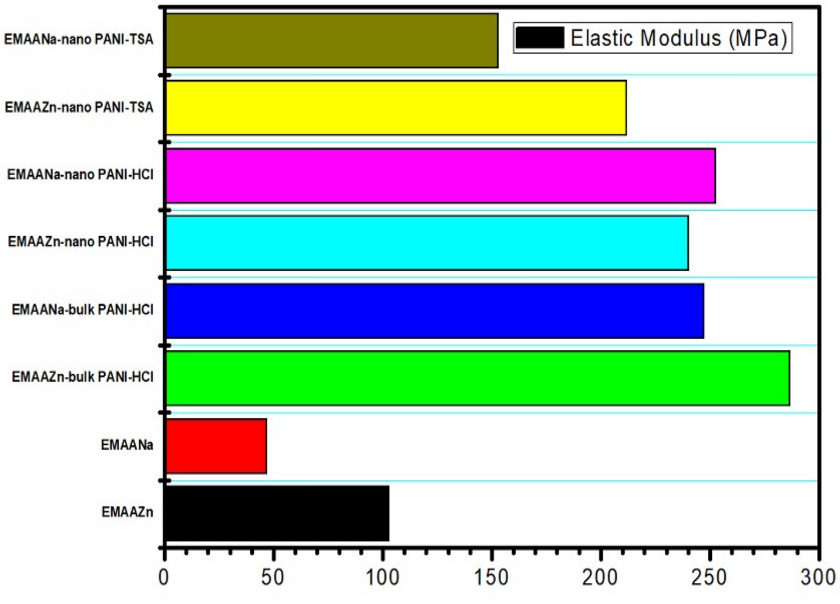

Figure 6.8. Elastic Modulus of EMAAZn, EMAANa, EMAAZn-Bulk PANI-HCl, EMAANa-Bulk PANI-HCl, EMAAZn-Nano PANI-HCl, EMAANa-Nano PANI-HCl, EMAAZn-Nano PANI-TSA and EMAANa-Nano PANI-TSA

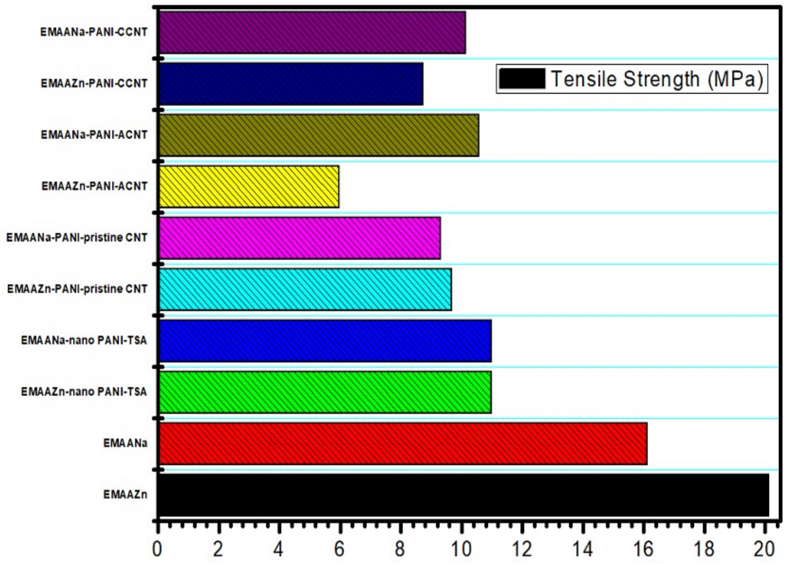

Figure 6.9. **Tensile of EMAAZn, EMAANa, EMAAZn-Nano PANI-TSA, EMAANa-Nano PANI-TSA, EMAAZn-PANI-pristine CNT, EMAANa-PANI-pristine CNT, EMAAZn-PANI-ACNT, EMAANa-PANI-ACNT, EMAANa-PANI-CCNT and EMAANa-PANI-CCNT**

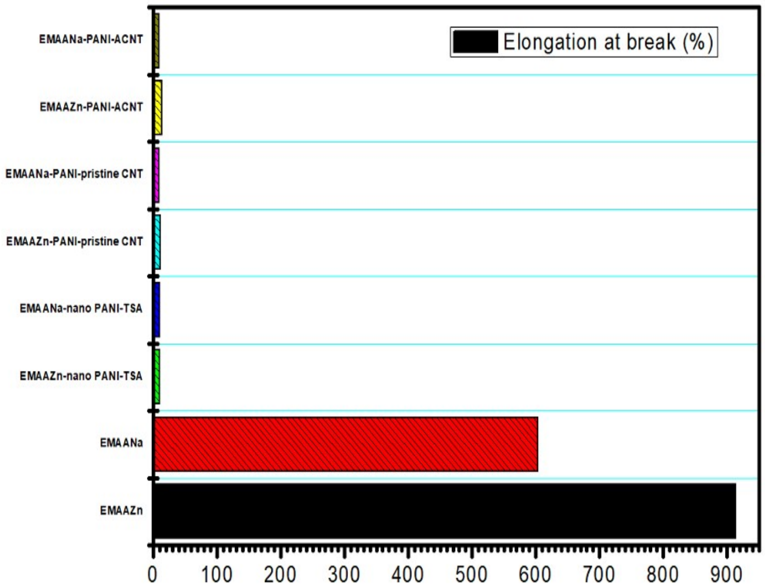

Figure 6.10. **Elongation of EMAAZn, EMAANa, EMAAZn-Nano PANI-TSA, EMAANa-Nano PANI-TSA, EMAAZn-PANI-pristine CNT, EMAANa-PANI-pristine CNT, EMAAZn-PANI-ACNT, EMAANa-PANI-ACNT, EMAANa-PANI-CCNT and EMAANa-PANI-CCNT**

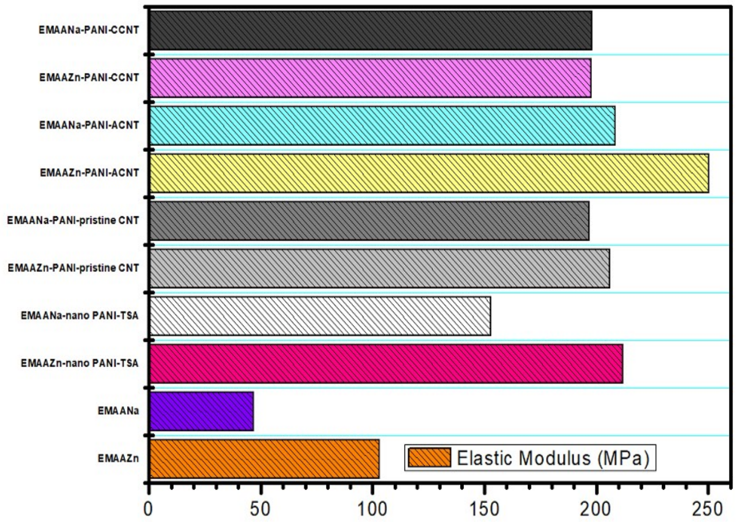

Figure 6.11. Elastic Modulus of EMAAZn, EMAANa, EMAAZn-Nano PANI-TSA, EMAANa-Nano PANI-TSA, EMAAZn-PANI-pristine CNT, EMAANa-PANI-pristine CNT, EMAAZn-PANI-ACNT, EMAANa-PANI-ACNT, EMAANa-PANI-CCNT and EMAANa-PANI-CCNT

6.4 Conclusion

Incorporation of PANI to the ionomer matrix produce widely varying results in the mechanical properties of the composites depending on the chemical structure of the ionomer macromolecules. PANI in bulk form drastically reduces the tensile strength of EMAAZn while increasing the same in the case of EMAANa composites. Nano sized PANI could not improve mechanical properties even in the case of EMAANa apparently due to its tendency to agglomerate in the host matrix. In all cases the addition of PANI transforms the ductile fracture behavior of the ionomers to a brittle one with a drastic decrease in elongation and an increase in modulus. Contrary to expectations, incorporation of MWCNT in the composites could not achieve any improvement in the tensile properties of the composites. It may be due to the embedment of MWCNT in PANI which prevents direct interaction MWCNTs and ionomer matrix. The uneven distribution of the fillers in the polar and nonpolar phases of the ionomer and resulting agglomerations may also be responsible for the reduction in mechanical properties.

Reference

[1] Mathias LJ, 2018. Available: www.pslc.ws/macrog/Polymer Science Learning Center/ionomer. Accessed on 2nd June 2018.

[2] Tant M and Wilkes GL, 1987. Viscoelastic behaviour of ionomers in bulk and solution, in structure and properties of ionomers, Pineri M and Eisenberg A (Eds), Reidel, Dordrecht, NATO ASI Series, p. 191-226.

[3] Schlick S, 1996. Ionomers: characterization, theory and applications. Boca Raton, Florida: CRC Press LLC.

[4] Eisenberg A and Joon-Kim J-S, 1998. Introduction to ionomers. Wiley Interscience, New York, p 327.

[5] Castillo-Ortega MM, Encinas JC, Rodriguez DE, Olayo R, 2001. Preparation and characterization of electroconductive polypyrrole-thermoplastic composites. J Appl Polym Sci, 81 1498-1506.

[6] Castillo-Ortega MM, Rodriguez DE, Encinas JC, Plascencia M, Mendez-Velarde FA, Olayo R, 2002. Conductometric uric acid and urea biosensor prepared from electroconductive polyaniline-poly (n-butylmethacrylate) composites. Sens Actuat B, 85 19-25.

[7] Ameen S, Akhtar SM, Song M and Shin HS, 2013. Solar cells - research and application perspectives. In Arturo Morales-Acevedo (Eds) Metal oxide nanomaterials, conducting polymers and their nanocomposites for solar energy. InTech, p 203-259.

[8] Palaniappan S and John A, 2008. Polyaniline materials by emulsion polymerization pathway. Prog Polym Sci, 33 732-758.

[9] Bakhishi AK and Bhalla G, 2004. Electrically conducting polymers: Materials of the twenty-first century. J Sci and Ind Res, 63 715-728.

[10] Subrahmanyam AR, Geetha V, Kumar A, Alakanandana A and Siva KJ, 2012. Mechanical and electrical conductivity studies of PANI-PVA and PANI-PEO blends. Int J Mater Sci, 2 (1) 27-30.

[11] Jia Z, Wang Z, Xu C, Liang J, Wei B, Wu D and Zhu S, 1999. Study on poly(methyl methacrylate)/carbon nanotube composites. Mater Sci Eng A, 271 (1-2) 395-400.

[12] Mathur RB, Pande S, Singh BP and Dhami TL, 2008. Electrical and Mechanical Properties of Multi-Walled Carbon Nanotubes Reinforced PMMA and PS Composites. Polym comp, 29 (7) 717-727.

……

Chapter 7

SUMMARY AND CONCLUSIONS

Conducting polymers are widely used in electrical/electronic devices, energy storage devices, sensors and EMI shielding applications. Among the conducting polymers, polyaniline (PANI) and PANI based materials have been studied most comprehensively for the reasons that they possess easier and inexpensive preparation methods, good environmental stability in both doped and undoped forms, excellent physical and chemical properties and high conductivity. However, PANI shows loss of conductivity in neutral and high pH environments and poor processability. Incorporation of CNTs in PANI can provide a vital role due to its unique structure, stable conductivity, non-corrosiveness, nominal processing cost and thermal and environmental stability. However, processability remains a major limitation even with the incorporation of CNTs. This justifies the necessity to fabricate either a binary composite of polymer matrix-PANI or hybrid composites of polymer matrix-PANI-CNTs. Polymer materials (thermoplastics, thermosets, elastomers, etc.) possess good melt strength to bind PANI, CNT or PANI-CNT particles together in order to make it processable without compromising its conductivity and other properties. One of the ways to achieve these benefits lies in the exfoliation of PANI or PANI-CNTs into the polymer matrix to generate particles of high aspect ratio.

Addition of CNTs into PANI with unstable electrical conductivity and the addition of PANI or PANI-CNTs into polymer matrix that is intrinsically highly insulating are of paramount industrial interest for enhancing the processability of PANI, CNTs or PANI-CNTs as well as enhancing the electrical conductivity of the insulating polymer. In the present study, a commercially important class of thermoplastic polymer known as ionomer is considered, which consists of random copolymers of ethylene and methacrylic acid where some of the acid groups are neutralized to form metal salts. Ionomers contains hydrophobic backbone chains and a small amount of polar ionic salt groups attached on either the backbones, side chains or on backbone terminals thereby making it hydrophilic too. The presence of a few salt groups (Na^+, K^+, Mg^{2+}, Zn^{2+}, Cu^{2+}, Mn^{2+} and Co^{2+}) impart enormous strength, stiffness and conductivity to the ionomers. However, despite its uniqueness as a class of polymeric materials that comprise repeat units of both electrically neutral units and a fraction of ionized units, it has low and poor conductivity which is dependent on water absorption, poor durability of wet films and poor mechanical and chemical stability at elevated temperatures. Mechanical and electrical properties of polymers are significantly influenced by the presence of fillers.

In this work, PANI, PANI-MWCNT hybrids, ionomer-PANI binary composites and ionomer-PANI- MWCNT hybrid composites are prepared for electrical and EMI shielding applications. PANI doped with hydrochloric acid (HCl) in bulk and nano dimensions (bulk PANI-HCl and nano PANI-HCl) and PANI doped with toluene sulfonic acid (TSA) (nano PANI-TSA) in nano dimensions were synthesized by chemical oxidative polymerization technique. The hybrid of polyaniline with MWCNTs were prepared by in situ polymerization of aniline in the presence of non-functionalized (pristine CNT), amine functionalized (ACNT) and carboxylic acid functionalized (CCNT) multi-walled carbon nanotubes using ammonium persulfate as initiator and TSA as dopant tagged as PANI-pristine CNT, PANI-ACNT and PANI-CCNT respectively. Binary composite films of ionomer-PANI and hybrid composite films of ionomer-PANI-MWCNT were fabricated by solution mixing in a blend of solvents (toluene (90%)/ 1-butanol (10%)) at 65 °C. The electrical properties and EMI shielding effectiveness of the conducting hybrid composites were also evaluated.

The preparation of PANI/MWCNT composites was successfully performed by in situ polymerization method. The incorporation of MWCNT in the PANI matrix was confirmed by (UV–Vis), FTIR, SEM, TEM, TGA and XRD studies. SEM and TEM images confirmed that, in all of the PANI-MWCNT samples, the polymers were coated over the CNTs. UV–Vis spectra supported the presence of quinoid and benzoid rings; however, the lower intensity of the exciton absorption band of the quinoid rings supported the dominance of the benzoid ring. FTIR analysis revealed the formation of PANI and the change in polymer structure due to the introduction of CNTs in the polymer matrix. Thermal analysis shows enhanced thermal stability of polyaniline. TGA provided evidence for better thermal stability in the different PANI-MWCNT composites. The formation of hybrid materials was confirmed by XRD analysis as the X-ray peaks became sharper and peak broadening occurred because of the superimposition of the peaks of the CNTs and polymers. The polymerization of PANI with MWCNT causes strong interfacial interactions between PANI and MWCNT crystallites, also suggested by FT–IR and XRD studies, thereby changing the molecular conformation of PANI from compact structure to an expanded structure. The electrical-transport properties of the samples were measured at room temperature. The maximum conductivity was found in the PANI CCNT composite at ratio 1:1. So this composite may be used as the best electronic conductor. Consequently, there is a visible enhancement in the conductivity of composite of PANI up as the MWCNT concentration increases.

The ionomers (EMAAZn or EMAANa) matrix were successfully and effectively dissolved in the solvent blend of toluene and 1-butanol at 65°C. The composites of EMAAZn or EMAANa and PANI could be prepared by mixing the ionomer solution with PANI. The enhancement of the electrical conductivity and electromagnetic interference (EMI) shielding effectiveness (SE) of EMAAZn or EMAANa matrices upon mixing with PANI clearly indicates the successful introduction of PANI into matrices by solution mixing. Results of UV-visible spectroscopic analyses establish lower UV transmission in the binary composite films compared to the neat matrices (EMAAZn or EMAANa). Therefore the composite films could be used for UV shielding applications. The decomposition pattern of the ionomer matrices (EMAAZn or EMAANa) changed on mixing with PANI, which tend to retard the degradation of the molecules of the pure matrices at higher temperatures. The improvement in the decomposition temperature of the composites shows that the stability of neat matrices (EMAAZn or EMAANa) is increased with the introduction of PANI, owing to the reduction in segmental mobility. The results of DC electrical conductivity show that the composites containing nano PANI-TSA has higher conductivity compared to the nano PANI-HCl and bulk PANI-HCl based composites. This indicates that PANI in nano dimension are more conducting than in bulk form. The conductivity was in the order EMAA-nano PANI-TSA > EMAA-nano PANI-HCl > EMAA-bulk PANI-HCl for both sodium ionomer and zinc ionomer. Among the polymer composites studied, the highest electrical conductivity values was obtained for 1:1 EMAA-nano PANI-TSA composite. The electromagnetic interference (EMI) shielding effectiveness (SE) of the EMAA-PANI binary composites also showed the highest value in EMAA-nano PANI-TSA composite. The values of attenuation obtained in the EMAA-bulk PANI-HCl and EMAA-nano PANI-HCl composites are lower than the minimum attenuation that ensures the safety of electronic gadgets. EMAANa-PANI binary composites show better electrical conductivity and EMI shielding effectiveness compared to EMAAZn-PANI binary composite. The EMAA-nano PANI-TSA composites are a promising material for EMI shielding. The composite films may be utilized for static charge dissipation, lightweight devices and effective EMI shielding or microwave absorption materials. The results obtained revealed that the solution blending is an effective way to improve the processability of electrically conducting polyaniline as well as improve the thermal, electrical and EMI SE properties of EMAAZn or EMAANa.

PANI-MWCNT nanocomposites were successfully introduced into ionomers (EMAAZn or EMAANa) matrices by solution mixing method and then EMAAZn-PANI-MWCNT and EMAANa-PANI-MWCNT hybrid composite films were fabricated using a solvent mixture of 90:10

(toluene/1-butanol) at 65°C. During the sonication process, the PANI-MWCNT was dispersed to redistribute and also breakdown agglomerated particles and thus increased the chance of inter-connectivity between PANI-MWCNT nanocomposites and the ionomers (EMAAZn or EMAANa) matrices resulting in the improvement of the electrical conductivity of the matrices. The results showed that the hybrid composites displayed good electromagnetic interference shielding effectiveness. At ratio 1:1 of MWCNT with PANI, the EMI SE and electrical conductivity of the hybrid composites with CCNT were higher than those of the ACNT > pristine CNT composites. The higher EMI SE and electrical conductivity can be ascribed to the higher conducting networks established within PANI-MWCNT and the polymer matrix, thereby enhancing the composite's EMI SE and electrical conductivity. It was also found that the EMAANa-PANI-MWCNT hybrid composites exhibited much higher electrical conductivity hence better EMI SE compared to EMAAZn-PANI-MWCNT hybrid composites. The results of DC electrical conductivity show that the hybrid composites containing PANI-CCNT has higher conductivity compared to the PANI-ACNT and PANI-Pristine CNT based hybrid composites. The EMI SE and DC conductivity was in the order EMAA-PANI-CCNT > EMAA-PANI-ACNT > EMAA-PANI-Pristine CNT for both sodium ionomer and zinc ionomer. Among the polymer composites studied, the highest electrical conductivity values was obtained for 1:1 EMAA-PANI-CCNT hybrid composites. The electromagnetic interference (EMI) shielding effectiveness (SE) of the EMAA-PANI hybrid composites also showed the highest value in EMAA-PANI-CCNT hybrid composite. From the results obtained, it can be concluded that the higher thermal properties, EMI SE and electrical conductivity of the hybrid composites was influenced by strong interactions of MWCNTs type and loading compared to results obtained from EMAA-PANI binary composites in chapter 4. The prepared composites can find applications where better thermal resistance, EMI SE and conducting properties are required. The EMI SE obtained are very promising for some EMI shielding applications such as laptop and desktop computers shielding, as low-cost and could be utilized effectively as EMI shielding materials in X-band region, can be applied for building shielding applications in high frequencies. This work provides a promising novel methodology to fabricate flexible and lightweight microwave shields based on EMAAZn-PANI-MWCNT and EMAANa-PANI-MWCNT hybrid composites. Thus the utilization of ionomer matrices can be increased with its enhanced properties.

Incorporation of PANI to the ionomer matrix produce widely varying results in the mechanical properties of the composites depending on the chemical structure of the ionomer macromolecules. PANI in bulk form drastically reduces the tensile strength of EMAAZn while increasing the same in the case of EMAANa composites. Nano sized PANI could not improve mechanical properties even in the case of EMAANa which may be due to its tendency to agglomerate in the host matrix. In all cases the addition of PANI transformed the ductile fracture behavior of the ionomers to a brittle one with a drastic decrease in elongation and an increase in modulus. Contrary to expectations incorporation of MWCNT in the composites could not achieve any improvement in the tensile properties of the composites. It may be due to the embedment of MWCNT in PANI which prevents direct interaction MWCNTs and ionomer matrix. The uneven distribution of the fillers in the polar and nonpolar phases of the ionomer and resulting agglomerations may also be responsible for the reduction in mechanical properties.

The present work is an attempt to formulate an effective preparative route by which composite blends with high conductivity and processability could be obtained. Solution mixing of PANI or PANI-MWCNT hybrids with ionomers, either sodium salt of poly(ethylene-co-methacrylic acid) (EMAANa) or zinc salt of poly(ethylene-co-methacrylic acid) (EMAAZn) using a blend of polar and non-polar solvents at 65°C improves the processability of the composites and it is an effective material for using as EMI shielding materials. More emphasis is given to solution processing as it is a more economical method to achieve good homogeneity and rapid mixing of the component materials with minimum energy consumption. Since the conducting composites are stable and retain the mechanical properties of the host polymer, films can be fabricated by solvent evaporation or by melt-processing for use in anti-static applications, for electromagnetic shielding, microwave absorption devices, etc.

Future Outlook

There are numerous possibilities for continuation of the studies on ionomer-PANI binary composites and ionomer-PANI-MWCNT hybrid composites.

Some of the suggestions are listed below.

- Improvement of electrical and electromagnetic interference shielding properties of ionomer-PANI binary composites and ionomer-PANI-MWCNT hybrid composites at high PANI and PANI-MWCNTs loading.
- Improvement of plasticity of ionomer-PANI binary composites and ionomer-PANI-MWCNT hybrid composites at high PANI and PANI-MWCNTs loading.
- Evaluation of the effect of solution mixing and melt mixing on the mechanical, electrical and electromagnetic interference shielding properties of ionomer-PANI binary composites and ionomer-PANI-MWCNT hybrid composites.
- Evaluation of the effect of solution mixing and melt mixing on the miscibility of ionomer-PANI binary composites and ionomer-PANI-MWCNT hybrid composites.
- Study of the dielectric performance of ionomer-PANI binary composites and ionomer-PANI-MWCNT hybrid composites to determine their suitability for capacitor applications.
- Study of actuated strain of ionomer-PANI binary composites and ionomer-PANI-MWCNT hybrid composites for application as actuators.

…..⁂…..

List of Publications

International Journals

(i) **Kingsley K. Ajekwene,** Jelmy E. Johny and Thomas Kurian, 2018. Sodium Salt of Polyethylene-Co-Methacrylic Acid Ionomer/Polyaniline Binary Blends for EMI Shielding Applications. *Progress in Electromagnetics Research C, Vol. 88, 207–218.*

(ii) **Kingsley Kema Ajekwene** and Thomas Kurian (2018) Bulk and nano-structured polyaniline: synthesis, characterization, thermal behaviour and dc conductivity. International Journal of Research in Advent Technology, Volume 6, Issue 9, 2385-2391.

(iii) **Kingsley Kema Ajekwene,** Jelmy E Johny and Thomas Kurian (2018), Preparation, Characterization, Thermal Behaviour and DC Conductivity of Nanopolyaniline and Polyaniline-Multi Walled Carbon Nanotube Nanocomposites. Journal of Emerging Technologies and Innovative Research, Volume 5, Issue 9, 374-386.

(iv) **Ajekwene K. K.,** Jelmy E J, and Thomas Kurian (2018), Preparation, characterization, thermal behaviour and dc conductivity of nano-structured polyaniline doped with HCl or TSA: A comparative analysis. *Journal of Emerging Technologies and Innovative Research, Volume 5, Issue 9, 294-299.*

(v) **Kingsley Kema Ajekwene**, Honey John and Thomas Kurian (2017), Progress in Preparation, Processing and Applications of Conducting Polymer-Ionomer Blends. *International Journal of Research and Scientific Innovation (IJRSI) | Volume IV, Issue IX, September 2017 | ISSN 2321–2705.*

Conference Proceedings

(i) **Kingsley Kema Ajekwene**, Thomas Kurian and Honey John (2016), Effect of particle size on the dielectric properties of polyaniline doped with HCl, *International Symposium on New Trends in Applied Chemistry (NTAC -2017) Sacred Heart College (Autonomous), Thevara, Kochi, India.*

(ii) **Ajekwene Kingsley Kema,** Thomas Kurian and Honey John (2017), Effect of synthesis conditions on the particle size, morphology and electrical conductivitybof polyaniline. Innovations in nanoworld: neoteric visions and emerging nanptechnologies (INNVENT)- 2017, IUCND, Cochin University of Science and Technology, Kochi, India; December 2017.

(iii) **Ajekwene Kingsley Kema,** Thomas Kurian and Honey John (2017), Electromagnetic interference shielding effectiveness of blends of polyaniline – zinc salt of poly(ethylene-co-methacrylic acid). National Conference of Current Trends in Polymer Science (CTPS)- 2018, Cochin University of Science and Technology, Kochi, India; February, 2018.

(iv) **Ajekwene K. K.,** Jelmy E J, and Thomas Kurian (2018), Preparation, characterization, thermal behaviour and dc conductivity of nano-structured polyaniline doped with HCl or TSA: A comparative analysis. 2nd International Conference on Research Trends in Engineering, Applied Science and Management (ICRTESM-2018), Osmania University Centre for International Programmes, Osmania University Campus, Hyderabad, Telangana State, India. 23rd September 2018, ISBN: 978-93-87433-40-3

……

Curriculum Vitae

1 **Names in full:** **Kingsley Kema Ajekwene**

1. **Date of Birth:** 28th February, 1972

2. **Place and Date of Birth:** Ukpodo Ifeku-Island, Edo State.

3. **Nationality:** Nigerian

4. **Marital Status:** Married

5. **Number and Ages of Children:** Three (14, 12 and 10 years)

6. **Permanent Home Address:** Techo D, Flat 15, Yabatech, Staff Quarters, Yaba, Lagos.

7. **Present Postal Address:** P.O. Box 2085, Shomolu, Lagos, Nigeria.

8. **Email:** kemaking@gmail.com
kingsley.ajekwene@yabatech.edu.edu.ng

9. **Tel:** +234-8035611170, +234-8020624990

10. **Present Employment Status:** Lecturer I CONPCASS 06/09

11. **Educational Institutions Attended (with dates):**

(a) **Primary:** Island Primary School, Ifeku, Edo State.
1978-1984

(b) **Secondary:** Illushi Secondary School, Illushi, Edo State.
1984-1990

(c) Tertiary:

(i)	Cochin University of Science and Technology (CUSAT), Kochi, Kerala, India	2015-Date
(ii)	The Federal University of Technology, Akure, Nigeria	2008-2012
(iii)	The Federal University of Technology, Akure, Nigeria	2004-2005
(iv)	Auchi Polytechnic, Auchi, Edo State, Nigeria	1996-1998
(v)	Auchi Polytechnic, Auchi, Edo State, Nigeria	1993-1995

12. Academic Qualifications (degree/diploma *with dates*):

(i) MTECH., Industrial Chemistry (Polymer Group)
2012

(ii) PGD, Industrial Chemistry
2005

(iii) HND, Polymer Technology
1998

(iv) ND, Polymer Technology
1995

(v) West Africa Senior Sch. Cert. Exam. (W.A.S.S.C.E)
1994 & 2006

13. Membership of Professional Bodies:

(i) Polymer Institute of Nigeria (PIN)
1997

(ii) Materials Society of Nigeria (MSN)
2002

(iii) National Association of Textile Scientist and Technologists
2011

(iv) International Journal for Research Under Literal Access (IJRULA)
2018

14. Awards:

(i) **RULA Awards for International Innovations and Betterment Excellence in Technical Research; as INNOVATIVE SCIENTIST IN NANOCOMPOSITES - 2018**

15. Work Experience:

(a) Polytechnic/College:

(i) **Lecturer I:** Dept of Polymer/Textile Technology, Yaba College of Technology Yaba, Lagos. **Oct. 2013 – Till Date**

(ii) **Principal Technologist I:** Dept of Polymer/Textile Technology, Yaba College of Technology Yaba, Lagos. **Jan. 2011 – Oct. 2013**

(iii) **Senior Technologist:** Dept of Polymer/Textile Technology, Yaba College of Technology Yaba, Lagos. **Jan. 2008 – Dec. 2011**

(iv) **Technologist I:** Dept of Polymer/Textile Technology, Yaba College of Technology Yaba, Lagos. **Jan. 2005 – Dec. 2008**

(v) **Technologist II:** Dept of Polymer/Textile Technology, Yaba College of Technology Yaba, Lagos. **May 2001 – Dec. 2005**

(b) Industry:

i. **Quality Control Officer:** Ben Plastics Ltd, Iganmu, Lagos.
Industrial Training Programme. **(May 1996 – July 1997)**

ii. **Quality Control Officer:** Poly Products Nig PLC, Ilupeju, Lagos.
National Youth Service Programme. **(March 1999 – Feb. 2000)**

iii. **Quality Controller-in-Charge:** Poly Products Nig PLC, Ilupeju, Lagos. **(March 2000 – May 2001)**

……